

✓

479144
7471667

COMPONENTS

R & D

LABORATORIES

LAND LOCOMOTION LABORATORY

Report No. 7841

LL 79

Copy No.

**RIGID WHEEL STUDIES
BY MEANS OF DIMENSIONAL ANALYSIS**

By

E. T. Vincent, H. H. Hicks, Jr.
E. I. Oktar, D. K. Kapur

1 April 1963

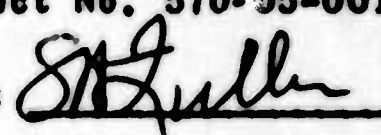
Project No. 5510.11.82200

D/A Project No. 570-95-001

Authenticated:



Approved:





**U.S. ARMY TANK-AUTOMOTIVE CENTER
CENTER LINE, MICHIGAN**

OBJECT

Study rigid wheel behavior by means of dimensional analysis, and ascertain the range over which the cohesive and frictional moduli of sinkage of a soil can be controlled.

RESULTS

Proper master variables were found for sand.

Cohesive and frictional moduli of sinkage of artificial soil and mixtures used indicated control is possible to a moderate degree.

RECOMMENDATIONS

1. Extend similitude studies to cohesive soils.
2. Investigate additional artificial soil mixtures to obtain independent variation of their penetration parameters.

ADMINISTRATIVE INFORMATION

Work was performed by the University of Michigan under contract with Department of the Army, Detroit Ordnance District Contract No. DA-20-018-ORD-18955. Report was approved for publication 1 April 1963.

ACKNOWLEDGEMENT

This report, which was edited by Mr. Z. J. Janosi, Land Locomotion Laboratory, represents a summary of the work done by the University of Michigan under contract with the Department of the Army, U. S. Army Ordnance Corps, Detroit Ordnance District (Contract No. DA-20-018-ORD-18955).

The report is based on the following progress reports:

- a. "A Similitude Study of the Drag and Sinkage of Wheels Using the Sinkage-Parameter System of Soil-Values" by H. H. Hicks, Jr. and E. T. Vincent.**
 - b. "Performance Coefficients for Powered Wheels in Sand", by D. K. Kapur and E. T. Vincent.**
 - c. "Control of the Properties of Research Soil Systems", by H. H. Hicks, Jr., E. J. Otkar, and E. T. Vincent.**
- In addition, the editor used the material included in paper No. 38 of the First International Conference on the Mechanics of Soil Vehicle Systems, presented by H. H. Hicks, Jr. in Turin (Italy) 1961, "A Similitude Study of the Drag and Sinkage of Wheels Using a System of Soil Values Related to Locomotion".**

TABLE OF CONTENTS

	<u>Page No.</u>
Acknowledgement	1
Abstract	1
Introduction	2
List of Symbols	4
List of Tables	5
List of Figures	6
Background	11
Theory	13
Experiments	18
1. Driven wheels in Sand	
2. Towed Wheels	
3. Control of Properties of Soils	
Results and Discussion	24
1. Driven Wheels	
2. Towed Wheels	
3. Control of Properties of Soils	
Conclusions	49
References	50
Distribution List	51
Figures	53

ABSTRACT

In the work presented here, a successful similitude correlation of wheel performance in sand was obtained using the Bekker sinkage parameters. Tests were made in the laboratory under simulated field conditions and included an investigation of wheel sinkage, drag, and traction, as related to wheel shape, diameter, load and soil depth.

A series of experiments are reported using a precision Bevameter on sand and mixtures of sand with other materials. The object of the tests was to ascertain the range over which the cohesive and frictional moduli of sinkage of a soil could be controlled which would exert a controlling influence upon the dimensionless parameters developed.

The results indicate that such control is possible to a moderate degree when using the types of materials studied.

INTRODUCTION

A fundamental problem in land locomotion mechanics is the interaction of the wheel-soil system. Since the mechanics of this system involves the properties of all its constituents, the problem is related to the physical properties of the soil in contact with the wheel as well as those of the wheel itself.

The soil can vary from a more or less plastic clay to sands. Little is known about the mechanics of soils. The result is that an empirical approach is necessary to solve the immediate problems, at least for the present.

The most general empirical approach has been introduced by Bekker⁽¹⁾. He expressed the average pressure under a footing which penetrates into the ground vertically by means of three empirical factors as follows:

$$p = \left(\frac{k_c}{b} + k_\phi \right) z^n \quad (1)$$

It is well recognized that the pressure p and the sinkage z are not accurately represented by the relation shown for all values of p and z . However, the main error involved at which difficulties develop is at small values of z , outside the range of significant vehicle sinkages. Thus, the relation permits considerable theoretical analysis and prediction,

the development of trends and consequent economies in money and time.

Equation (1) can be used for the solution of land locomotion problems provided that the soil values k_0 , k_g and n are known for the soil in question.

There is another approach to the subject where these parameters assume considerable importance: in dimensionless analysis where the object is to use principles of similitude to employ small scale tests in the laboratory to predict full-scale vehicle performance. In other words, the approach is to employ in land locomotion the equivalent of wind tunnel tests of airplanes, a technique which has been used for many years to check drag, stability, etc. of a model of the plane before its actual construction.

LIST OF SYMBOLS

p	Average pressure under a footing	lbs/in^2
k_c	Cohesive modulus of sinkage	lbs/in^{n+1}
k_ϕ	Frictional modulus of sinkage	lbs/in^{n+2}
n	Sinkage exponent	N.D.
z	Sinkage	in.
R	Horizontal component of the total force on the Wheel (motion resistance)	lbs
T	Torque applied to drive a wheel	lbs. in.
d	Diameter of a wheel	in.
α	Wheel aspect ratio (width/diameter).	N.D.
D	Soil-bed depth	in.
W	Vertical load applied on the wheel axis	lbs.
i	Slip	N.D.
μ	Coefficient of friction (soil to wheel)	N.D.
v_w	Tangential velocity of the wheel perimeter	in/sec
v_c	Linear horizontal velocity of the wheel	in/sec
b	Width of the Bevameter plate	in
S	Density	$\text{lbs sec}^2/\text{in}^4$
k	Bernstein's "sinkage coefficient"	lbs/in^{n+2}
ϕ	Angle of repose	(°)
r	Radius of a circular footing	in

LIST OF TABLES

TABLE NO.

- I. Independent Variables used for Powered Wheel Tests.
- II. Effect of Moisture Content on Soil Properties.
- III. Typical Properties of Barium Ferrite.
- IV. Soil Parameters for Indicated Materials, Obtained with Circular and Rectangular Footings.
- V. Calculated Maximum and Minimum Relations of Indicated Parameters.
- VI. Load-Sinkage Data for 75% Glass Beads, 25% Sand.

LIST OF FIGURES

Figure No.

- 1 Sign convention of velocities and forces on the wheel
- 1a Picture of wheel and motor drive
- 2 Plot of non-dimensional drag coefficient (R/W) versus non-dimensional load coefficient ($W/d^{n+2}k_d$) for rectangular cross-sectional wheels.
- 3 Plot of non-dimensional sinkage coefficient (z/d) versus non-dimensional load coefficient ($W/d^{n+2}k_d$) at various aspect ratios for rectangular cross-sectional wheels.
- 4 Plot of non-dimensional drag coefficient versus non-dimensional load coefficient at various aspect ratios for rectangular cross-sectional wheels.
- 5 Plot of non-dimensional sinkage coefficient vs. non-dimensional load coefficient for rectangular cross-sectional wheels.
- 6 The tow tank
- 7 The wheel carriage
- 8 Diagram of the penetrometer
- 9 Electric circuit
- 10 One range of sizes of feet employed for plunger
- 11 Plot of (R/W) versus % slip for ($W/d^{n+2}k_d = 1.328 \times 10^3$) under similitude conditions.
- 12 Plot of (R/W) versus % slip for ($W/d^{n+2}k_d = 2.656 \times 10^3$) under similitude conditions.

LIST OF FIGURES, Cont'd.

Figure No.

- 13 Plot of (R/W) vs. % slip for $(W/d^{n+2}k_{\phi} = 5.312 \times 10^3)$
under similitude conditions
- 14 Plot of (R/W) vs. % slip for $(W/d^{n+2}k_{\phi} = 7.368 \times 10^3)$
under similitude conditions
- 15 Plot of (R/W) vs. % slip for $(W/d^{n+2}k_{\phi} = 13.28 \times 10^3)$
under similitude conditions
- 16 Plot of (T/Wd) vs. % slip for $(W/d^{n+2}k_{\phi} = 1.328 \times 10^3)$
under similitude conditions
- 17 Plot of (T/Wd) vs. % slip for $(W/d^{n+2}k_{\phi} = 2.656 \times 10^3)$
under similitude conditions
- 18 Plot of (T/Wd) vs. % slip for $(W/d^{n+2}k_{\phi} = 5.312 \times 10^3)$
under similitude conditions
- 19 Plot of (T/Wd) vs. % slip for $(W/d^{n+2}k_{\phi} = 7.968 \times 10^3)$
under similitude conditions
- 20 Plot of (T/Wd) vs. % slip for $(W/d^{n+2}k_{\phi} = 13.28 \times 10^3)$
under similitude conditions
- 21 Plot of (z/d) vs. % slip for $(W/d^{n+2}k_{\phi} = 1.328 \times 10^3)$
under similitude conditions
- 22 Plot of (z/d) vs. % slip for $(W/d^{n+2}k_{\phi} = 2.656 \times 10^3)$
under similitude conditions
- 23 Plot of (z/d) vs. % slip for $(W/d^{n+2}k_{\phi} = 5.312 \times 10^3)$
under similitude conditions
- 24 Plot of (z/d) vs. % slip for $(W/d^{n+2}k_{\phi} = 7.968 \times 10^3)$
under similitude conditions

LIST OF FIGURES, Cont'd.

Figure No.

- 25 Plot of (z/d) vs. % slip for $(W/d^{n+2}k_\phi = 13.28 \times 10^3)$
under similitude conditions
- 26 Plot of (R/W) vs. % slip for $(W/d^{n+2}k_\phi = 1.328 \times 10^3)$
at various aspect ratios
- 27 Plot of (R/W) vs. % slip for $(W/d^{n+2}k_\phi = 2.656 \times 10^3)$
at various aspect ratios
- 28 Plot of (R/W) vs. % slip for $(W/d^{n+2}k_\phi = 5.312 \times 10^3)$
at various aspect ratios
- 29 Plot of (R/W) vs. % slip for $(W/d^{n+2}k_\phi = 7.968 \times 10^3)$
at various aspect ratios
- 30 Plot of (R/W) vs. % slip for $(W/d^{n+2}k_\phi = 13.28 \times 10^3)$
at various aspect ratios
- 31 Plot of (T/Wd) vs. % slip for $(W/d^{n+2}k_\phi = 1.328 \times 10^3)$
at various aspect ratios
- 32 Plot of (T/Wd) vs. % slip for $(W/d^{n+2}k_\phi = 2.656 \times 10^3)$
at various aspect ratios
- 33 Plot of (T/Wd) vs. % slip for $(W/d^{n+2}k_\phi = 5.312 \times 10^3)$
at various aspect ratios
- 34 Plot of (T/Wd) vs. % slip for $(W/d^{n+2}k_\phi = 7.968 \times 10^3)$
at various aspect ratios
- 35 Plot of (T/Wd) vs. % slip for $(W/d^{n+2}k_\phi = 13.28 \times 10^3)$
at various aspect ratios
- 36 Plot of (z/d) vs. % slip for $(W/d^{n+2}k_\phi = 1.328 \times 10^3)$
at various aspect ratios

LIST OF FIGURES, Cont'd

Figure No.

- 37 Plot of (z/d) vs. % slip for $(W/d^{n+2}k_\phi = 2.656 \times 10^3)$
at various aspect ratios
- 38 Plot of (z/d) vs. % slip for $(W/d^{n+2}k_\phi = 5.312 \times 10^3)$
at various aspect ratios
- 39 Plot of (z/d) vs. % slip for $(W/d^{n+2}k_\phi = 7.968 \times 10^3)$
at various aspect ratios.
- 40 Plot of (z/d) vs % slip for $(W/d^{n+2}k_\phi = 13.28 \times 10^3)$
at various aspect ratios
- 41 Plot of (DP/w) vs. $(w/d^{n+2}k_\phi)10^3$ at +25% slip
and various aspect ratios
- 42 Plot of DP vs. $(w/d^{n+2}k_\phi)10^3$ at +25% slip
and various aspect ratios
- 43 Composition of the 3- component substance
(water, clay, glycol) in equilibrium with
humid air at 75°F, 1 atmos. pressure
- 44 Pressure and sinkage relationship of sand
with stirring
- 45 Pressure and sinkage relationship of non-
magnetic barium ferrite with stirring
- 46 Pressure vs. sinkage of a flat plate in sand.
- 47 Pressure on sinkage plot for various depths
of sand layers.
- 48 Pressure vs. sinkage plots for various plates
in glass beads
- 49 Pressure or sinkage plots for various plates
in magnetic barium ferrite.

LIST OF FIGURES, Cont'd.

Figure No.

- | | |
|----|---|
| 50 | Effect of speed of penetration in sand. |
| 51 | Averaged values of actual test points. |
| 52 | k_c vs. degree of magnetization |
| 53 | Typical lead-sinkage curves |

BACKGROUND

Bekker's system approaches the problem of wheels in soils by assuming that there exists an analogy between the vertical penetration test and the wheel-soil interaction. Accordingly, an important factor in the validity of the Bekker system is whether the analogy is adequate. As it stands, this question can not be positively answered in a general sense, but experience has shown that the system is applicable under a wide range of conditions.

About a decade ago Nuttall conducted an investigation of wheel performance by testing scale models in the laboratory⁽²⁾. This work is also incorporated in Bekker's book "Theory of Land Locomotion", in Chapter XI, where the author discusses the application of dimensionless analysis techniques in Land Locomotion problems. In Nuttall's investigation, two of the sinkage parameters proposed by Bernstein were redefined in terms of soil properties introduced by Coulomb.

Good correlations were obtained over a limited range of test conditions, but even so there are several objections to be made to this work. For example, no rational argument is given for discarding some of the sinkage parameters. Furthermore, it is nearly certain that cohesion and friction are inadequate to describe the unconsolidated soils on which vehicles frequently operate.

McGowan and Nuttall presented a paper entitled "Scale Models of Vehicles in Soils and Snow" at the First International Conference on the Mechanics of Soil-Vehicle Systems, in Turin (Italy) in 1961⁽³⁾. The results shown and the functional relationships derived are valid for snow and sand where Bekker's sinkage exponent $n = 1$. It will be seen that Nuttall's relationship is basically a special case of that presented in this report. McGowan and Nuttall suggested the following relationships:

$$z = d f_1 \left(\frac{W}{c_s d^2}, \phi, S, h/d \right)$$

$$D = W f_2 \left(\frac{W}{c_s d^2}, \phi, S, h/d \right)$$

here, d is the wheel diameter; W is the load; ϕ is the angle of internal friction; S is the slip; h is the total depth of the soil layer of interest; z is the sinkage and D is the drawbar pull. The value of c_s is derived from a penetration test.

I. THEORY

Rational analysis indicates⁽⁴⁾ that there is an intimate correlation between wheel sinkage and drag. Thus, it is reasonable to assume that they are both functions of the same independent variables. Among these variables are those termed the sinkage parameters (k_c , k_ϕ and n) advocated by Bekker, which are obtained from the stress-strain relationship recorded when forcing a flat plate into the soil. Thus, the following variables are considered influential in describing the wheel-soil system.

a. Dependent variables:

R Horizontal component of the total force
on the wheel (lb)

z Wheel sinkage (in.)

T Wheel torque (in.lb)

b. Independent variables:

d Wheel diameter (in.)

λ Wheel aspect ratio (non-dimensional)

μ Coefficient of friction - soil to wheel
(non-dimensional)

D Soil bed depth (in.)

W Load (lb.)

i Wheel slip (non-dimensional)

k_ϕ Sinkage modulus, (lb/in.ⁿ⁺²)

k_c Sinkage modulus (lb/in.ⁿ⁺¹)

n Sinkage exponent (non-dimensional)

The dependent variables R , z and T are unknown functions of the independent variables listed previously. These may be expressed functionally as:

$$R = f_1 (d, \alpha, \mu, D, W, i, k_\phi, k_c, n) \quad (2a)$$

$$z = f_2 (d, \alpha, \mu, D, W, i, k_\phi, k_c, n) \quad (2b)$$

$$T = f_3 (d, \alpha, \mu, D, W, i, k_\phi, k_c, n) \quad (2c)$$

Each of the unknown functional relationships involves ten variables. An analysis of the dimensionless matrix of these variables, using the M, L, T system of units reveals that the rank of the matrix is to be of order two. As a consequence of Langhaar's rule (5) the number of master variables which can be formed for each equation is $10-2 = 8$.

The dimensionless master variables are found by a method attributed to Lord Rayleigh. Equation (2a) can be written as:

$$\frac{R}{W} = (W)^{a_1} \dots (D)^{a_2} \cdot (d)^{a_3} \cdot (i)^{a_4} \cdot (\mu)^{a_5} \cdot (n)^{a_6} \cdot (k_\phi)^{a_7} \cdot (k_c)^{a_8} \cdot (\alpha)^{a_9} \quad (3)$$

In this expression the exponents are arbitrary constants. In dimensional form Eq. (3) becomes:

$$0 = (MLT^{-2})^{a_1} \cdot (L)^{a_2} \cdot (L)^{a_3} \cdot (ML^{-(n+1)}) \cdot (T^{-2})^{a_7} \cdot (ML^{-n} T^{-2})^{a_8} \quad (4)$$

Equating the exponents of M, L, T, produces:

$$a_1 + a_7 + a_8 = 0$$

$$a_1 + a_2 + a_3 - (n+1)a_7 - n a_8 = 0$$

Thus:

$$a_3 = - (n+2)a_1 - a_2 - a_8$$

$$a_7 = - a_1 - a_8$$

Equation (3) may be rewritten as:

$$\frac{R}{W} = (W)^{a_1} (D)^{a_2} (d)^{-(n+2)a_1 - a_2 - a_3} \cdot (1)^{a_4} \cdot (\mu)^{a_5} \cdot (n)^{a_6} \\ \cdot (k_\phi)^{-a_1 - a_8} \cdot (k_c)^{a_8} (\alpha)^{a_9}$$

or

$$\frac{R}{W} = \left(\frac{W}{d^{n+2} \cdot k_\phi} \right)^{a_1} \cdot \left(\frac{D}{d} \right)^{a_2} \cdot (1)^{a_4} (\mu)^{a_5} (n)^{a_6} \cdot \left(\frac{k_c}{dk_\phi} \right)^{a_8} (\alpha)^{a_9} \quad (5)$$

Similarly from equations (2b) and 2c) one may derive two more relationships, so that:

$$\frac{R}{W} = f_1 \left\{ \left(\frac{W}{d^{n+2} k_\phi} \right), \left(\frac{k_c}{dk_\phi} \right), \left(\frac{D}{d} \right), (\alpha), (\mu), (n), (1) \right\} \quad (6a)$$

$$\frac{T}{W_d} = f_2 \left\{ \left(\frac{W}{d^{n+2} k_\phi} \right), \left(\frac{k_c}{dk_\phi} \right), \left(\frac{D}{d} \right), (\alpha), (\mu), (n), (1) \right\} \quad (6b)$$

$$\frac{W}{d} = \left\{ \left(\frac{W}{d^{n+2}k_c} \right) \cdot \left(\frac{k_c}{dk_c} \right) \cdot \left(\frac{D}{d} \right) \cdot (\alpha) \cdot (\mu) \cdot (n) \cdot (i) \right\} \dots (6c)$$

Let us distinguish between a scale model and a full-size prototype by using indices "m" and "p" respectively. Then complete similitude requires that the following conditions be met:

$$\left(\frac{W}{d^{n+2}k_c} \right)_p = \left(\frac{W}{d^{n+2}k_c} \right)_m \dots \dots \dots (7a)$$

$$\left(\frac{k_c}{dk_c} \right)_p = \left(\frac{k_c}{dk_c} \right)_m \dots \dots \dots (7b)$$

$$\left(\frac{D}{d} \right)_p = \left(\frac{D}{d} \right)_m \dots \dots \dots (7c)$$

$$(\alpha)_p = (\alpha)_m \dots \dots \dots (7d)$$

$$(\mu)_p = (\mu)_m \dots \dots \dots (7e)$$

$$(n)_p = (n)_m \dots \dots \dots (7f)$$

$$(i)_p = (i)_m \dots \dots \dots (7g)$$

A simplification of these conditions occurs if the same soil is used in both the prototype and the model testing. For sand, k_c is frequently zero. As a consequence, the

conditions necessary for similitude under these circumstances reduce to:

$$\left(\frac{W}{d^{n+2} k_\phi} \right)_p = \left(\frac{W}{d^{n+2} k_\phi} \right)_m \dots \dots \dots (8a)$$

$$\left(\frac{D}{d} \right)_p = \left(\frac{D}{d} \right)_m \dots \dots \dots (8b)$$

$$(\alpha)_m = (\alpha)_p \dots \dots \dots (8c)$$

$$(i)_m = (i)_p \dots \dots \dots (8d)$$

For towed wheels the slip is not considered to be an influential factor, hence, the last term in equation (6a) may be omitted and equation (8d) is of no importance here. Hence, towed wheels were investigated in sand ($k_c = 0$) by considering equations 8a, 8b, and 8c only.

To extend the studies to soils possessing values for both k_c and k_ϕ it follows equations (7a) and (7b) that means must be found to vary independently k_c , k_ϕ and n if at all possible. The experiments to be described represent an attempt to produce stable soils accompanied with at least a moderate independent variation in both k_c and k_ϕ and their ratio of the materials, using the Bekker Sinkage Parameters.

II. EXPERIMENTS

1. DRIVEN WHEELS IN SAND:

An experimental investigation was conducted to verify the validity of the foregoing similitude parameters for powered rigid wheels in sand. The investigation utilized rigid smooth-aluminum wheels of rectangular cross-section operating in dry beach sand. Tests were conducted using a 12.5 inch diameter wheel and an 8.56 inch diameter wheel, both of which had an aspect ratio of 0.52.

Tests were also conducted to explore the effect of aspect ratio on the dependent variables R , T , and z for the larger 12.5 inch diameter wheel. For the selected wheel diameter d , the sand bed depth D , aspect ratio α , and wheel load W were varied in accordance with the requirements of similitude as expressed by Eqs. (8a-d). The particular values selected and their range are summarized in the chart below. The dependent variables, R , T , and z were measured for each individual test.

TABLE I.

INDEPENDENT VARIABLES USED FOR POWERED WHEEL TESTS

<u>Wheel Diameter (in.)</u>	<u>Aspect Ratio</u>	<u>Wheel Load (lb.)</u>	<u>Bed Depth (in.)</u>
12.50	0.27		
12.50	0.52	10, 20, 40 60 & 100	8.0
12.50	0.84		
8.56	0.52	3.25, 6.50, 13.0 20 & 33	5.5

The beach sand used during the tests had an average set of properties characterized by $k_c = 0$, $k_\phi = 3.4$ and $n = 1.05$. The wheel slip was independently varied from $i = -100\%$ to $i = +100\%$. In this program the slip is computed as:

$$i = \frac{v_w - v_c}{v_c}$$

where v_w = Tangential velocity of surface of wheel

and v_c = Linear horizontal velocity of wheel

Figure 1 shows the assigned directions for positive torque and net horizontal force exerted by the sand on the wheel. It also shows the positive directions of linear and angular velocities.

APPARATUS:

The equipment employed in the research is described in detail in Ref. 12, with the exception that, for the tests under discussion, the wheel was driven by an electric motor,

trunnion-mounted for torque reaction measurements to record both torque and power inputs when necessary.

The wheel-carrying assembly had been modified somewhat to accommodate the components required for driving the wheel. The drive motor, speed reducer, and the power source (batteries) were all mounted on the test carriage. A detail view of the wheel-carrying assembly is shown in Fig. 1-a, where it is seen that the wheel is now mounted on a counter-balanced beam which can be loaded by the addition of weights over the wheel axle. The beam is kept horizontal by the vertical adjustment of the complete carriage, described in a previous report (12).

2. TOWED WHEELS:

In accordance with the preceding theory, Equation 8, low-speed drag and sinkage tests were conducted on two geometrically similar, solid, aluminum wheels of rectangular cross-section, the diameters of the wheels being 6.625 in. and 12.50 in. The aspect ratios of the wheels tested were 0.27, 0.52 and 0.84. The soil used was a sand for which $k_p = 3.40$, and $n = 1.05$ are most probable values. The tests with variable aspect ratio were conducted in deep beds of soil corresponding to semi-infinite conditions, while the tests conducted in various depths of soil were made at the single aspect ratio $\lambda = 0.27$. All

tests were conducted at the relatively low speed of 0.25 ft/sec. This speed was used because experimental difficulties are minimized at low speed, and it was justified by the results of other tests which showed the effect of speed to be negligible below a speed of 5.0 ft/sec. with a 12.5 inch diameter wheel.

It should be noted that unexpected experimental difficulties are encountered in work of this type. The principal difficulty is the preparation of the soil to a uniform and repeatable consistency. This problem has never completely been solved and consequently the data presented here represents the mean of many test runs, in some cases numbering twelve. Another problem is associated with the large span of forces to be measured, covering a range of approximately a hundred to one. This demands considerable precision and ruggedness in the test apparatus, qualities that are somewhat mutually exclusive.

The test results are given in Figs. 2 thru 5. In Figs. 3 and 5, the sinkage and drag coefficients are given vs. the load coefficient with the depth ratio as a parameter. In Figs. 2 and 4, the sinkage and drag coefficients are given vs. the load coefficient with the aspect ratio as a parameter.

A general view of the tow tank is shown in Fig. 6, and a detailed view of the wheel carriage is shown in Fig. 7.

3. CONTROL OF PROPERTIES OF SOILS:

To obtain soil properties with a high degree of precision, and thus obtain closely reproducible test results, a special penetrometer was developed at this laboratory. This equipment removed much of the scatter and many of the discontinuities of previous beavimeters employed. The equipment consists of a hydraulically-operated plunger to which the penetrating foot is attached, held in place by a sensitive ring gauge to which strain gauges are attached to record the load on the foot. Displacement of the foot is recorded by a linear potentiometer driven by the plunger movement. This equipment is similar to many others employed for the purpose in question. The differences are (1) the size, and thus the sensitivity of the ring; and (2) the supply of fluid to the plunger is via a constant-flow control valve, permitting accurate control of the plunger velocity regardless of the loads applied. (This appears to be responsible for the absence of steps in the curves). The pressure-sinkage data are plotted directly on Autograf X-Y recorder.

Fig. 8, is a diagram of the system. The electrical circuit is shown in Fig. 9. The footings employed for the plunger are shown in Fig. 10. The size of the box containing the soil was considered large enough to render the boundary effects of bottom and sides negligible. The soil thus was

considered homogeneous with semi-infinite boundary conditions.

Figures 44 and 45, show the type of data recorded for sand and barium ferrite, respectively. The material was well-stirred between runs. Several runs are shown superimposed on one another, indicating the degree of reproducibility particularly when allowance is made for the difficulty of accurately determining the position of zero sinkage for the start of the graph.

III. RESULTS AND DISCUSSION

1. DRIVEN WHEELS:

Dimensional equations express a certain unknown functional relationship between the measured (dependent) master variables and a number of fixed (independent) master variables. If the functional relationship between all of the master variables were specifically known, the solution would be unique when all pertinent variables of the system were included in the analysis. Experimental studies with scale models enable a direct verification of a set of dimensional equations describing a particular physical problem. Verification is accomplished by conducting two or more different tests with scale models under conditions where values of independent master variables remain unaltered. Under these test conditions the measured values of all the dependent master variables should be the same for the range of test conditions.

The dimensionless parameters obtained from the experimental measurements made on powered rigid wheels operating in sand are shown in Fig. 5 and Figs. 11 thru 25. These figures present the values of the measured master variables R/W (Figs. 11-15), T/Wd (Figs. 16-20), and z/d (Figs. 21-25), for two different test conditions which satisfy the similarity requirements of Eqs. (8a-d). These figures all display

a marked degree of similitude, thus attesting to the validity of the selected dimensional parameters for powered rigid wheels in frictional soils. Figures 11 and 12 at low load coefficients show some scatter in the observations, but here the equipment was operating with forces so small that the sensitivity of the measuring devices was just approached.

Figures 26 thru 40 indicate the effect of varying aspect ratio, \mathcal{L} , on the various dependent master variables. The occurrence of negative values of the motion resistance R , indicate the development of a net tractive effort by the wheel. The net tractive effort of a wheel is often characterized by a quantity known as drawbar-pull. Drawbar-pull is defined as the difference between the gross traction force produced by the shearing strength of the soil and the motion resistance of the wheel.

Drawbar-pull (DP) and the dimensionless ratio DP/W for a slip of +25% are shown as a function of load coefficient in Figs. 40 and 41. These figures are typical of the results obtained and the tests displayed the following characteristics:

(1) DP/W decreased with increasing load W for all values of \mathcal{L} .

(2) DP/W increased with increasing \mathcal{L} for the same load.

(3) DP/W increased with increasing positive slip up to about 25%. Above this value it remained essentially constant.

(4) DP increased with increasing loads initially and then began to decrease, ultimately reaching a negative value.

(5) DP/W and DP were positive for a narrow range of load coefficient, especially for low aspect ratios.

(6) Aspect ratio had a pronounced effect on R/W and Z/d, and an almost negligible effect on T/Wd.

(7) T/Wd approached a constant value of 0.24 for large positive slip, irrespective of wheel diameter and aspect ratio, for all load coefficients.

In frictional soils the gross traction developed varied directly with load and was independent of the area of contact of wheel to soil. From the results presented in Figs. 26 through 32, it is seen that motion resistance decreases with increasing α for the same load and wheel diameter.

2. TOWED WHEELS:

The plotted data, Figs. 2 through 5, make it apparent that a high degree of similitude was attained in the tests, and that the independent variables selected were appropriate to the system. Accordingly, the results should be applicable to wheels of any scale as long as the assumed parameters are maintained. It is consequently important to consider carefully what this condition requires.

The sinkage parameters used were those obtained with a single (1 by 3 in.) Bevameter plate, penetrating a semi-infinite bed of homogeneous soil. This means that the

parameters obtained depend only on the inherent mechanical properties of the soil and on the shape and size of the bevameter plate. If a different soil is placed under the bevameter plate, changes in the sinkage parameters will result which can be due only to changes in the mechanical properties of the soil.

Consistent with this framework of ideas, there exists a particular wheel having some diameter and aspect ratio, whose sinkage characteristics are similar to those of the bevameter plate used. In other words, an analogy exists, and because of this any variations in the basic mechanical properties of the soil will not only produce changes in the sinkage parameters as measured by the bevameter, but also cause a change in the sinkage of the wheel. Consequently the sinkage of the analogous wheel is uniquely related to the measured sinkage parameters.

If a fixed quality soil and variable geometry wheel are considered instead of the converse above, then variations in the size and shape of the wheel produce sinkages that are related to the sinkage of the analogous wheel and hence to the sinkage parameters through these geometrical variations alone. The preceding reasoning is now repeated, but the soil is considered to be of finite depth and the first effect to be observed is that a new set of sinkage parameters is obtained related to the original set by some factor that

describes the relative "infiniteness" of the boundaries. The ratio of the characteristic dimension "b" of the beva-meter plate to the soil depth "D" or specifically the b/D ratio is a factor that satisfies this requirement. It is further evident that the analogous wheel will describe a new sinkage that is uniquely related to the new sinkage parameters, and also to the original sinkage parameters through the b/D ratio. Similarly, new relationships describing the effects on sinkage of changes in wheel geometry and soil quality will be obtained that are related to the original relationships through the b/D ratio. Finally, since there exists an analogous wheel of characteristic dimension "d", all effects of changes in soil depth may be related to the ratio d/D instead of the ratio b/D . It is thus possible to construct a self-consistent system based on analogy, which preserves the idea of sinkage parameters that are determined by soil properties only and which accounts for variations in wheel geometry and soil depth. In this system, it is obviously necessary to take account of the d/D ratio in the correlation of test results, as this is the source of a scale effect that enters the system. Failure to do this can lead to difficulties in obtaining correlations. This was observed by Czako and Bekker⁽⁷⁾ in an attempt to obtain sinkage parameters from the analysis of tests on wheels. Wheels of

a range of diameters were tested in a bed of soil of fixed depth, and only one of these wheels having a particular diameter gave sinkage parameters comparable to those obtained with the Bevameter. Apparently the analogy of wheel, soil, and bed depth to Bevameter, soil and bed depth was an optimum for this particular wheel. This observation is a manifestation of the scale effect and this difficulty has been entirely overcome in the present tests by observing the depth ratio (d/D).

An infinite variety of conditions exists with natural soils in the field, but since the most frequently occurring condition is that of an approximately homogeneous soil overlying a hard pan at some depth, the results given here should be applicable to natural soils in the field.

It was noted earlier that prior theory and experiment had produced working formulas for wheel drag that were accurate over limited ranges of conditions. One of these equations, due to Bernstein (6), can be expressed in the form

$$R/W = 0.86 (W/\rho k d^3)^{0.33}$$

and another, due to Nuttall (2), and applicable to sand, can be expressed as

$$R/W = 0.50 (W/\rho^{0.3} g p d^3)^{0.4}$$

Both of these equations, especially Nuttall's, predict drag coefficients that are in reasonable agreement with selected

areas of the data presented here, but neither of them closely follow the trend of aspect ratio. A better understanding of the source of this divergence can be obtained by writing these equations for a wheel of variable width which carries a constant load "c" per unit of width. For these conditions, the formulas reduce to

$$R/W = 0.86(c/k d^2)^{0.33}$$

and

$$R/W = 0.50(c/g p d^2)^{0.4} \mathcal{L}^{0.2}$$

In the first case it is seen that the aspect ratio drops out entirely, implying that shape has no effect on the drag coefficient and that end effects are negligible. In the second case, it is apparent that

$$R/W \rightarrow \infty$$

$$\mathcal{L} \rightarrow \infty$$

and

$$R/W \rightarrow 0$$

$$\mathcal{L} \rightarrow 0$$

Physical reasoning contradicts these mathematical conclusions; their experimental verification is not possible.

One of the more interesting features of the drag data is the way the drag coefficient decreased with large loads in shallow soils.

The effect, due to variation of aspect ratio also has some interesting features. The increase of the drag and

sinkage coefficients of the low-aspect-ratio wheels is apparent. Considerations in logic indicate that the drag coefficient may become infinite for zero-aspect-ratio wheels but approaches a limiting finite value for infinite-aspect-ratio wheels.

3. CONTROL OF PROPERTIES OF SOILS:

Various possible laboratory soils composed of clay, sand, and glycol are described in Ref. 8. Other possible soil ingredients also proposed but not used in that previous work were employed in the research described in this report.

The ideal soil mass, as defined in Ref. 8, should have the following characteristics:

- a. Stability of the solid state regardless of time, oxidation, or other chemical interaction.
- b. Controllability of soil values and parameters.
- c. Reproducibility of the mass in any quantity using standard or easily obtained materials.

The materials employed at the Land Locomotion Laboratory satisfy these requirements to a high degree, but the glycol is also hygroscopic, and thus will pick up moisture from the atmosphere. The properties of the soil can change somewhat

with time, particularly those mixtures representing viscous muds where high glycol contents are employed. Figure 43 shows the three-phase diagram of clay, glycol and water, plainly indicating the wide range of soil properties that could be expected from any one blended combination of clay and glycol, given sufficient time and atmospheric humidity. Fortunately, with proper organization the test data can be secured before such time elapse occurs.

The importance of moisture content in a given soil (an average sandy farm soil of Wayne County, Michigan) can be seen from Table I:

TABLE II.
EFFECT OF MOISTURE CONTENT ON SOIL PROPERTIES

Moisture, %	Soil Properties				
	ϕ , deg	c	k_{ϕ}	k_c	n
19	36	0.60	9.00	20.00	0.16
20	38	0.53	7.00	16.00	0.17
22	36	0.25	2.20	2.50	0.18

It follows that stable soils under all conditions of time, temperature, and humidity are necessary, or else the magnitudes of the soil parameters must be determined at each testing.

The research on the value of the soil parameters, covered by this report, can be considered an investigation

of the manner in which the individual parameters k_c , k_p , etc., can be controlled and varied by other means than the variation of moisture content or glycol constituent. Variations are introduced by controlling the shape of soil particle, the size of particle, or its cohesive force as measured by its degree of magnetization, i.e., the effect of artificial materials on the control of soil parameters is examined as set out below.

a. MAGNETIC SOILS:

As already pointed out, it is very desirable to be able to vary k_c without material change of k_p , if the relationship given by Eq. (7b) is to be satisfied for complete fulfillment of the model rules. At least the ratio of k_c and k_p must be variable over a wide range, even if individual variation proves impossible.

In considering this problem, it occurred to us that a material capable of being magnetized might present a variable k_c with little change in k_p ; in other words varying magnetic attraction between the particles might represent a soil with variable cohesion. To this end, a supply of barium ferrite was obtained from the D. M. Steward Manufacturing Company of Chattanooga, Tennessee, which gave the properties, listed in Table II, of the material when magnetized.

TABLE III.

TYPICAL PROPERTIES OF BARIUM FERRITE

Residual Induction, B_r (Gauss)	2190
Coercive Force, H_c (Oersteds)	1850
Intrinsic Coercive Force, H_c (Oersteds)	3450
Maximum Energy Product, $B_d H_d$	1.03×10^6
Permeance Coefficient, B_m/H_m at $B_d H_d$ max.	1.160
Temperature Coefficient of Residual Induction	0.18%/°C
Coefficient of Linear Thermal Expansion	$10 \times 10^{-6}/^\circ\text{C}$
Curie Temperature (°C)	450
Apparent Density	4.70 gr/cm ³
Electrical Resistivity (ohm/cm at 25°C)	10×10^6

Samples of this material in the nonmagnetized state show very little cohesion. At the same time, the angle of repose (ϕ) is extremely small; a sample spreads out over a wide area and has little depth even in the center. When magnetized, it has considerable magnetic attraction which appears to have the same effect on a mass as cohesion. At the same time, such a mass will form into a distinct cone-like mound having a definite angle of repose compared to the nonmagnetic variety, which might indicate a change in k_ϕ also. It follows that variation of the degree of magnetization may produce a reasonably wide variation of k_c , k_ϕ , and n . An additional advantage is relative economy, as compared with glycol.

NOTE: The relative economy could be formed in iron ore which has similar properties, but not in barium ferrite which is fairly expensive. The barium ferrite was used because it was readily obtainable in the desired powdered form.

b. GLASS BEADS:

One other material considered for the control of soil properties was spherical glass beads, with an average diameter of 0.010 to 0.015 in. Thus in particle size the beads are approximately in the same range as the sand particles in use; but by themselves they have no value of ϕ , the angle of repose, since, being almost perfect spheres, they will roll out to a single layer, provided they are dry and not mixed with oil or other viscous or cohesive binder. But if they are mixed with the sand employed in the routine tests, the frictional characteristics of the soil may change sufficiently to be of practical importance. The inclusion in plastic soils with or without the sand of Ref. 10 could also contribute to a possible increased range of k_c , k_ϕ , etc.

To study these effects, Bevameter⁽¹¹⁾ tests were run with a series of both circular and rectangular plates, with the object of obtaining the range of soil properties that could be produced by the use of the materials being considered.

c. RESULTS:

The results obtained from the apparatus (Fig. 8) are typified by the curves of Figs. 44 and 45, which show that the reproducibility of the results is good.

Such force-sinkage curves were then averaged and the results were plotted on log-log paper as shown in Fig. 46.

For Eq. (1) to represent the recorded results exactly, the points of Fig. 46 should lie on a straight line. A typical line has been drawn in; although it is not strictly through all the points, a close approximation to the straight line is seen over a portion of the graph, particularly if:

(1) The first one or two points plotted from such figures as Figs. 44 and 45, are neglected where the sinkage is small, say < 0.5 in.;

(2) The last few points at high load are also disregarded, where the sinkage is $> 4-5$ in.

These points can be neglected to a first approximation for the following reasons. (a) It is very difficult to determine the exact point at which the bevameter foot first touches the soil and the point at which pressure is exerted by it on the sand, since the top layer appears to be compressed to some extent and, in some cases, voids are taken up with practically no sinkage. Thus the zero setting of pressure and sinkage has some error; since the first point plotted on curves of the type shown in Fig. 46 has been for $z = 0.25$ in., an error of 0.05, which is easily possible in the zero setting, would change the picture a great deal.

(b) Secondly, it seemed that the upturn at the upper end of the diagram could be due to boundary effects from the bottom of the containing vessel. This was checked by running beva-meter tests with soils of varying thickness relative to the

size of the penetrometer. The results are shown in Fig. 47: four depths of a given sand were employed and the p - z relationships were obtained. The graphs show a high degree of agreement, except at the readings for $z = 0.25$ and for $z > 4\frac{1}{2}$ in. approximately. The upper part of the curves show that, for a 6 in. depth of soil and a $2\frac{1}{2}$ in. diameter foot, or $r = 1\frac{1}{4}$ in., departure from the approximate straight line occurs at about $z = 3\frac{1}{2}$ in. or $a(r/Z-D) = 0.5$ approximately, where D = depth of soil above the hard surface to the penetrating plate at its point of departure from the straight line. For the 9 in. depth, departure occurs at $z = 4\frac{1}{2}$ in., or, $r/Z-D = 0.28$; for both the 12 and $14\frac{1}{2}$ in. depths of soils, departure from the straight line occurs at about 5 in., or, $r/Z-D = 0.3$ and 0.18 . It is concluded that for a $2\frac{1}{2}$ in. -diameter footing, the soil should be at least 12 in. deep. Basing the relationship on the radius of the foot, the required depth of soil below the foot at the maximum penetration should be about five times the dimension "b" of Equation (1) if depth effect is to be avoided. Since only one size of foot was employed for Fig. 47, the values of k_c and k_p cannot be determined. However, for the sand in question, we can write

$$p = 3.5 z^{0.95}$$

which agrees well with other experiments with similar materials.

As a result of the above tests, the analytical relationships between p , z , and n which follow were all determined by neglecting the value of z for sinkages < 0.5 and > 4 in. and using a total soil depth of at least 12 in.

With the above limitations, tests with the following materials were carried out:

- a. Sand
- b. Nonmagnetic barium ferrite
- c. Magnetic barium ferrite
- d. Glass bead of from 0.010 to 0.015 in. in diameter (approximately)
- e. A mixture of 25% glass beads and 75% sand
- f. A mixture of 50% glass beads and 50% sand
- g. A mixture of 75% glass beads and 25% sand

All the above materials were dry. It follows that the cohesive force would be expected to be quite small and $k_c = 0,0$. Tests were made with three sizes of both circular and rectangular footings; theoretically, since k_c is zero or at least quite small, all the p - z curves should almost superimpose on one another and cross the line of $z = 1$ in. almost at one point. The results substantiate this. Typical plots for some of the materials are shown in Figs. 48 and 49, the former is for the circular plates and the latter for rectangular ones. The soil parameters obtained from all the graphs are as shown in Table III. Substantial agreement existed between the two types of footings. When more than one such set of curves were averaged (as was generally the case), the results tended to be closer than those given here.

In Fig. 51, the actual test points are plotted to show the rather tight grouping of most of the points at their averaged values, plus a few scattered results which in almost all cases still do not change the sign of the coefficients. The values given in Table III result from averaging several runs using the straight-line log-log relationship $p = (k_c/b + k_p)z^n$ in the conventional manner. Employing the appropriate values from Table III in this formula and calculating the pressure and sinkage values, the calculated points correlate well with the mean plotted values. It is concluded that no major error in k_c and k_p exists by employing the average of a number of runs with small, medium, and large plates, at least for z between 0.7 and 4.5 inches.

Table IV, indicates that for the range of materials examined, change in the value of "n" for all these dry, large particle materials is negligible. But for the fine powdery barium ferrite this parameter has been reduced to $n = 0.68$, which, when magnetized, is re-established at 1.0, as for the other materials.

VALUES OF k_c :

The object of the tests was to produce an independent variation in the magnitude of k_c . The average data indicate a possible variation of its magnitude from -0.7 to +0.93 for circular plates and -0.53 to +1.21 for rectangular ones.

The variation produced in k_c is small as is to be expected since all the materials, with the exception of the barium ferrite, were granular, with little if any cohesion. A cohesive coefficient of 0.9 to 1.2 was recorded with the magnetic barium ferrite.

In general, it was observed of all the test results that there was less variation between tests for rectangular plates than for circular ones.

VALUES OF k_ϕ :

The corresponding variation of k_ϕ is from 0.37 to 3.95 for circular plates and from 0.69 to 3.7 for rectangular ones. Here a significant change of values has been achieved. Taking the sand and bead combinations only, where for sand $k_\phi = 3.1$ to 3.7 and for beads $k_\phi = 1.96$, a variation of about 1.8:1 is seen, a range of considerable interest as far as similitude study is concerned. If the ferrite is included, a range from 0.5 to 3.5 or 7:1 is possible.

VALUE OF n :

Table III shows that the value of " n " in Eq. (1) changes from 0.65 to 1.06. If the nonmagnetic barium ferrite is neglected, the range is from 0.9 to 1.06. In other words, " n " for the materials so far tested is approximately constant at $n = 1$.

The effect of the speed with which the footing penetrated the soil was examined for any change of magnitude of n , k_c and k_p that might have resulted. This effect is recorded in Fig. 11. Table IV gives the maximum and minimum relations as calculated.

Since the speed-effect curves for rectangular and circular feet are all recorded with but one size of plate, the individual values of k_c and k_p cannot be determined in this case. But it is safe to assume $k_c = 0.0$, since this has been determined for this material by the Land Locomotion Laboratory.

TABLE IV..

**SOIL PARAMETERS FOR INDICATED MATERIALS,
OBTAINED WITH CIRCULAR AND RECTANGULAR FOOTINGS**

Material	n		k _c		k _s	
	Circular	Rect.	Circular	Rect.	Circular	Rect.
Dry Sand	0.95	0.95-1.0	-0.60	-0.64	3.1	3.3-3.7
100% Glass Beads	0.9-0.91	0.91-1.06	+0.175	+ .182	1.96	1.96
25% Glass Beads and 75% Sand	0.9	0.95	-0.7	-0.53	3.95	3.68
50% Glass Beads and 50% Sand	1.0	1.0	-0.36	-0.48	2.97	3.01
75% Glass Beads and 25% Sand	1.06	1.06	-0.703	-0.461	2.79	2.43
Nonmagnetic Barium Ferrite	0.68	0.65	0.93	1.21	0.37	0.69
Magnetic Barium Ferrite	1.0	1.00	0.34	0.43	1.22	1.05

TABLE V.

**CALCULATED MAXIMUM AND MINIMUM RELATIONS
OF INDICATED PARAMETERS**

Speed, fpm	Circular Footing, 2 in. Diam.	
	n	k _s
5.0	0.95	2.9
6.5	0.95	3.0

It may be an advantage to list the similitude relationships in a slightly different form. If W , D , d , and α are considered the independent variables and z and R the dependent ones, where

- W = Load on wheel, lb.
- D = Depth of soil above hardpan, in.
- d = diameter of wheel, in.
- α = aspect ratio of wheel
- z = Depth of sinkage, in.
- R = Drag of wheel, lb.

then for similitude the following conditions must be met:

$$\frac{k_{\phi}}{k_c} d = \text{Constant} \quad (9)$$

$$\frac{W}{k_{\phi} d^{n+2}} = \text{Constant} \quad (10)$$

$$\frac{D}{d} = \text{Constant} \quad (11)$$

When $k_c = 0$, Eq. (9) disappears and thus, for sand where $k_c = 0$, model work is a possibility by the use of Eqs. (10 and 11). It follows that the main importance of the present test program arises as soon as k_c has some magnitude. Then to provide a sufficient band of model tests to cover all practicable wheels, as d is varied the ratio k_{ϕ}/k_c must also vary if true similitude is desired for all cases.

The work to date has shown that there are some possible ways in which the cohesive and deformation moduli of the Bekker soil-value system can be varied independently, at least over a moderate range of values. The important feature is the ratio of the two [see Eq. (9)]. Figure 52 shows the range of k_c and k_ϕ , together with values of their ratio for the magnetic soil (the degree of magnetization is unknown). For the sand and glass bead combination, the value of k_c is so close to zero, actually varying from positive to negative values, that it is believed that the ratio of the parameters loses some of its significance. But the variation of k_ϕ is a reasonable amount and could have a significant effect in extending the range of similitude testing for full scale and models, particularly when the limitation arising from Eq. (9) is taken into account for a given soil bin with a fixed value of D , the soil depth.

If the curve of Fig. 51 for k_c is taken as drawn, then the ratio k_ϕ/k_c varies from -4.4 for pure sand to +9.7 for glass beads. The major change occurs as the composition approaches 100% glass beads.

Typical load-sinkage curves with various sizes of rectangular plates are shown in Figs. 53a, 53b, and 53c. The initial portion of the record consists of an almost vertical rise in load with a negligible deformation. Examining the initial part of the curves on the basis of the pressure per

unit are under the plate, one obtains the data of Table V. An approximately constant stress under the various plates is seen.

TABLE VI. LOAD SINKAGE DATA
FOR: 75% GLASS BEADS, 25% SAND

Plate and Area sq. in.	Load, lb.	Penetration, Z, in.	Stress, psi
2-1/4" x 3/4" 1.687 sq in.	1.2	Too small to read	0.71
2-1/2" diam. 1.767 sq in.	1.5	Too small to read	0.85
3" x 1" 3 sq in.	2.7	.015	0.90
2" diam. 3.14 sq in.	2.5	.02"	0.80
3-3/4" x 1-1/4" 4.675 sq in.	4.7	.02"	0.99
2-1/2" diam. 4.906 sq in.	5.0	.02"	1.02

The exact process occurring during this phase of the load-sinkage curve is difficult to establish. It is believed that the very first load increase must take place with an almost negligible sinkage, perhaps as follows:

- a. The sand is left in some state of particle arrangement and density for some depth by the soil-conditioning process employed.

b. When load is applied, no penetration occurs until a force is exerted sufficient to cause the uppermost sand particles to reorientate themselves against the friction between particles, and to slide or shear on one another an insignificantly small amount to produce a more or less rigid solid surface in contact with the penetrating plate on one side and the sand at greater depths on the other.

c. Further increase in load produces an increased boundary layer attached to the plate accompanied by some small measurable sinkage resulting from further compaction and slip with the start of flow away from the stressed region to places of no stress, most probably toward the sand surface as shown in Ref. 10.

d. When the attached boundary has been completely formed to the penetrating plate, the remaining operation is mainly one of flow from below the boundary layer outward and upward.

The result is the curves as shown in Fig. 54, with little or no sinkage for a given increase in load, followed by a fairly rapid increase in sinkage for a further moderate increase in load, and finally a more or less constant functional change of p and z approximating Eq. (1).

One other explanation could be the assumption of an initial elastic phase where the modulus of compression would have to be of very considerable magnitude. This does not seem to fit all the observations.

That this initial change of stress without sinkage is in some manner associated with the material of the soil is established by comparison of Figs. 44 and 45 (the latter showing the load-sinkage curve for nonmagnetic barium ferrite). For this material, due to its finely powdered state, there is little or no need to apply load of much magnitude to reorient the particles and produce a flow. Also due to the fine nature of the material and its powdered condition, its density is probably below that of its natural compacted state that is, unless it has been consolidated. It follows that the first portion of Fig. 45 shows a very small vertical rise followed by sinkage, producing mainly compaction. With little or no applied pressure, some of this sinkage is definitely due to flow of the finely powdered loose surface material; how much, is difficult to say. It is seen that after some consolidation the load-sinkage curve does assume the normal shape. The great difference between Figs. 44 and 45 establishes that the soil itself and its preparation does control the resulting curves obtained in Bevameter tests.

As a result of analysis of the test data it can be concluded that:

a. It is possible to control the values of k_c and k_ϕ with some degree of independence over a range of values that should prove useful for similitude testing when employing frictional materials.

b. The value of the ratio k_{ϕ}/k_c can be varied from approximately -4.0 to +10.0 by the use of various combinations of sand and glass beads of approximately the same particle size.

c. By the use of barium ferrite in the nonmagnetized and magnetized states, the values of k_c and k_{ϕ} can be moderately varied; however, the ratio k_{ϕ}/k_c varies only from 0.28 to 0.34 in the process.

d. Additional tests with materials having greater magnitudes of k_c are desirable to evaluate fully the usefulness of the methods employed.

e. To cover the total possible variation of the parameters and their ratios, further test work should be undertaken, such as:

(1) variation of bead size in relation to sand particles;

(2) variation (and measurement) of the degree of magnetization;

(3) combinations of these materials with clays and loams, etc.

CONCLUSIONS

1. It has been found that dimensional analysis techniques are applicable to land locomotion studies for sand. The following master variables satisfy the similitude requirements for driven wheels: R/W , T/Wd and z/d , under the above conditions.

2. It has been shown that it is necessary to take account of the d/D ratio in the correlation of test results.

3. When the cohesive soil parameter is not negligible ($k_c \neq 0$), the Bekker soil values must be varied according to equations 7b or 9 to obtain completely analogous conditions for wheels of different size.

4. The Bekker soil values may be changed by use of "magnetic soils", glass beads or other artificial soil-like material.

5. Equation (1) represents the true pressure-sinkage relationship within the sinkage range of 0.5 - 4.5 inches for sand and sand mixtures. These limits were found to be valid for a soil layer of 12 inch depth.

REFERENCES

1. Bekker, M. G., "A Proposed System of Physical and Geometric Terrain Values for the Determination of Vehicle Performance and Terrain Trafficability", Research Report No. 4, Land Locomotion Laboratory, OTAC, U. S. Army, Center Line, Mich., 1956.
2. Nuttal, C. J., "The Rolling Resistance of Wheels in Soil", Stevens Institute of Technology, Experimental Towing Tank, Report No. 418, Hoboken, N. J., July 1957.
3. McGowan, R. P. and Nuttal, C. J., "Scale Models of Vehicles in Soils and Snows", paper No. 39, First International Conference on the Mechanism of Soil-Vehicle Systems, Turin (Italy), 1961.
4. Bekker, M. G., "Theory of Land Locomotion", The University of Michigan Press, Ann Arbor, 1956.
5. Langharr, H. L., "Dimensional Analysis and Theory of Models", John Wiley, New York, 1951.
6. Bernstein, R., "Problem Einer Experimentellen Motorpflugmechanik", Der Motorwagen, 16, 1913.
7. Czako, T. and Bekker, M. G., "Determination of Vehicle Sinkage Parameters by Means of Rigid Wheels", Report No. 33, Land Locomotion Laboratory, OTAC, U. S. Army, Center Line, Mich., 1958.
8. Hanamoto, B., "Artificial Soils for Laboratory Studies in Land Locomotion", Report No. 20, Land Locomotion Laboratory, OTAC, U. S. Army, Center Line, Mich.
9. Bekker, M. G., "Off-the-Road Locomotion", The University of Michigan Press, Ann Arbor, Mich., 1961.
10. Leis, R., "Soil Value System as Determined with a Precision Bevameter", University of Michigan, ORA Report 036026-2-P, December 1961.
11. Harrison, W. L. et al, "A Soil Value System for Land Locomotion Mechanics", Research Report No. 5, Land Locomotion Laboratory, Ordnance Tank Automotive Command, U. S. Army, Center Line, Mich., 1958.
12. Vincent, E. T., et al, "Research in Vehicle Mobility", UMRI Report 2544-31-F, Ann Arbor, Mich., July 1960.

DISTRIBUTION LIST

Commanding General Aberdeen Proving Gd, Md. ATTN: Tech Library 4	Commanding Officer Office of Ordnance Research Box CM, Duke Station Durham, North Carolina 3
Commandant Ordnance School Aberdeen Proving Gd, Md. 1	Headquarters Ordnance Weapons Command Research & Development Div Rock Island, Illinois ATTN: ORDOW-TB 2
Commander Canadian Army Staff 2450 Massachusetts Avenue Washington, D. C. ATTN: CAS (W) 4 ATTN: DRB 1	Chief of Ordnance ATTN: Chief, ORDTP-P Washington 25, D. C. 2
Director Waterways Experiment Station Vicksburg, Mississippi 3	Detroit Arsenal 10 Hq, U.S.CONARC Liaison Office
Unit X Documents Expediting Project Library of Congress Washington, D. C. Stop 303 4	Detroit Arsenal Technical Library 2
Exchange and Gift Div Library of Congress Washington 25, D. C. 1	Commanding General Engineer R & D Laboratory Fort Belvoir, Virginia 1 ATTN: Technical Reference & Analysis Branch
United States Navy Industrial College of the Armed Forces Washington, D. C. ATTN: Vice Deputy Commandant 1	Superintendent U.S. Military Academy West Point, New York 1 ATTN: Prof. of Ordnance
Chief of Ordnance Department of the Army Washington, D. C. ATTN: ORDTB 1 ATTN: ORDTW 1	Chief of Transportation Corps Washington 25, D. C. 1
Chief Office of Naval Research Washington, D. C. 1	Army Research Office Arlington Hall Station Arlington 12, Virginia 1
	ASTIA Arlington Hall Station Arlington 12, Virginia 10

DISTRIBUTION LIST (Cont'd)

**Superintendent
U. S. Naval Academy
Annapolis, Md.**

1

**Commander
British Army Staff
3100 Massachusetts Ave., N.W.
Washington 8, D. C.**

6

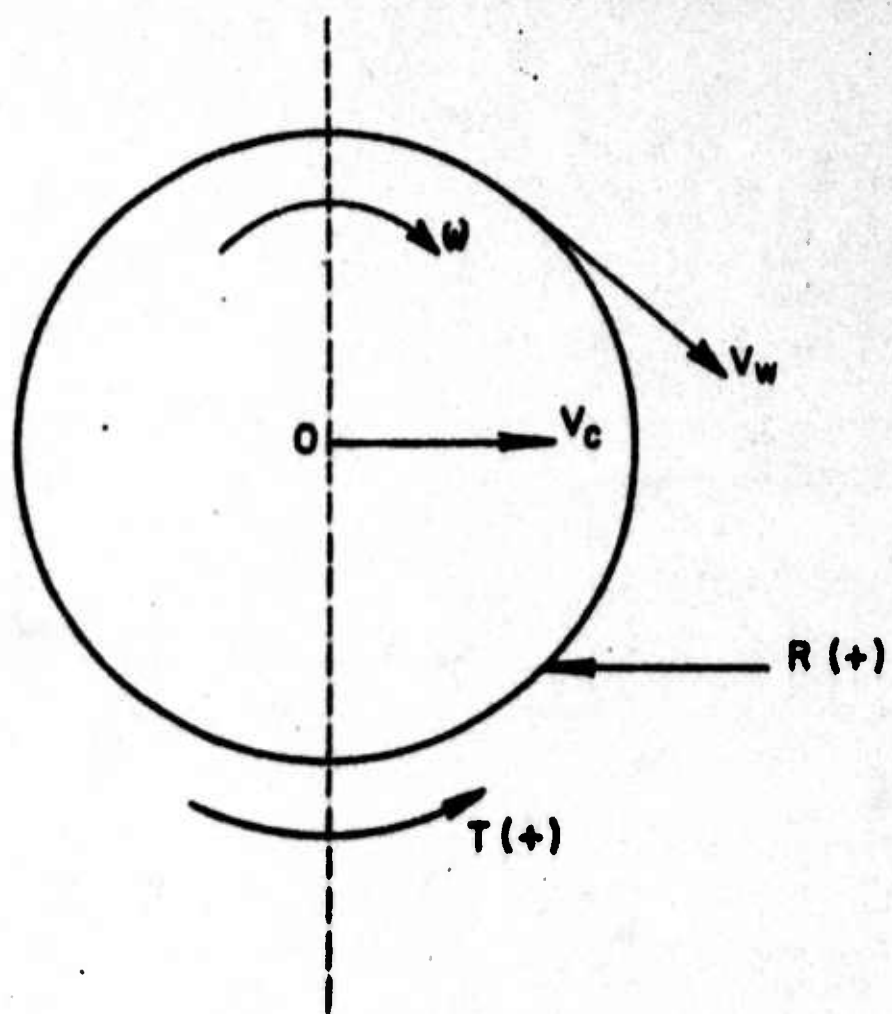


Fig. 1. Sign convention of velocities and forces on the wheel.

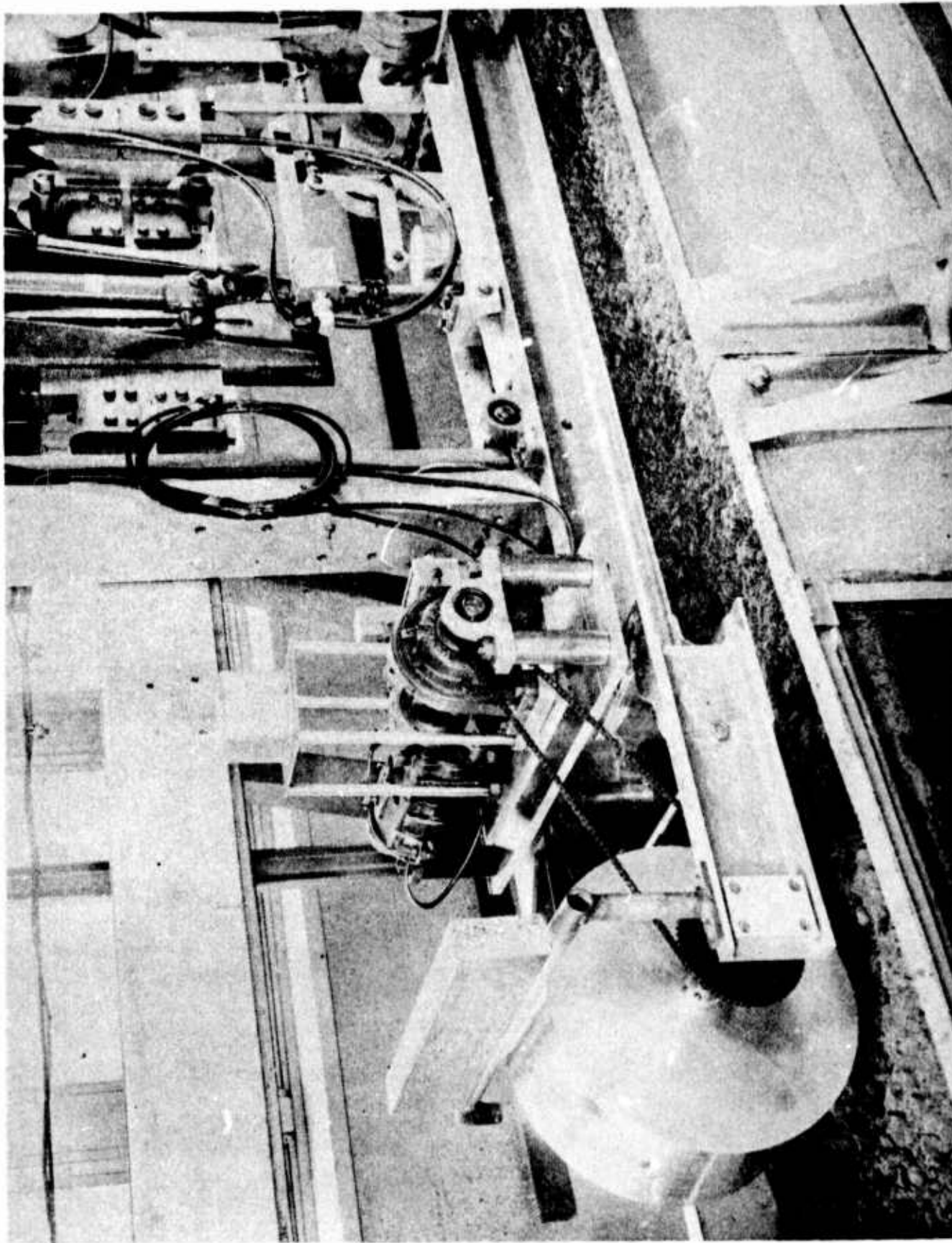


Fig. 1a Picture of wheel and motor drive.

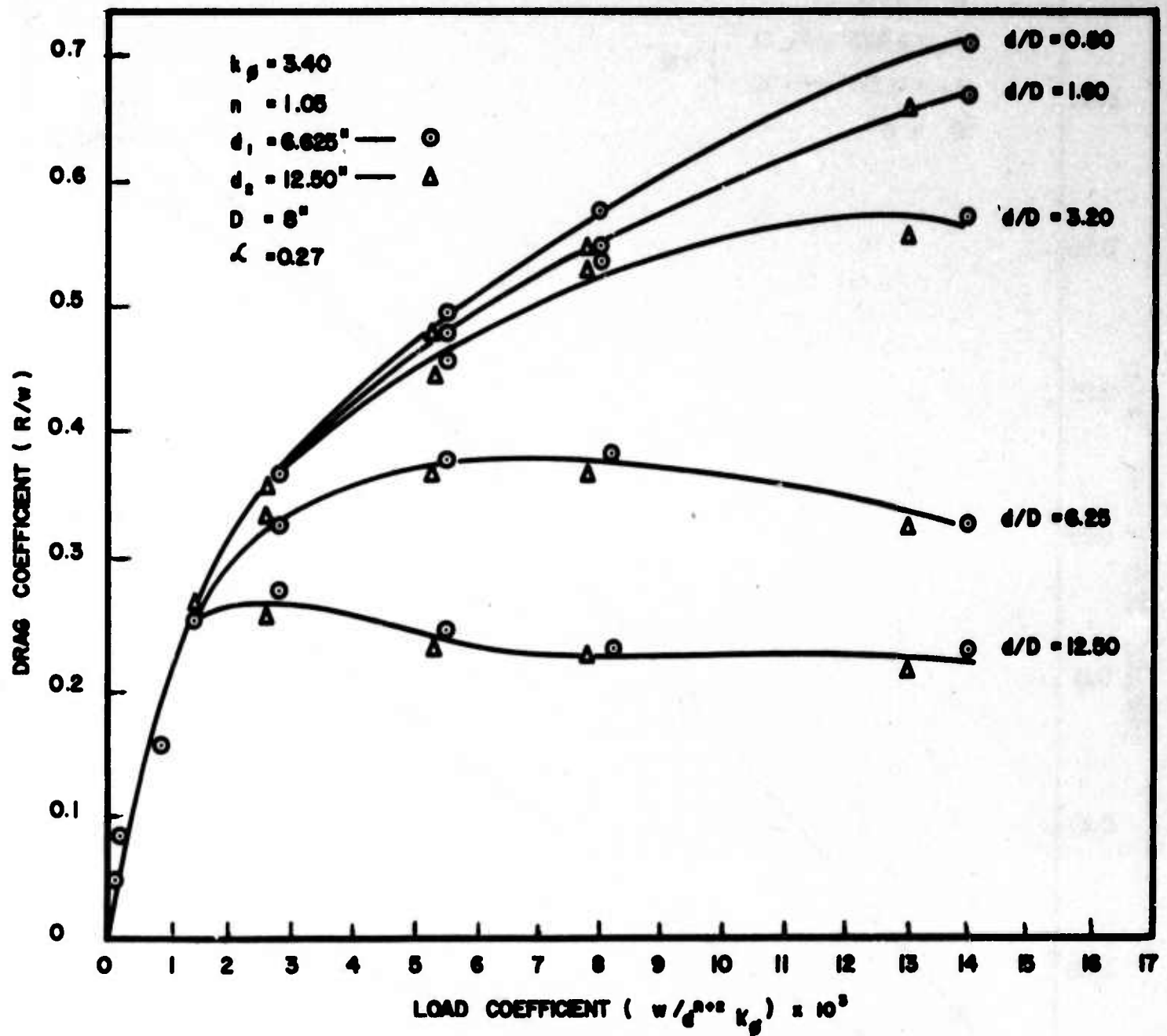


Fig. 2. Plot of non-dimensional drag coefficient (R/w) vs. non-dimensional load coefficient ($w/d^{n+2} k_p$) for rectangular cross-sectional wheels.

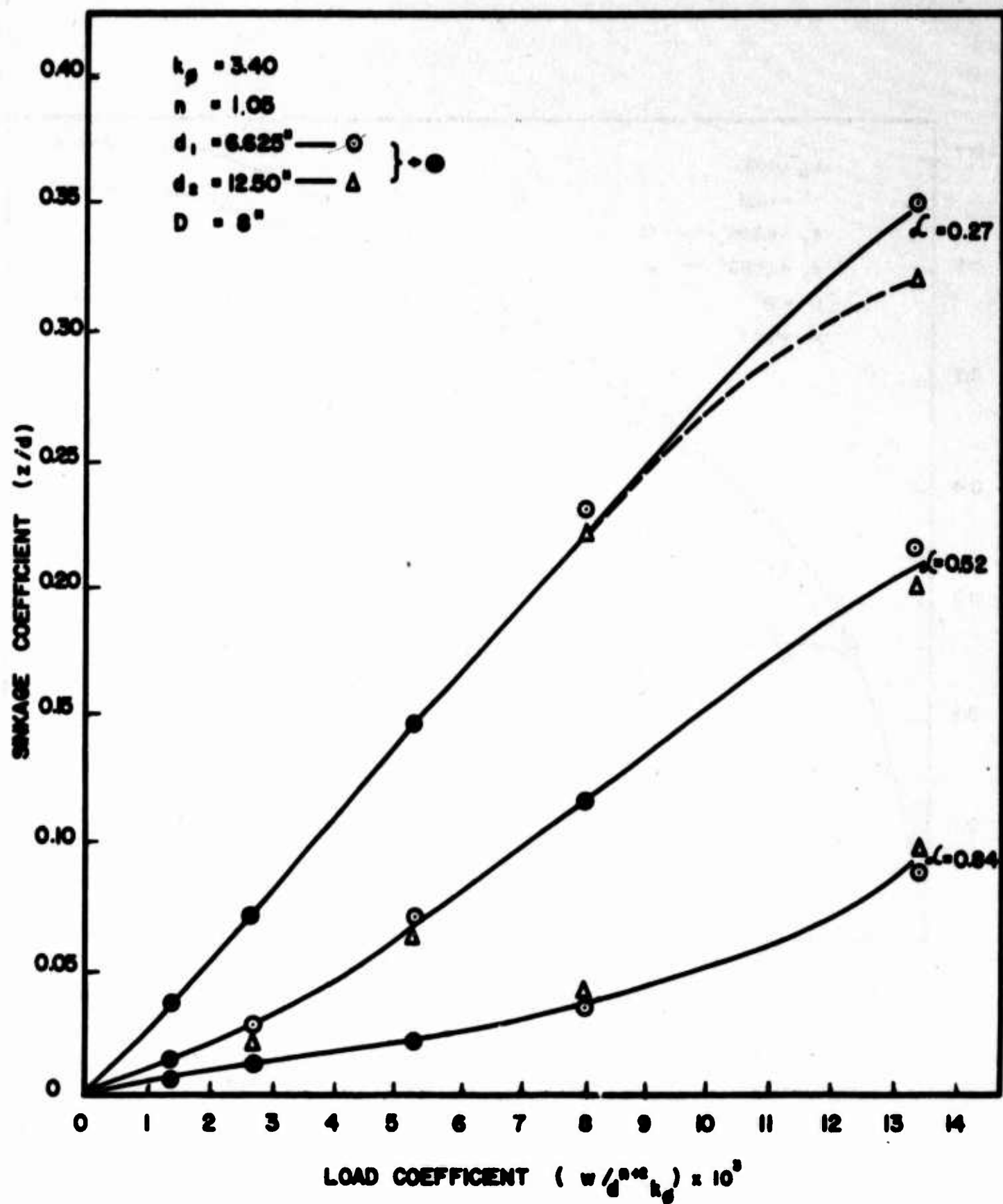


Fig. 3. Plot of non-dimensional sinkage coefficient (z/d) vs. non-dimensional load coefficient $(w/d^{n+2}k_p)$ at various aspect ratios for rectangular cross-sectional wheels.

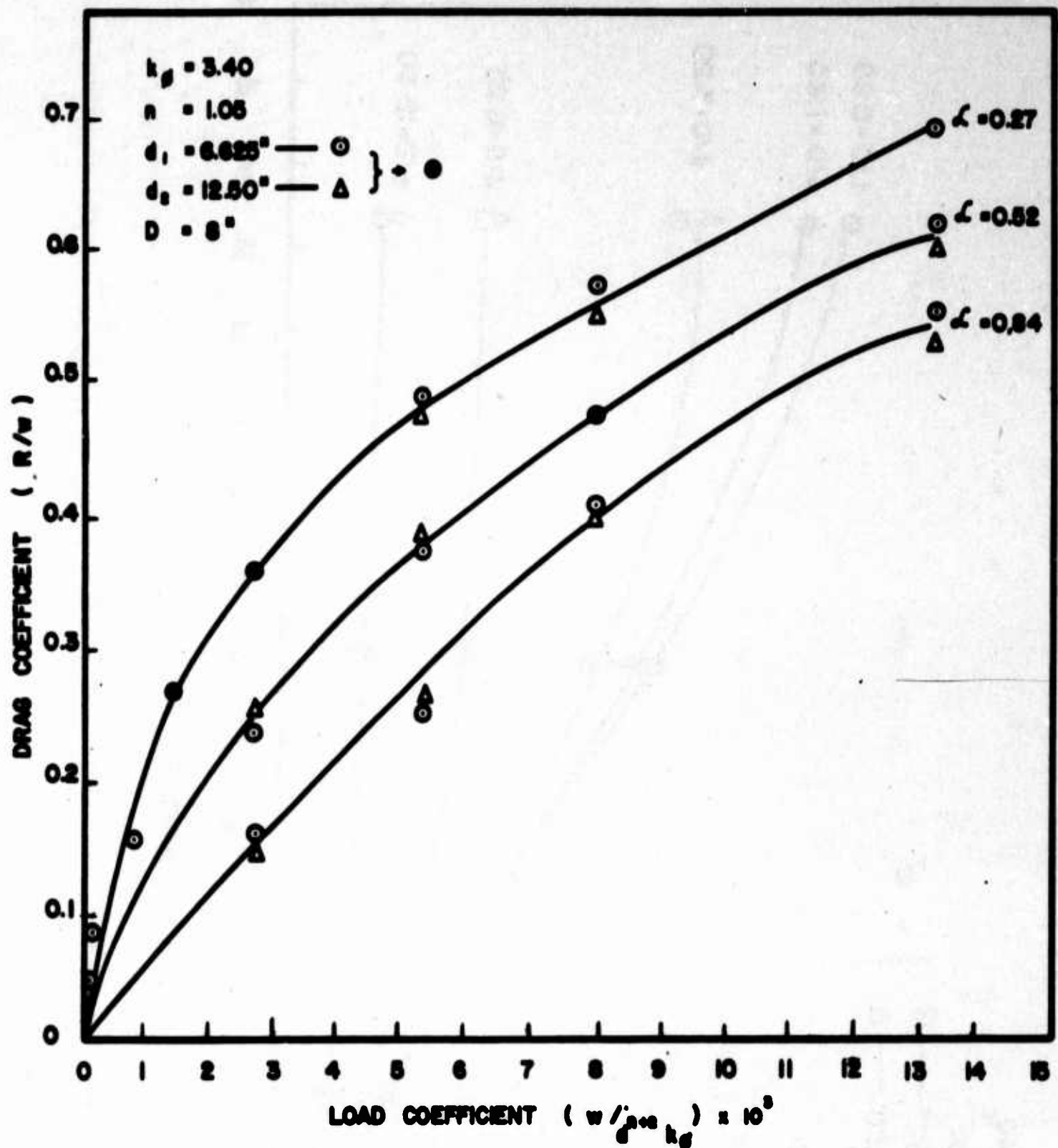


Fig. 4. Plot of non-dimensional drag coefficient (R/w) vs. non-dimensional load coefficient ($w/d^{2+n}k_p$) at various aspect ratios for rectangular cross-sectional wheels.

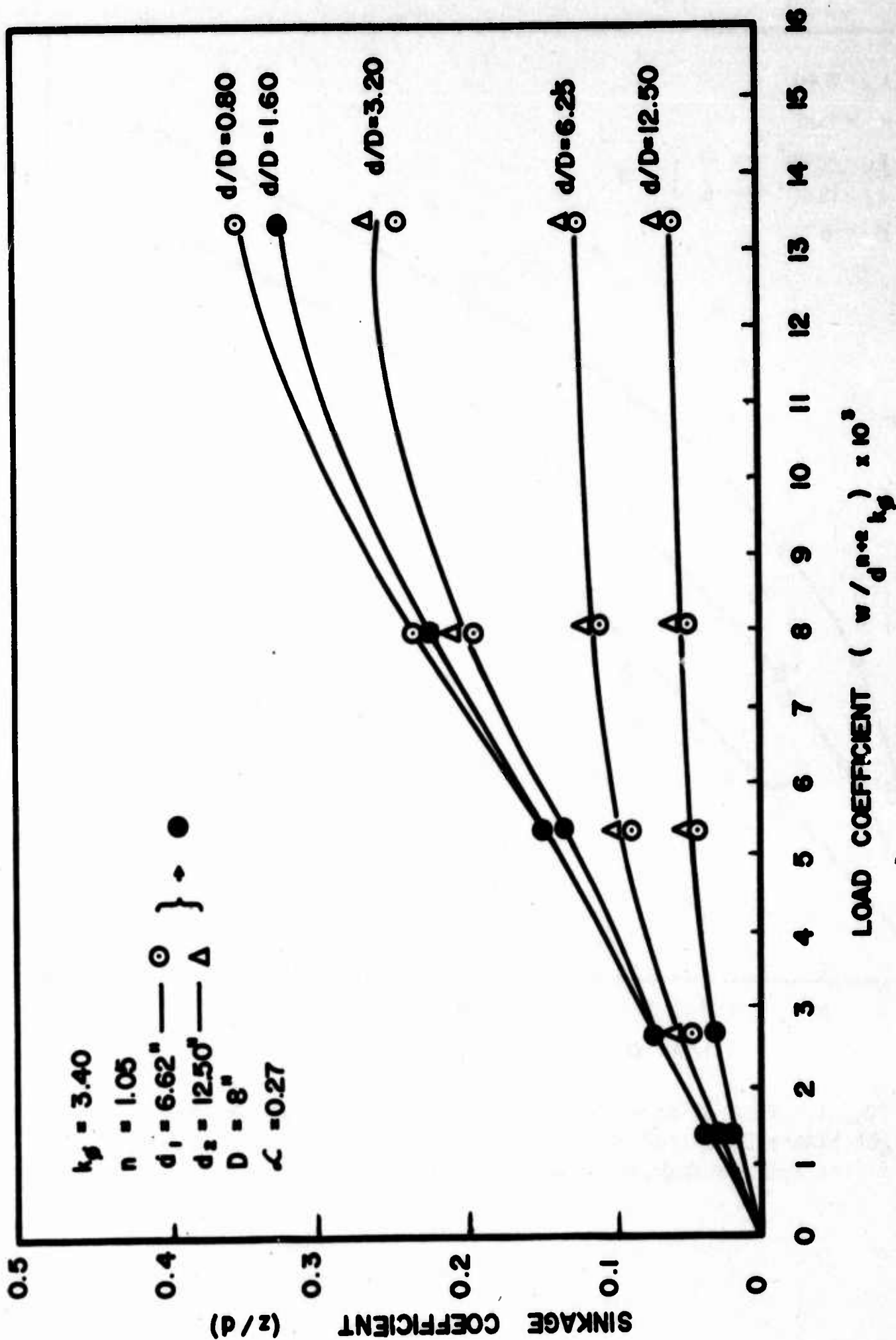


Fig. 5. Plot of non-dimensional sinkage coefficient (z/d) vs. non-dimensional load coefficient ($w/d^{n+2} k_p$) for rectangular cross-sectional wheels.

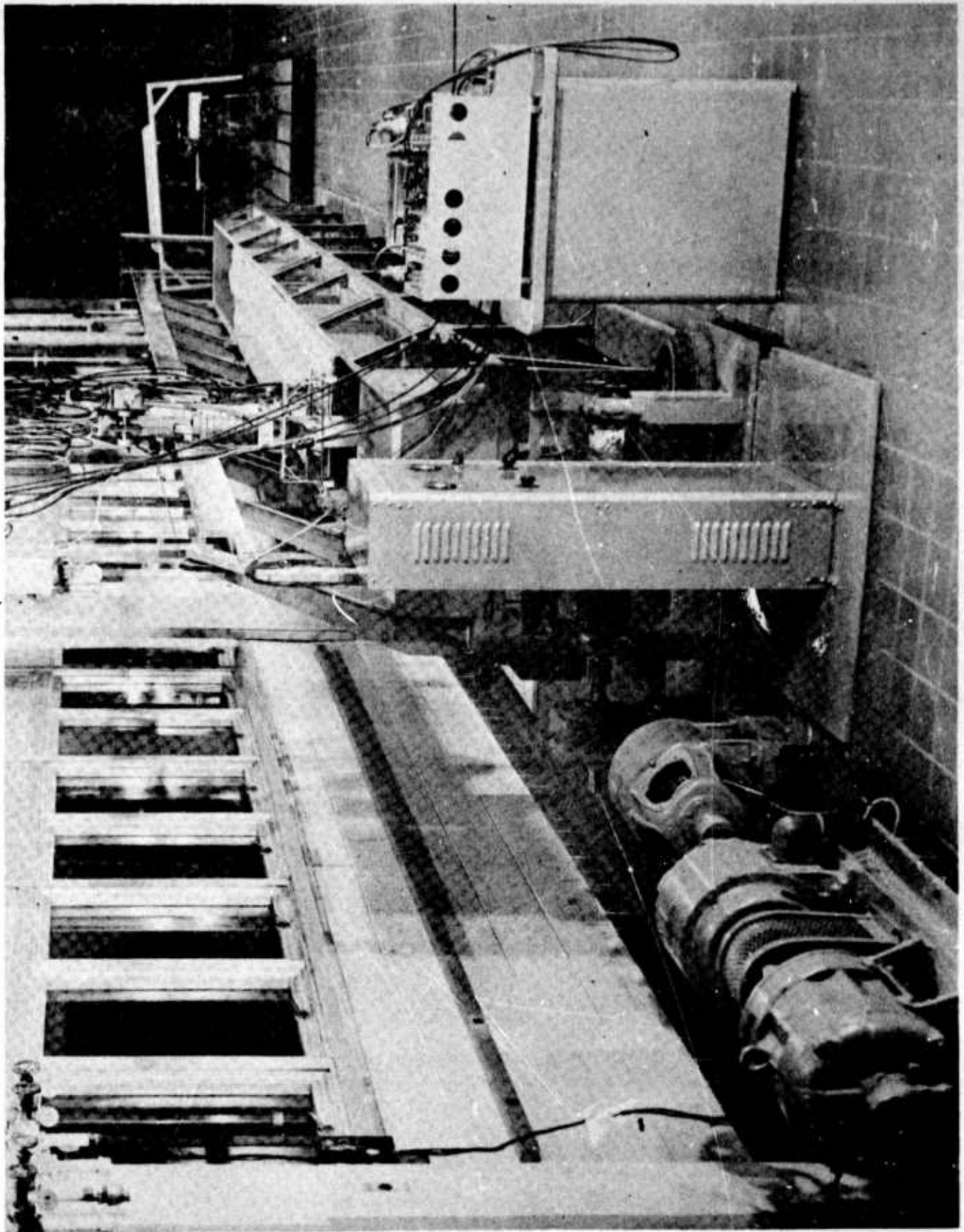


Fig. 6. The tow tank

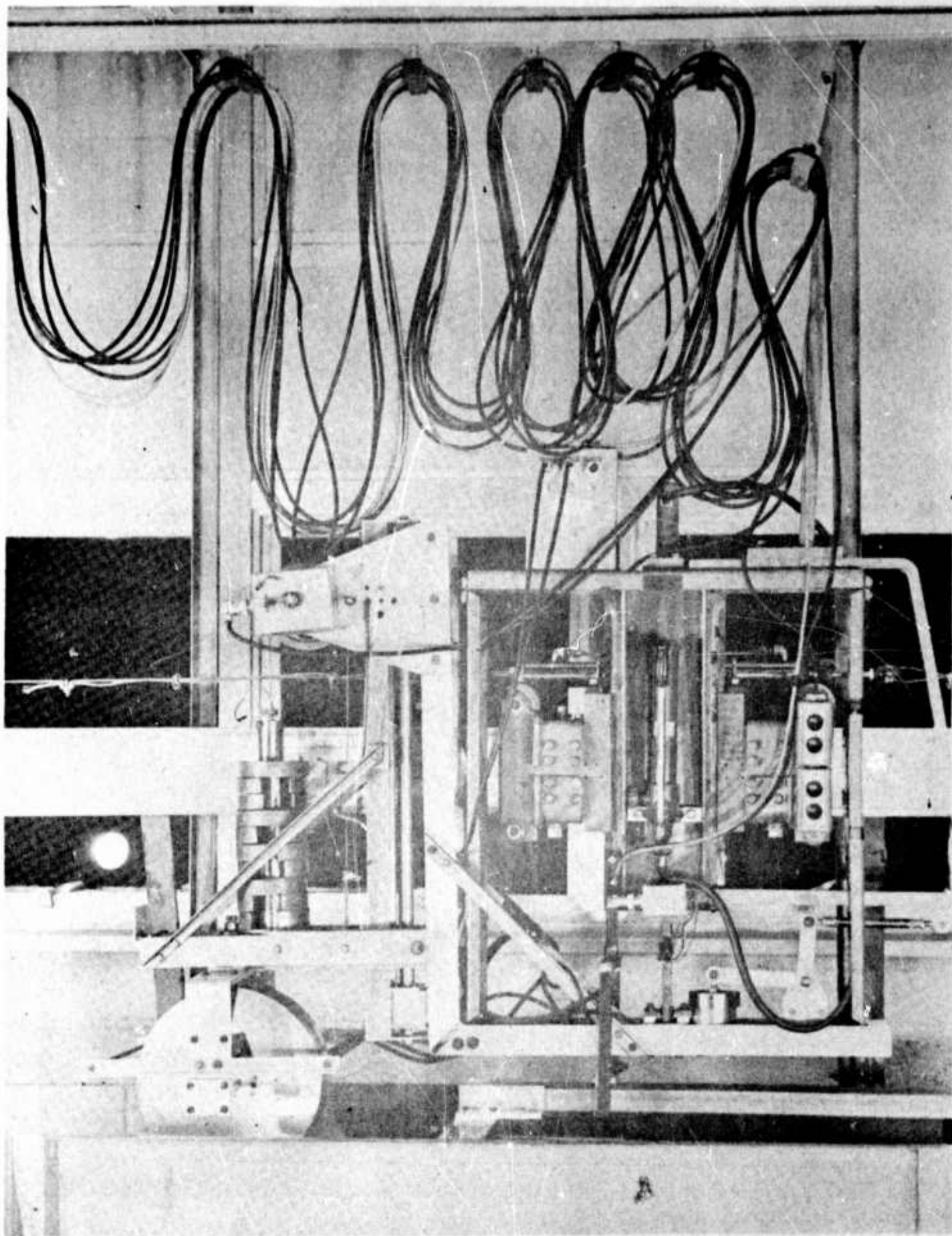


Fig. 7. The wheel carriage.

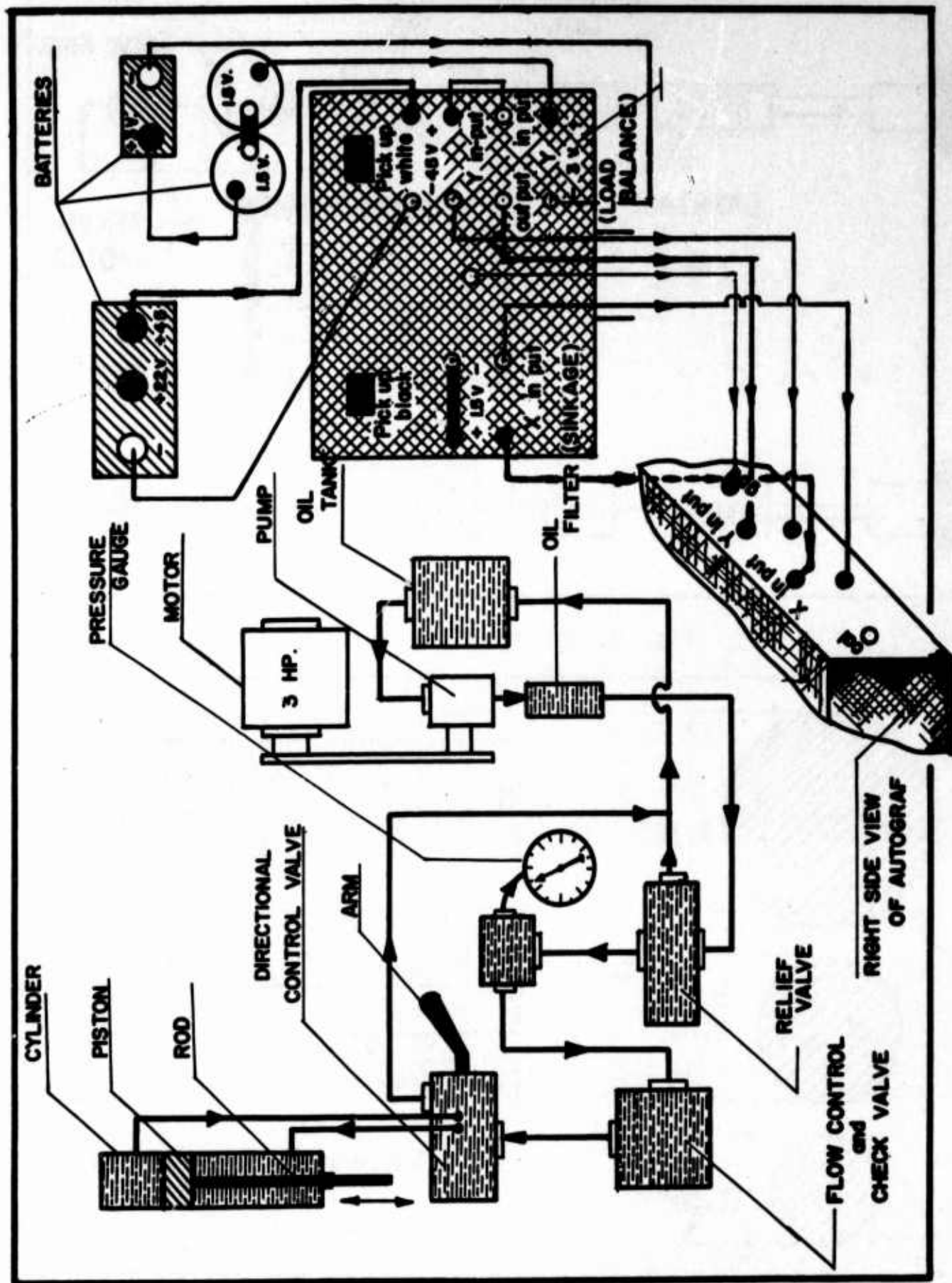


Fig. 8. Diagram of Penetrometer

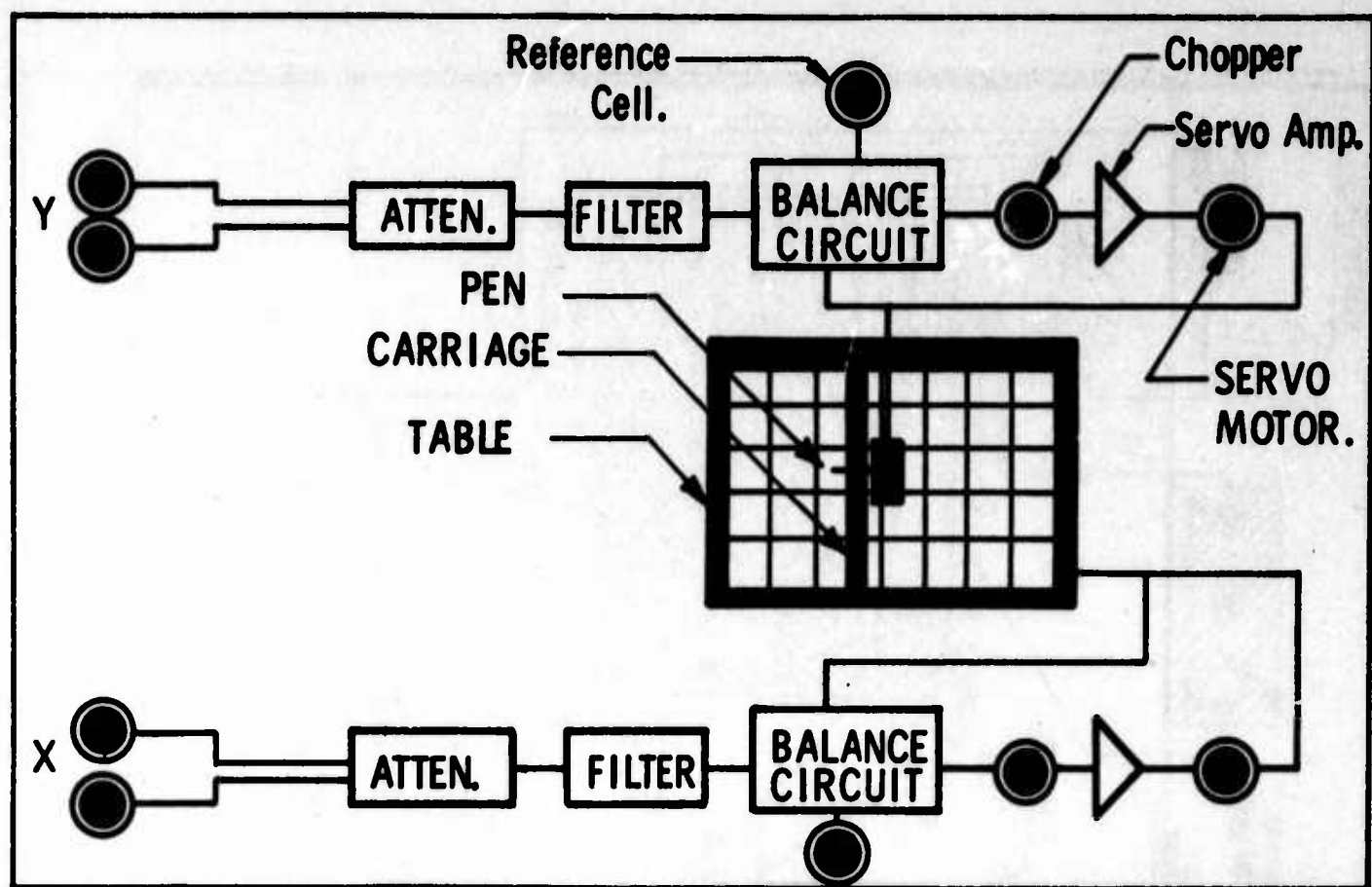


Fig. 9. Electrical circuit.

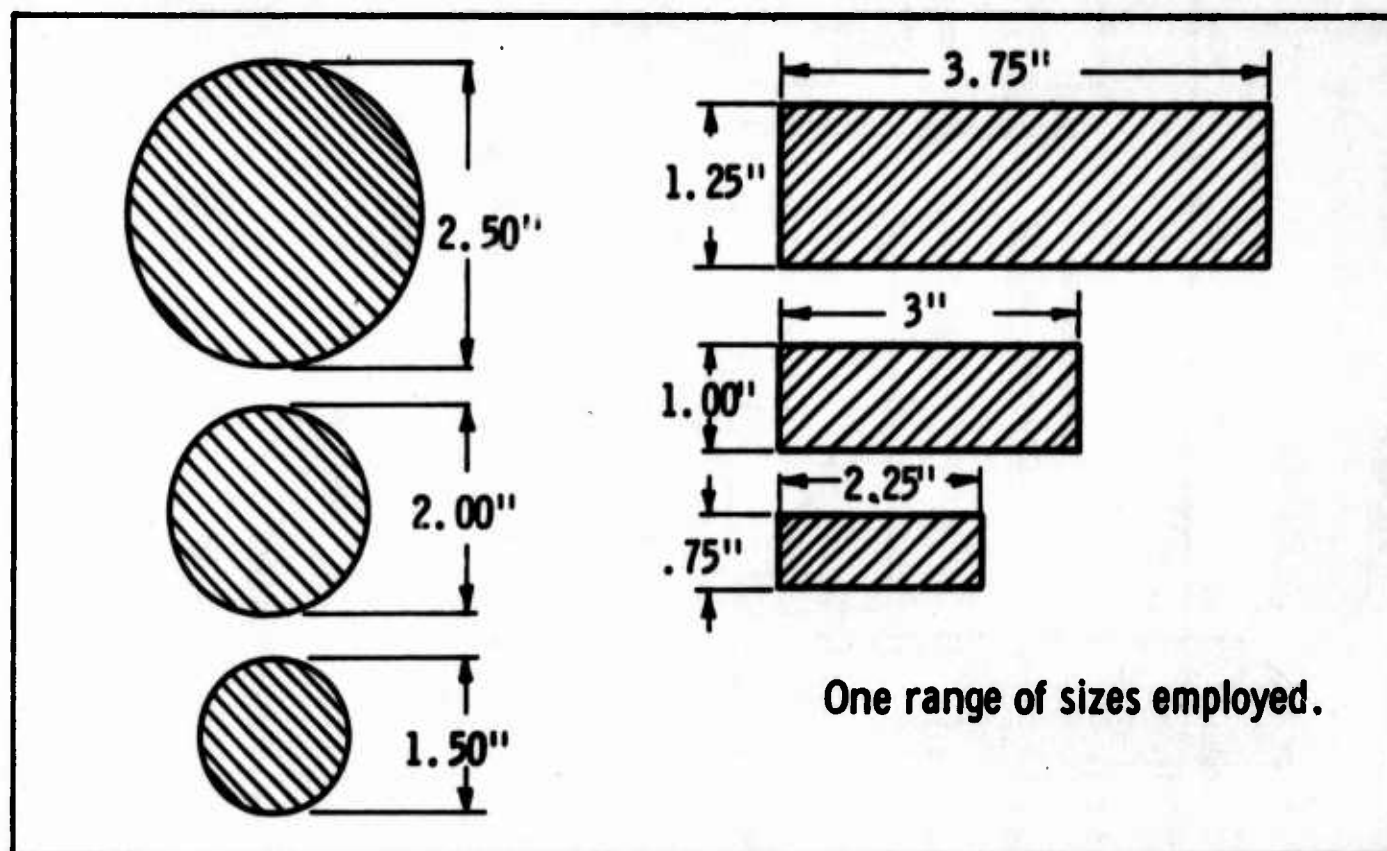


Fig. 10. One range of sizes of feet employed for plunger.

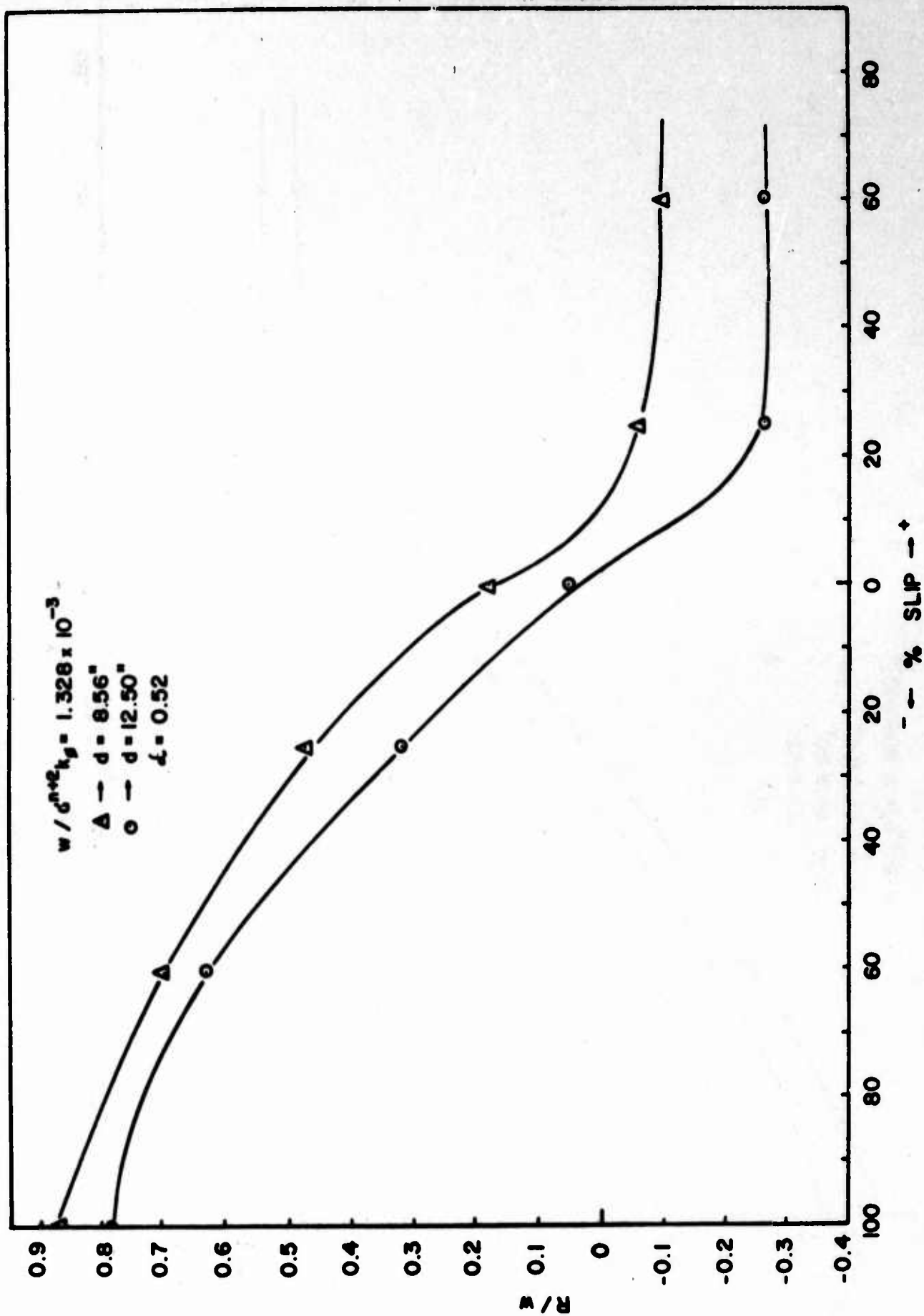


Fig. 11. Plot of (R/w) vs. $\% \text{ slip}$ for $(w/d^{n+2} k_g = 1.328 \times 10^{-3})$ under similitude conditions.

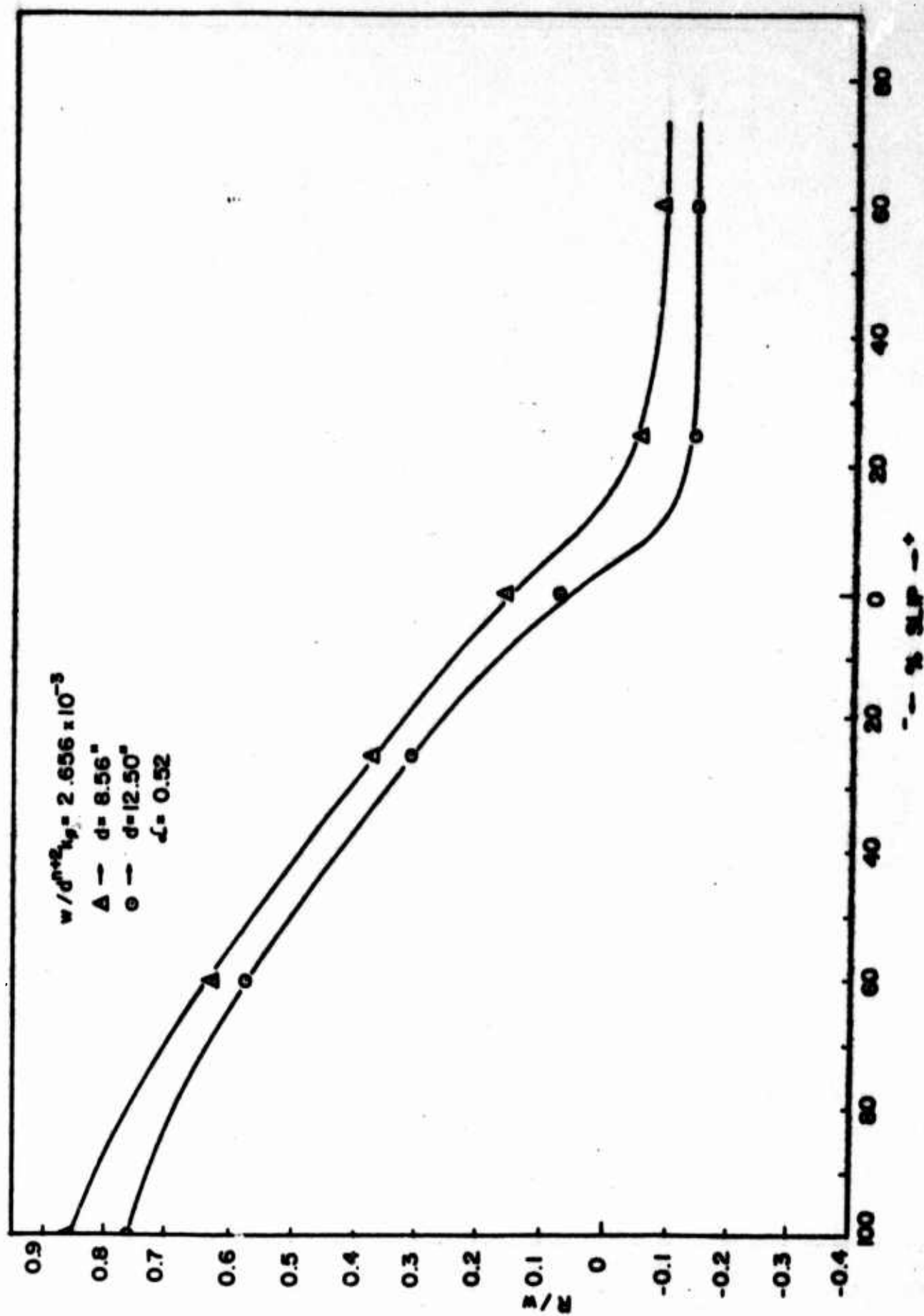


Fig. 12. Plot of (R/w) vs. ξ slip for $(w/d^{n+2}k_0 = 2.656 \times 10^{-3})$ under similitude conditions.

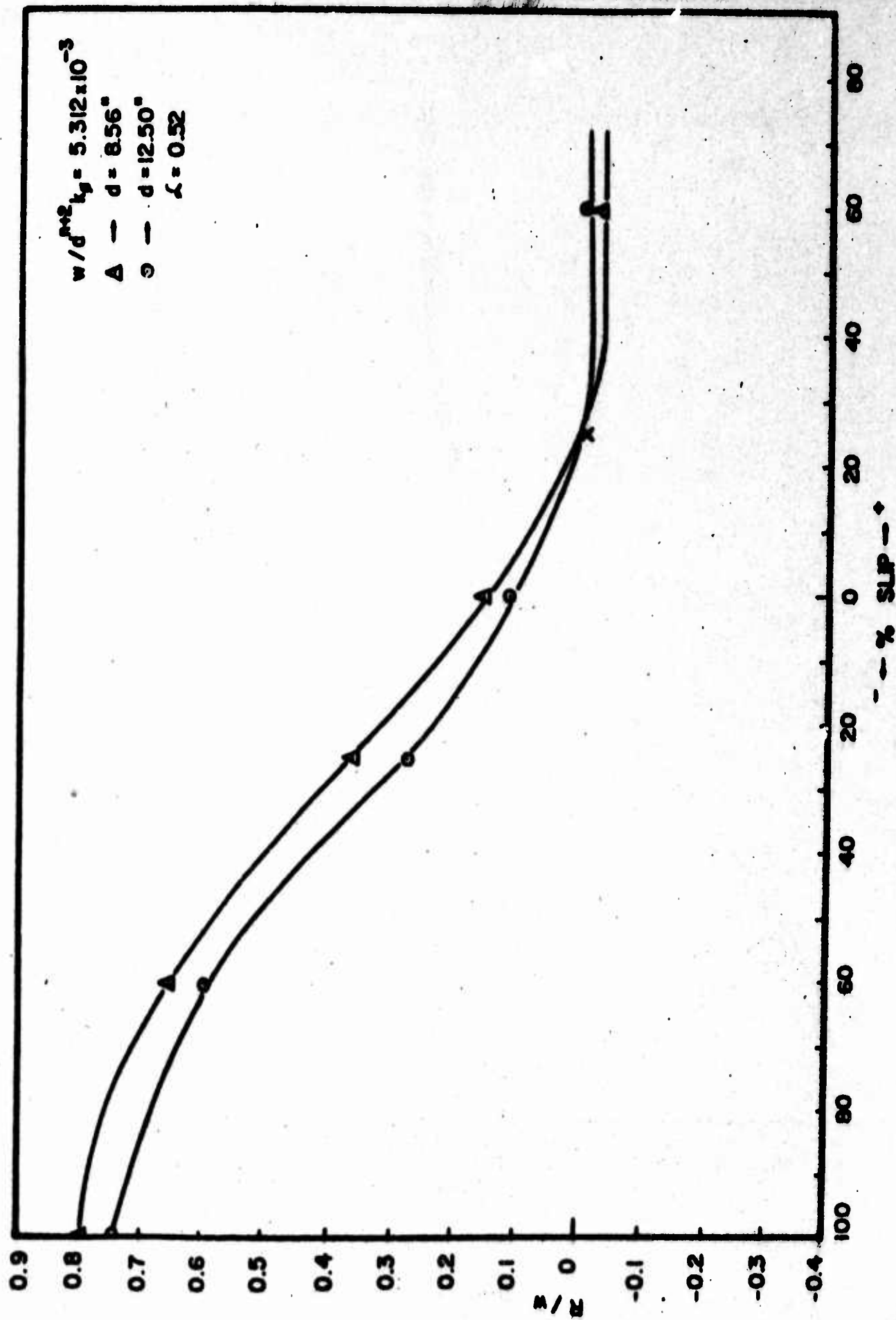


Fig. 13. Plot of (R/w) vs. % slip for $(w/d^{P+2}k_p = 5.312 \times 10^{-3})$ under similitude conditions.

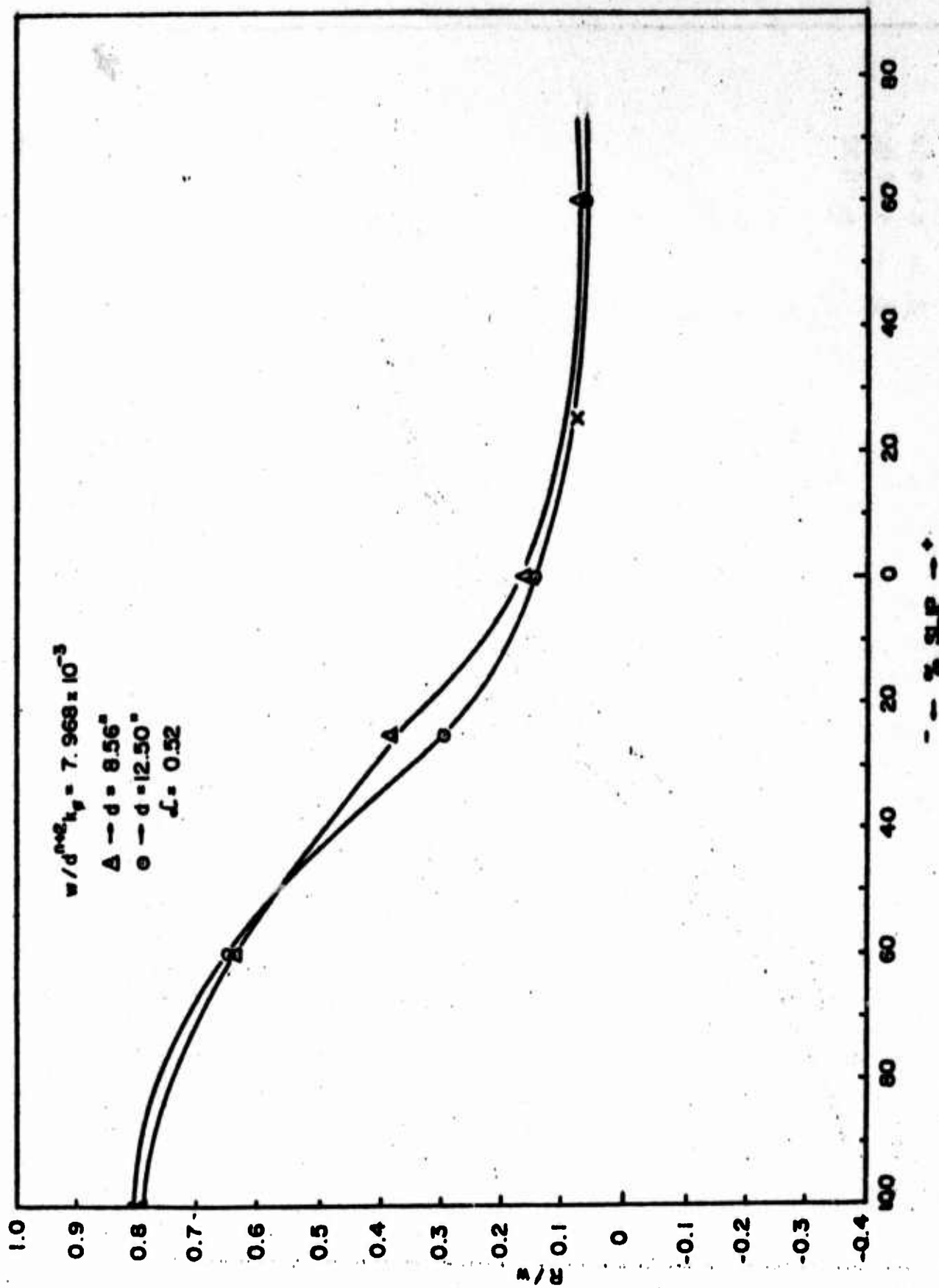


Fig. 14. Plot of (R/w) vs. % slip for $(w/d^{n+2} k_p = 7.968 \times 10^{-3})$ under similitude conditions.

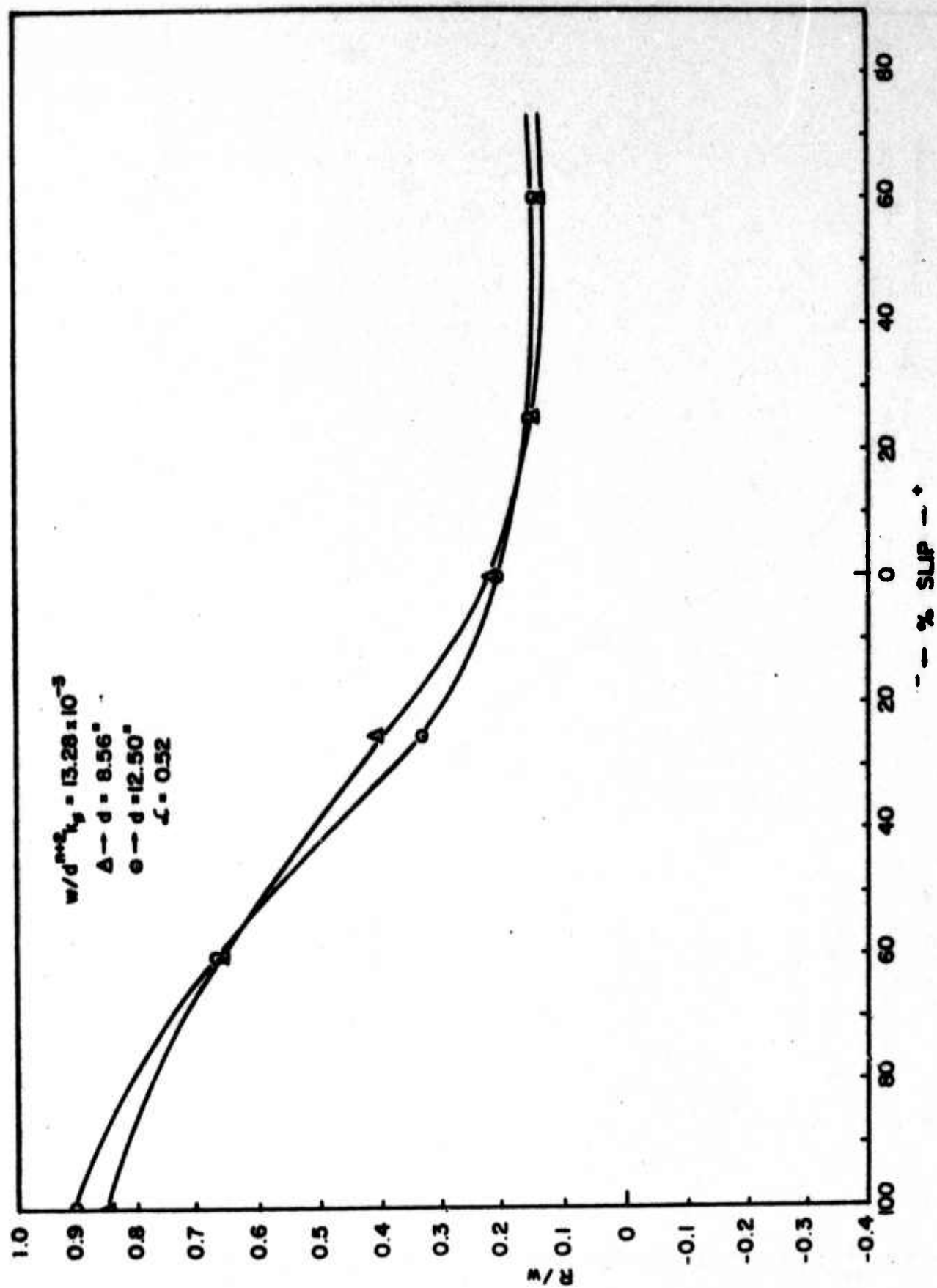


Fig. 15. Plot of (R/w) vs. % slip for $(w/d^{n+2} k_p = 13.28 \times 10^{-3})$ under similitude conditions.

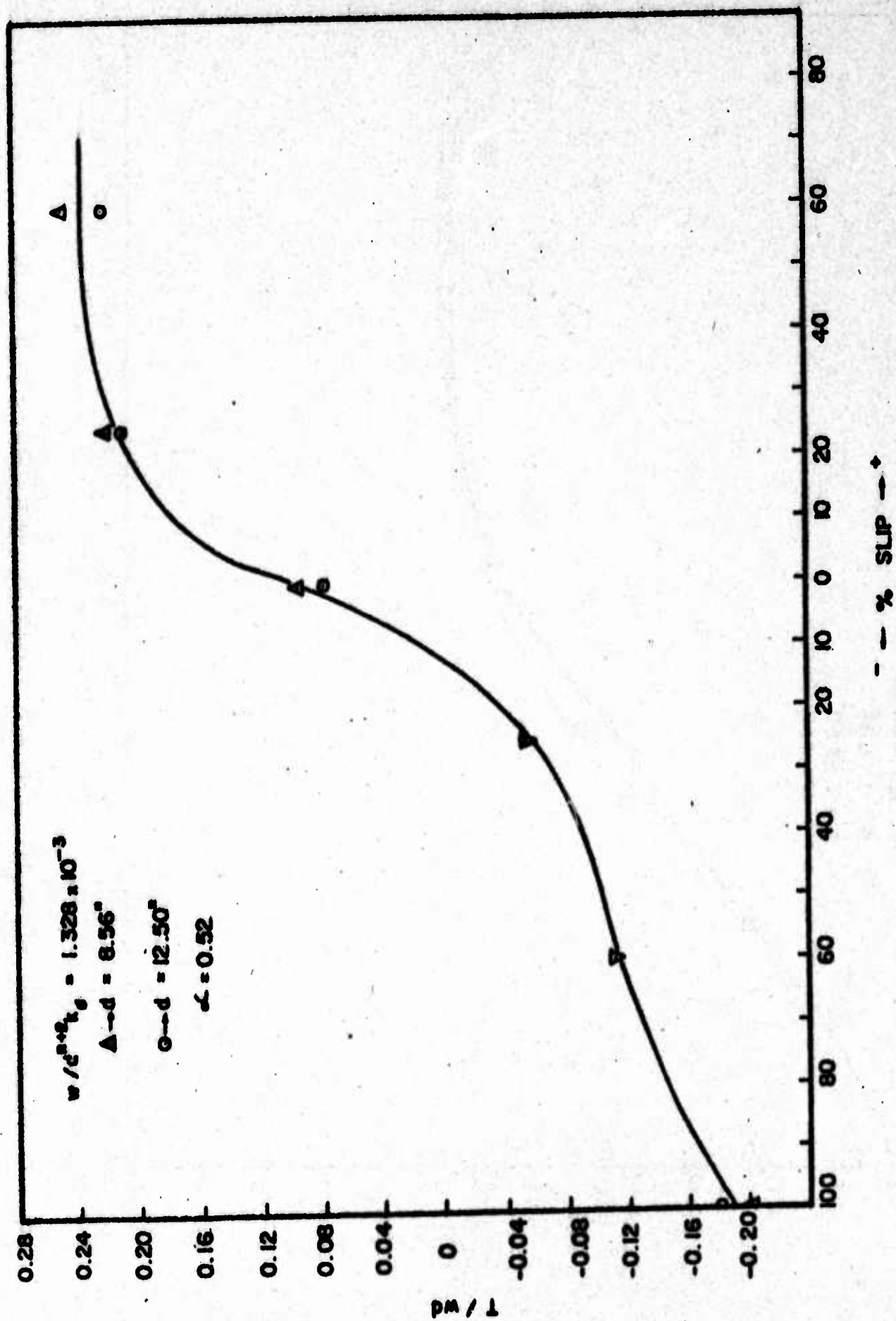


Fig. 16 Plot of (T/wd) vs. % slip for $(w/d^{n+2}k_0 = 1.328 \times 10^{-3})$ under similitude conditions.

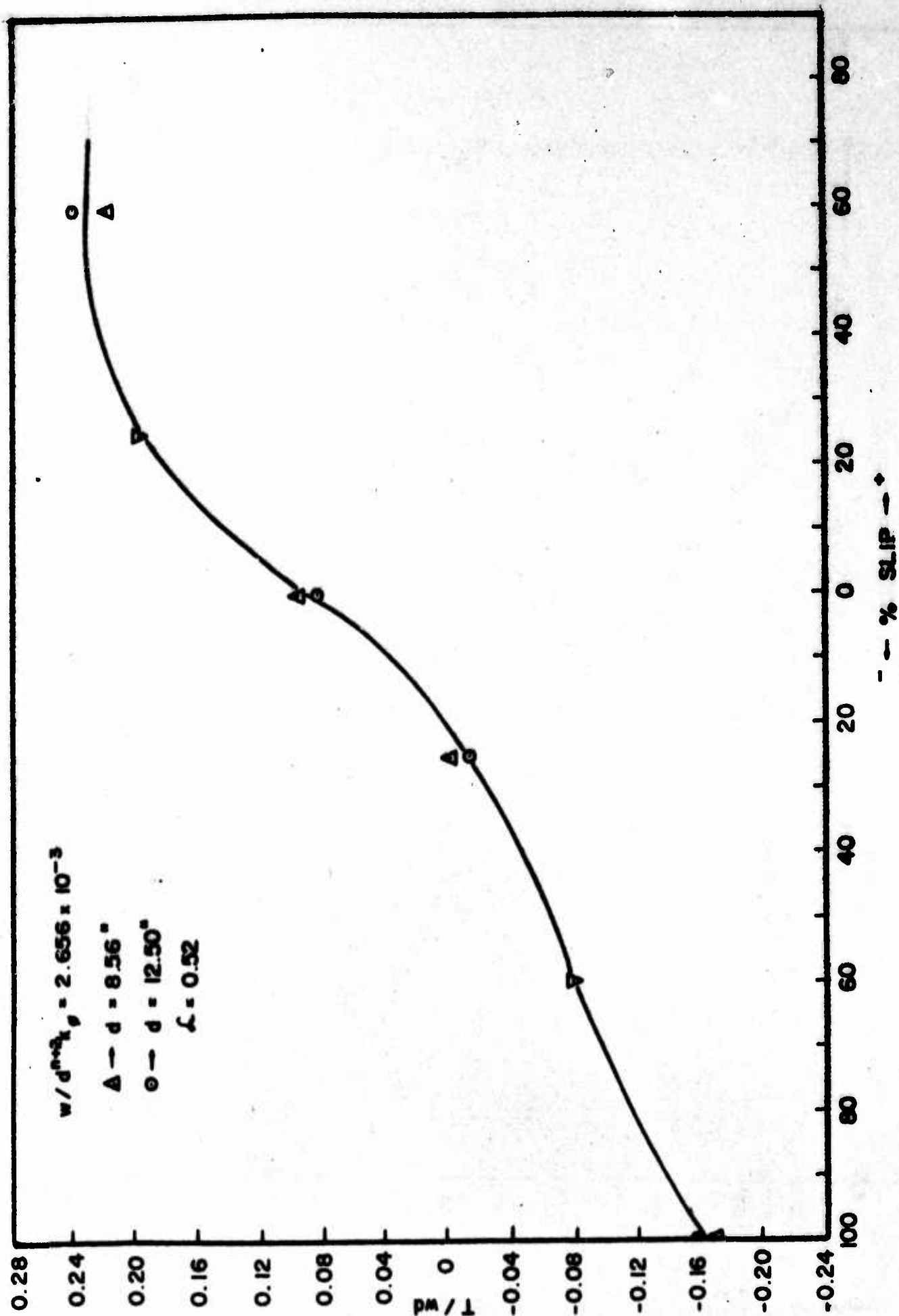


Fig. 17 Plot of (T/wd) vs. % slip for $(w/d^{n+2}k_0 = 2.656 \times 10^{-3})$ under similitude conditions.

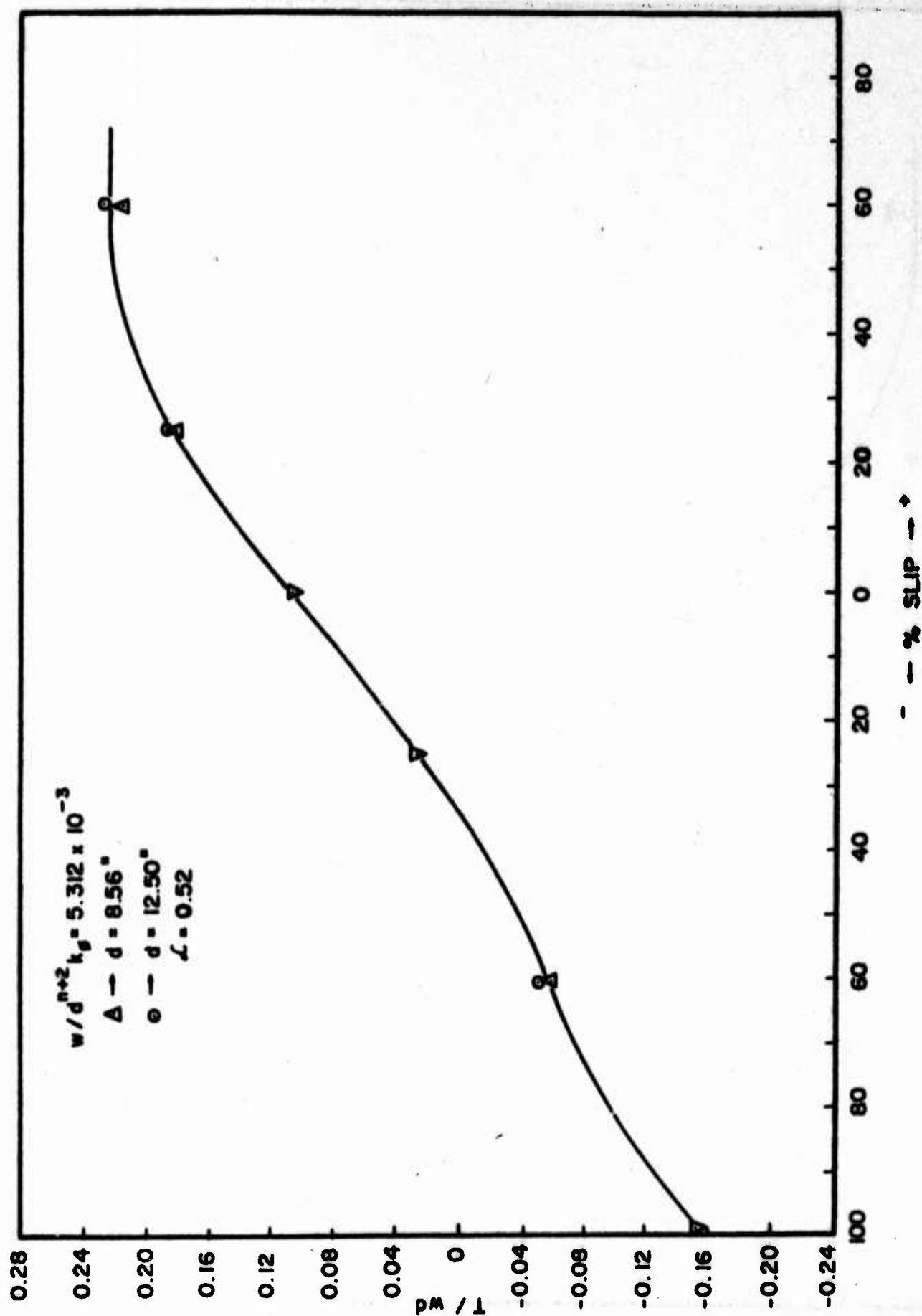


Fig. 18 Plot of (T/wd) vs. % slip for $(w/d^{3/2} k_g = 5.312 \times 10^{-3})$ under similitude conditions.

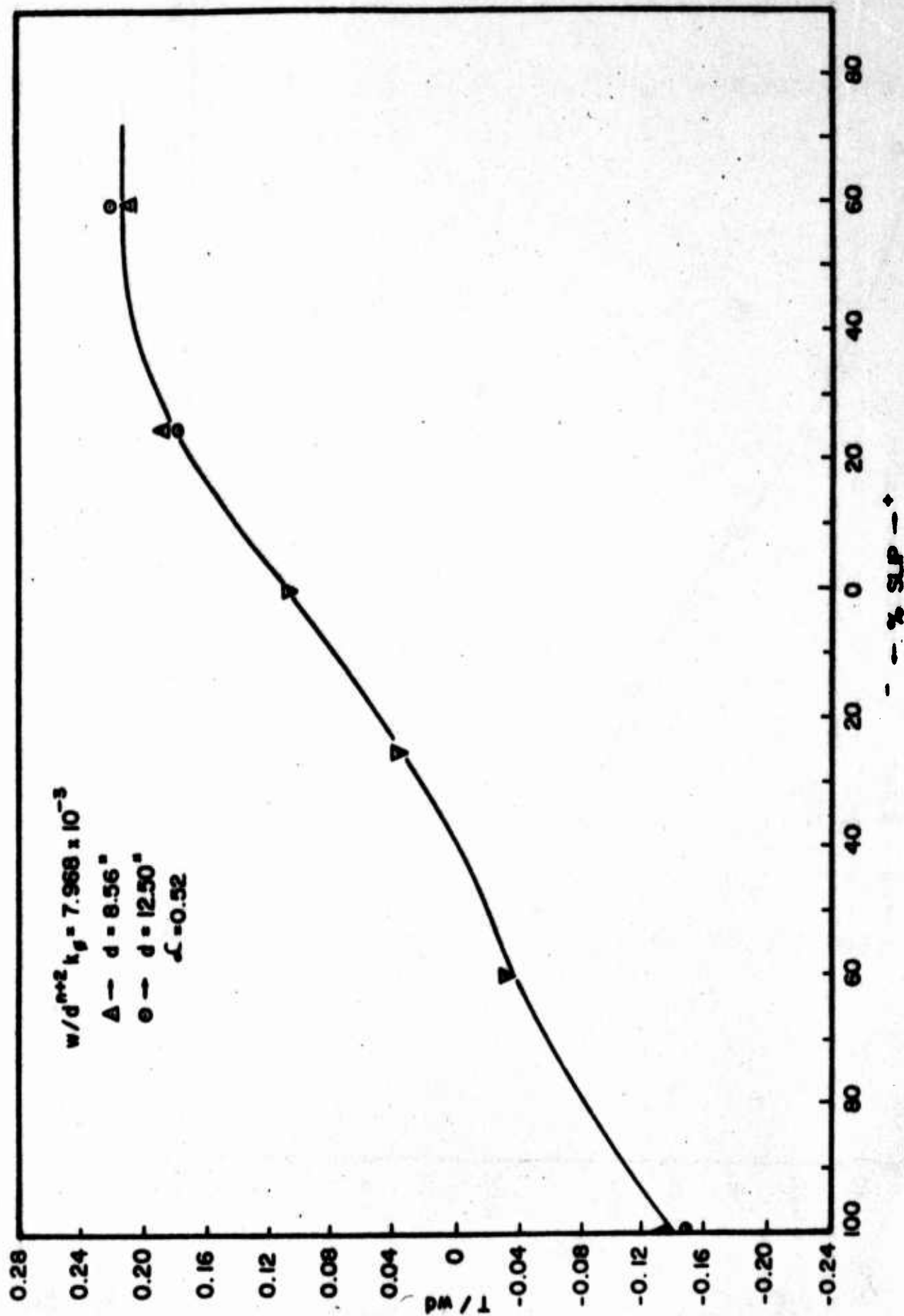


Fig. 17 Plot of (T/wd) vs. $\%$ slip for $(w/d^{n+2} k_g = 7.968 \times 10^{-3})$ under similitude conditions.

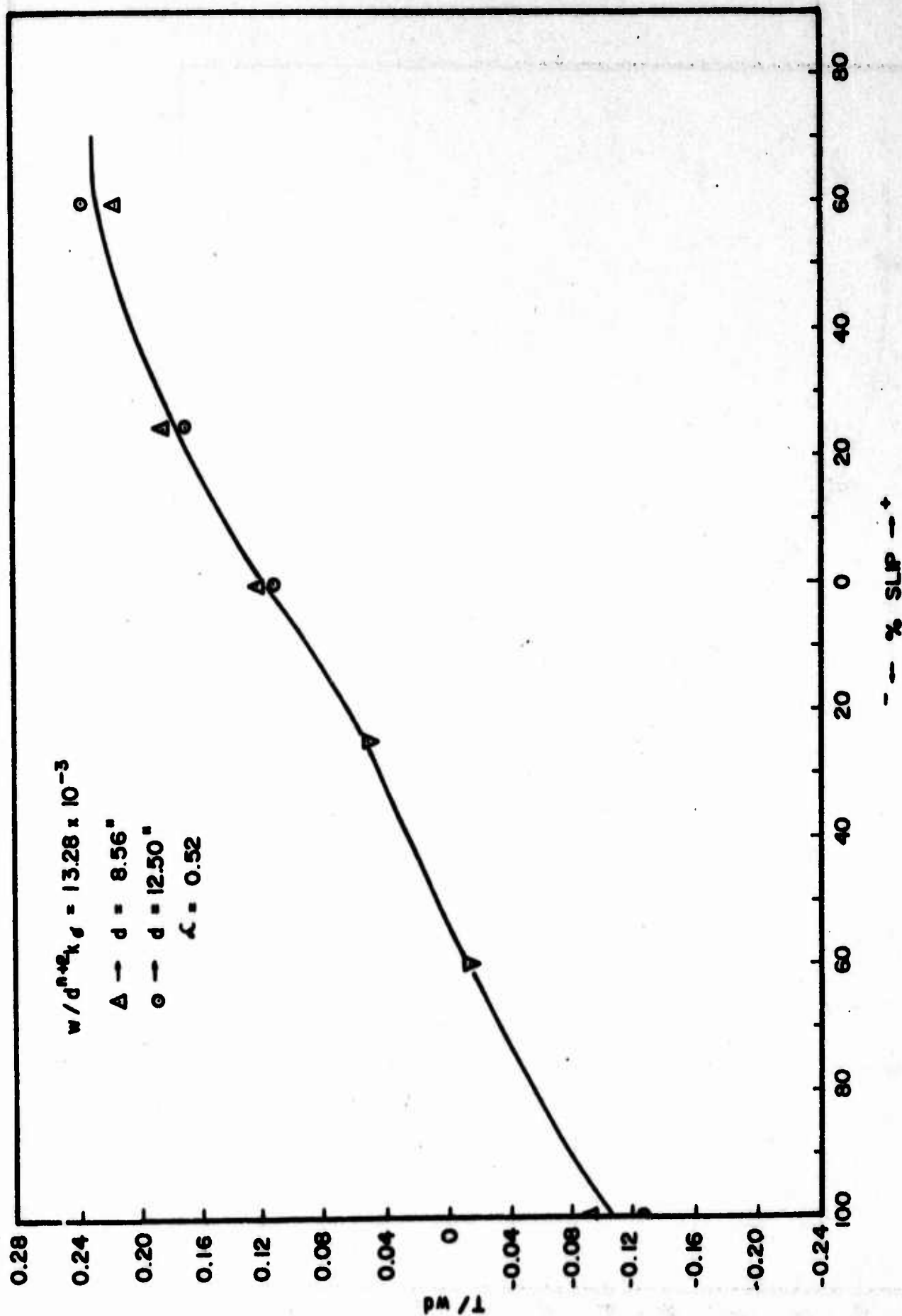


Fig. 20 Plot of (T/wd) vs. % slip for $(w/d^{0.42}k_0 = 13.28 \times 10^{-3})$ under similitude conditions.

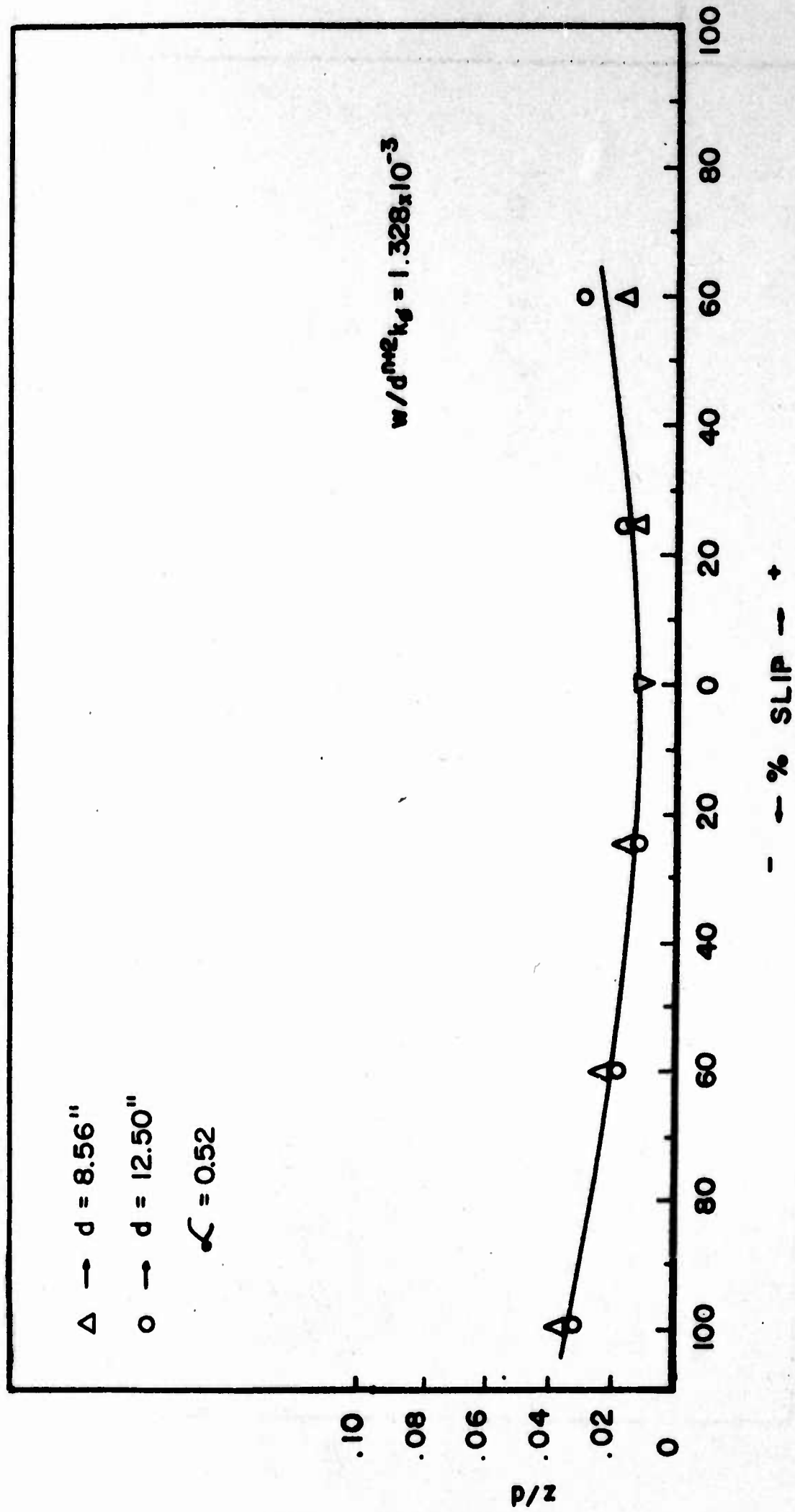


Fig. 21 Plot of (z/d) vs. % slip for $(w/d^{n+2} k_g = 1.328 \times 10^{-3})$ under similitude conditions.

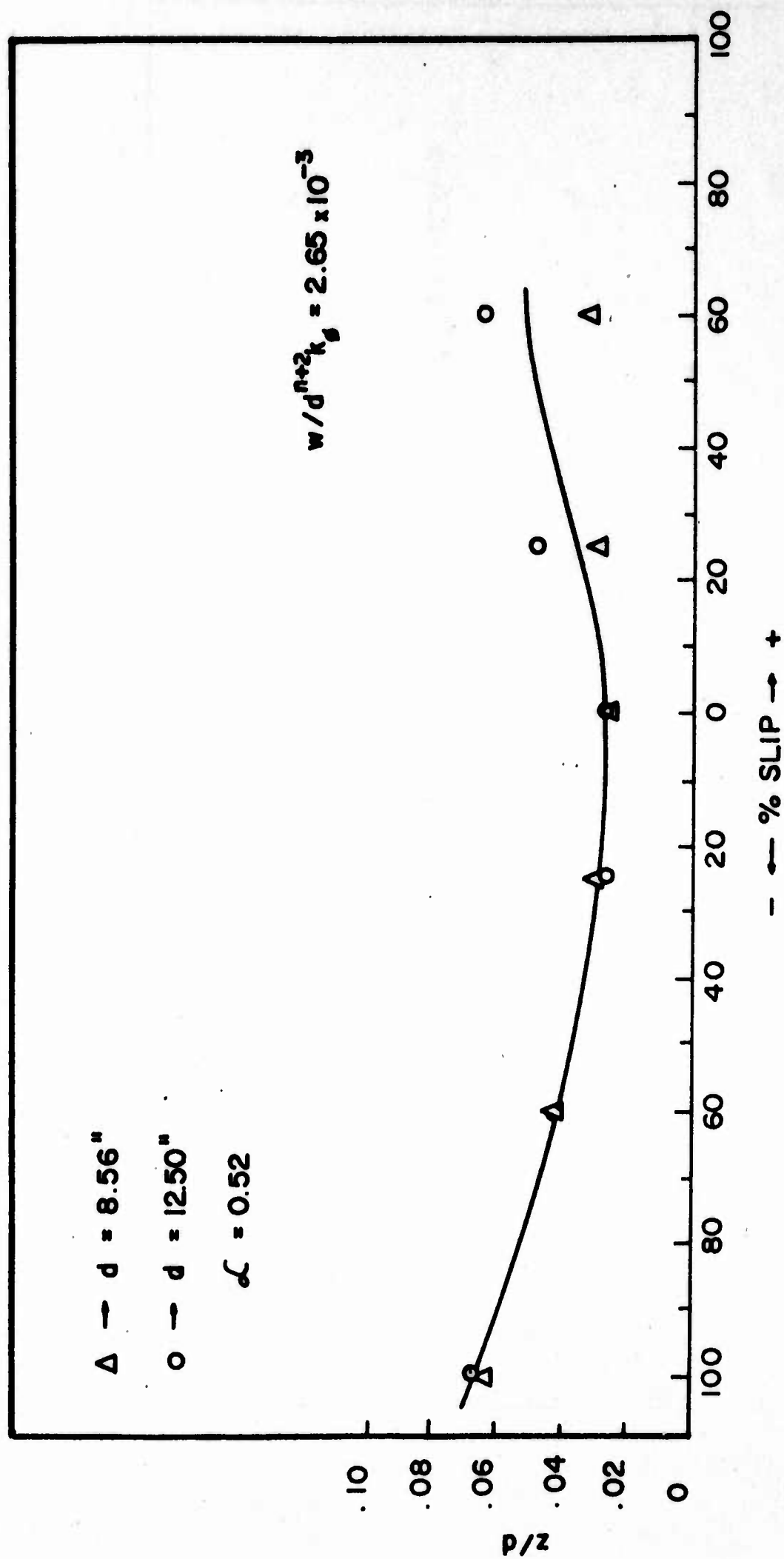


Fig. 22. Plot of (z/d) vs. % slip for $(w/d^{n+2}k_g = 2.656 \times 10^{-3})$ under similitude conditions.

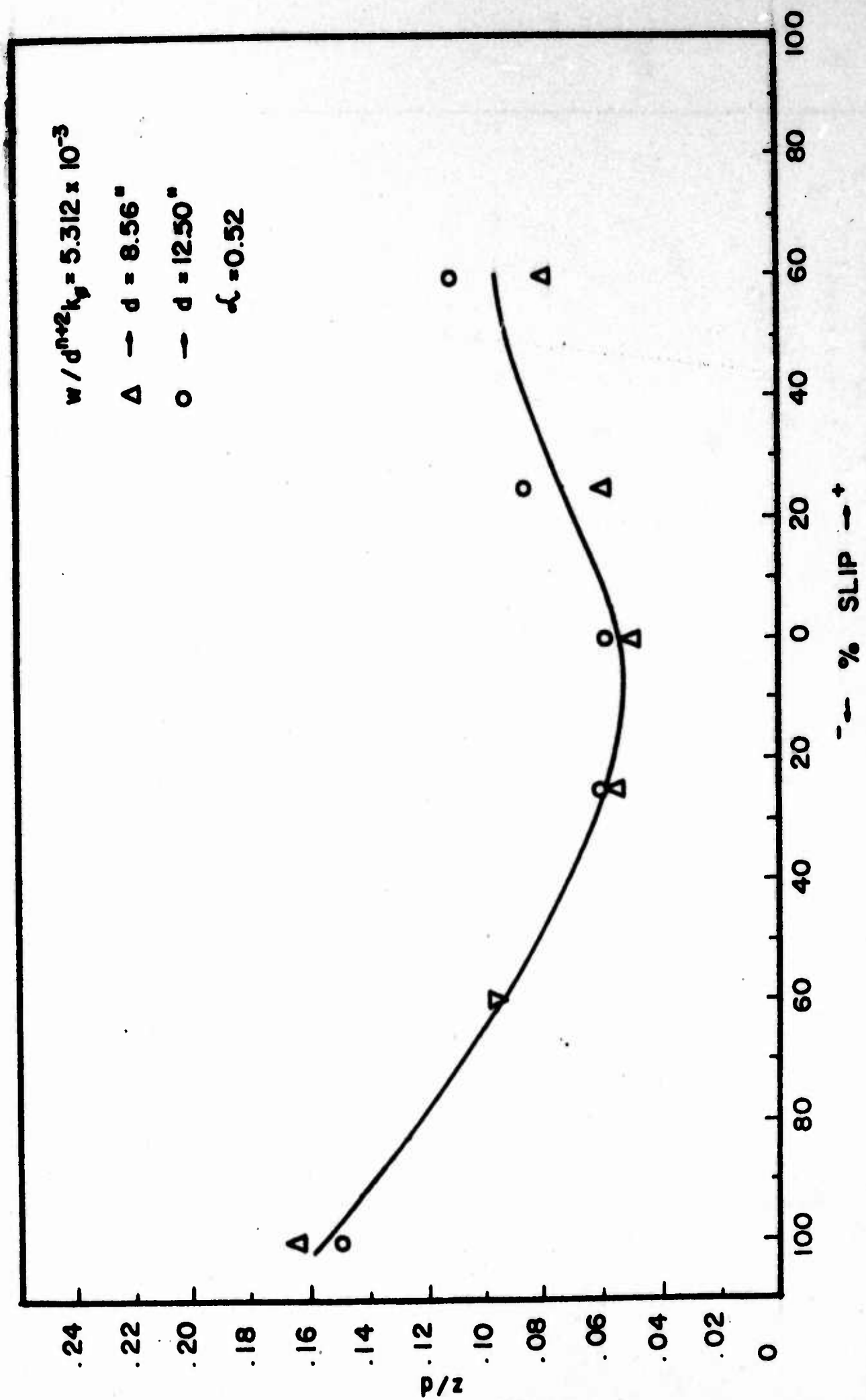


Fig. 23. Plot of (z/d) vs. % slip for $(w/d^{n+2}k_p = 5.312 \times 10^{-3})$ under similitude conditions.

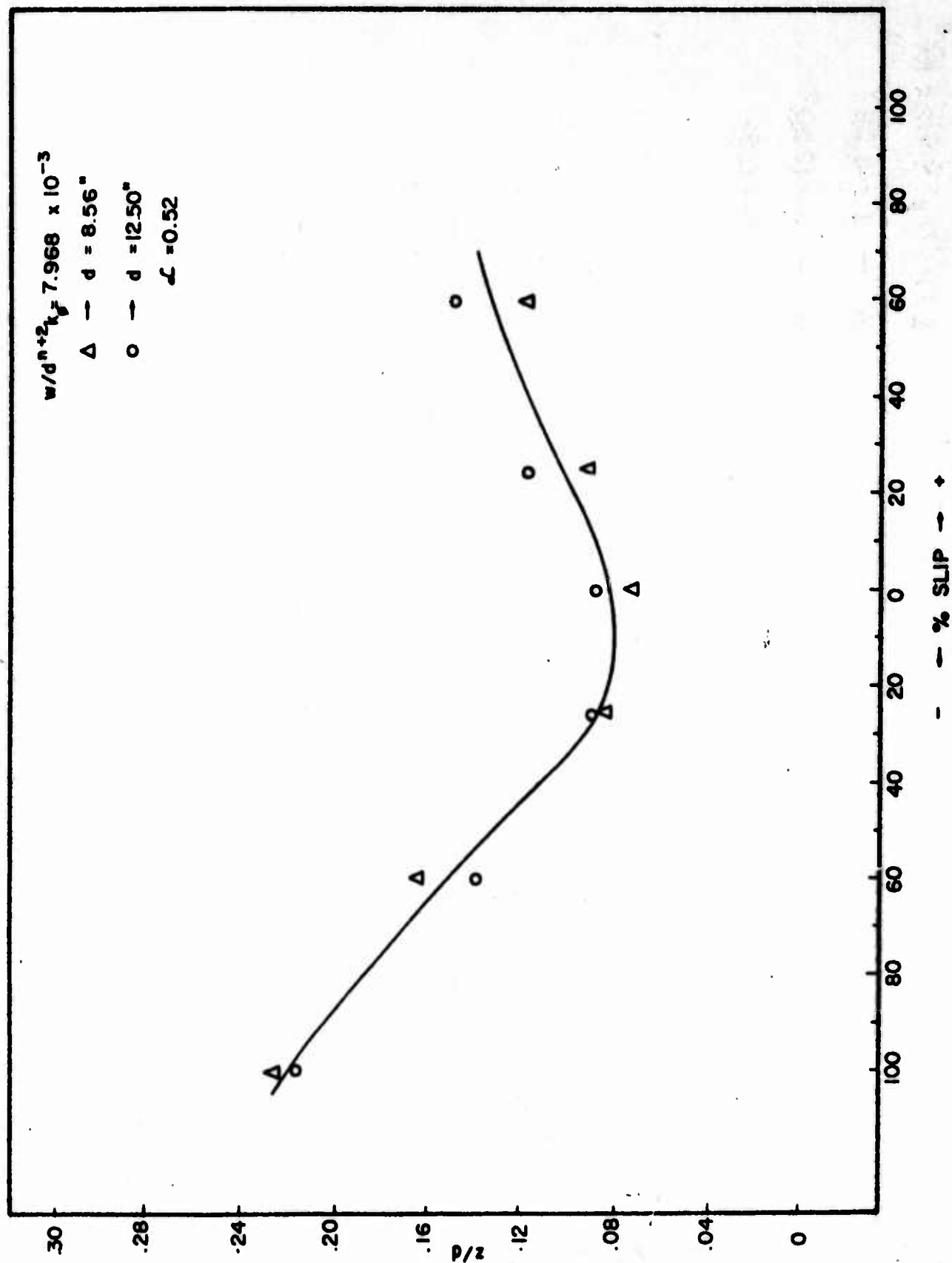


Fig. 24. Plot of (z/d) vs. % slip for $(w/d^{n+2}k_p = 7.968 \times 10^{-3})$ under similitude conditions.

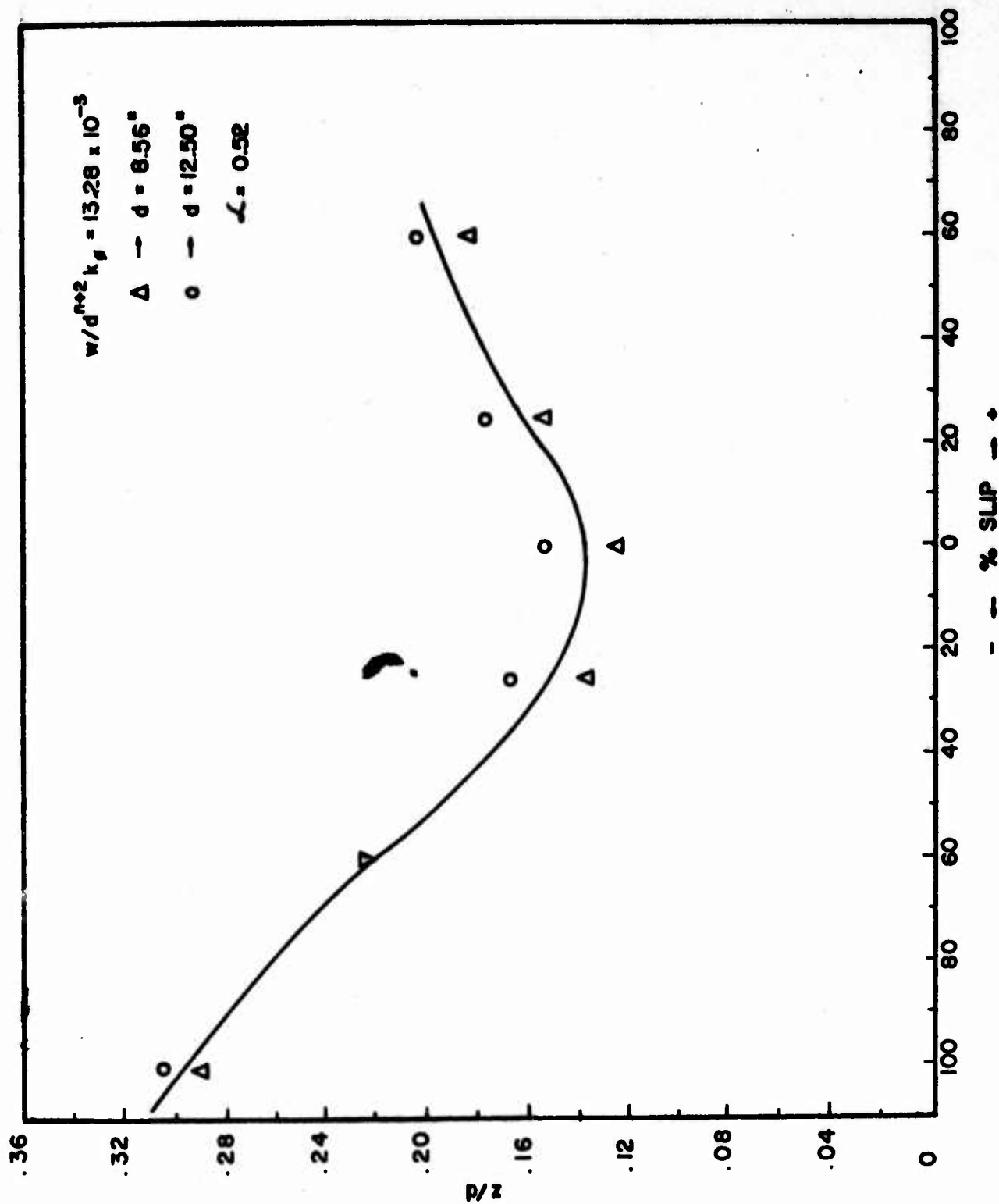


Fig. 25. Plot of (z/d) vs. % slip for $(w/d^{n+2} k_g = 13.28 \times 10^{-3})$ under similitude conditions.

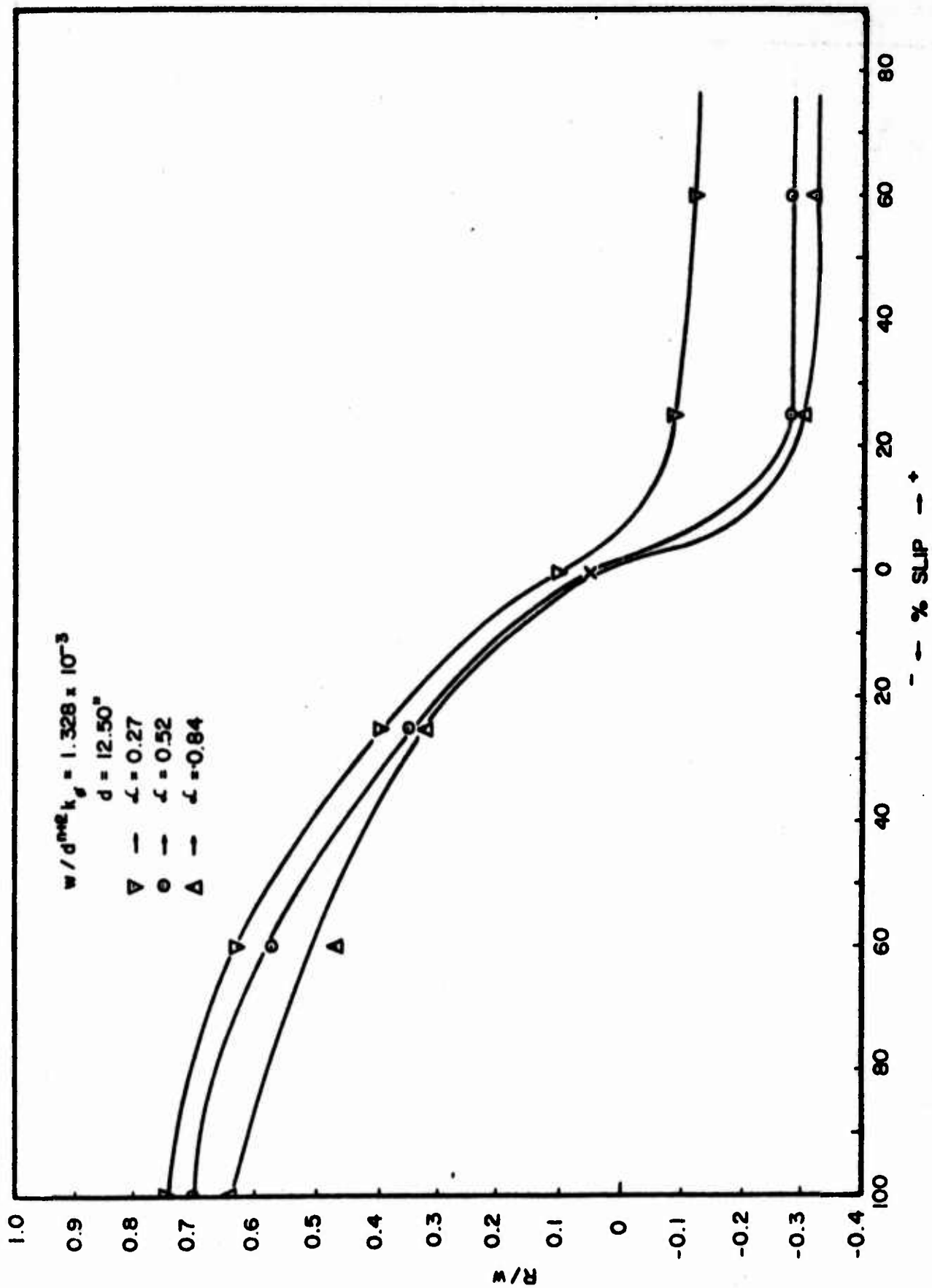


Fig. 26 Plot of (R/w) vs. % slip for $(w/d^{n+2} k_g = 1.328 \times 10^{-3})$ at various aspect ratios.

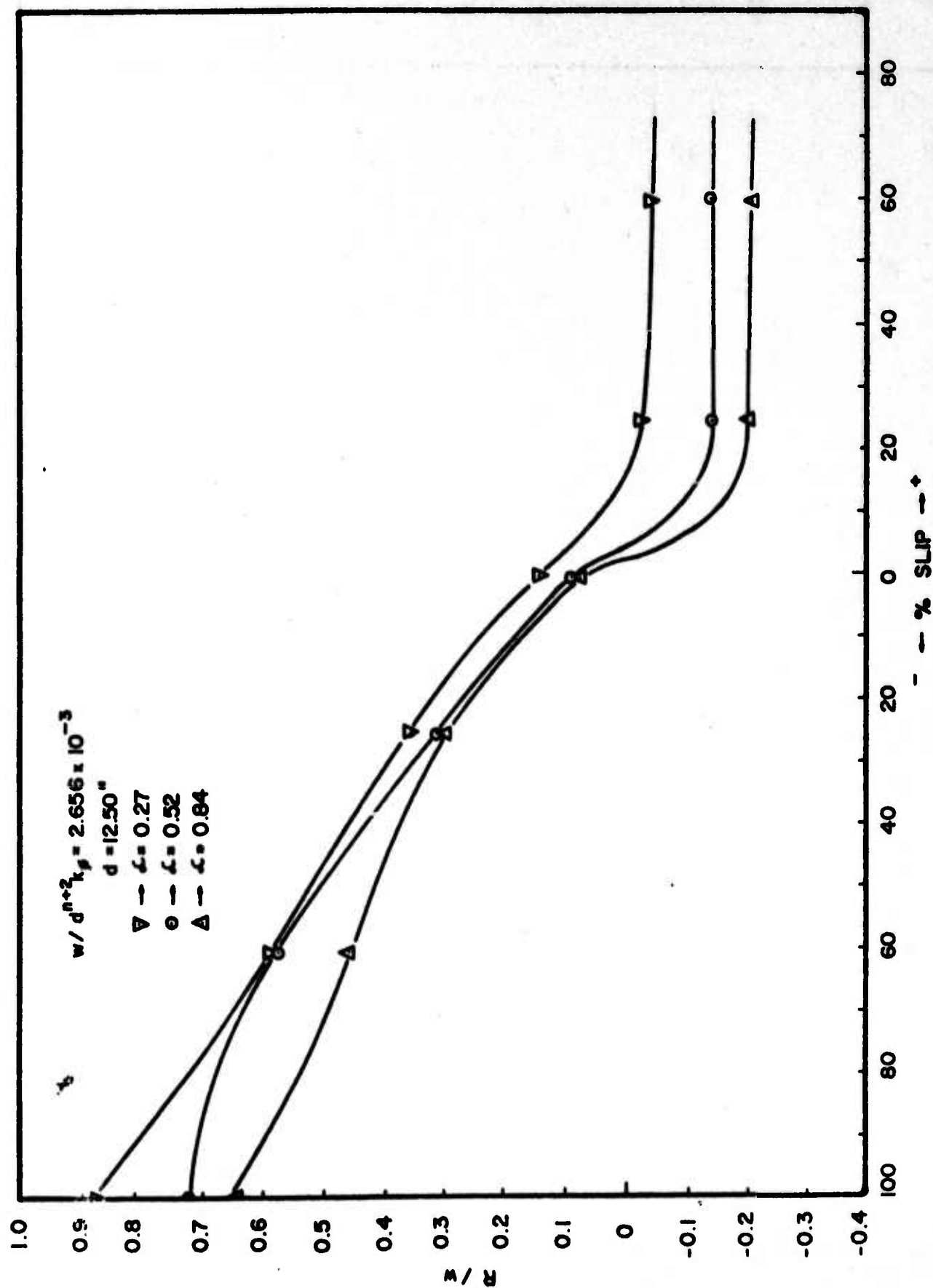


Fig. 27. Plot of (R/w) vs. % slip for $(w/d^{n+2}k_\phi = 2.656 \times 10^{-3})$ at various aspect ratios.

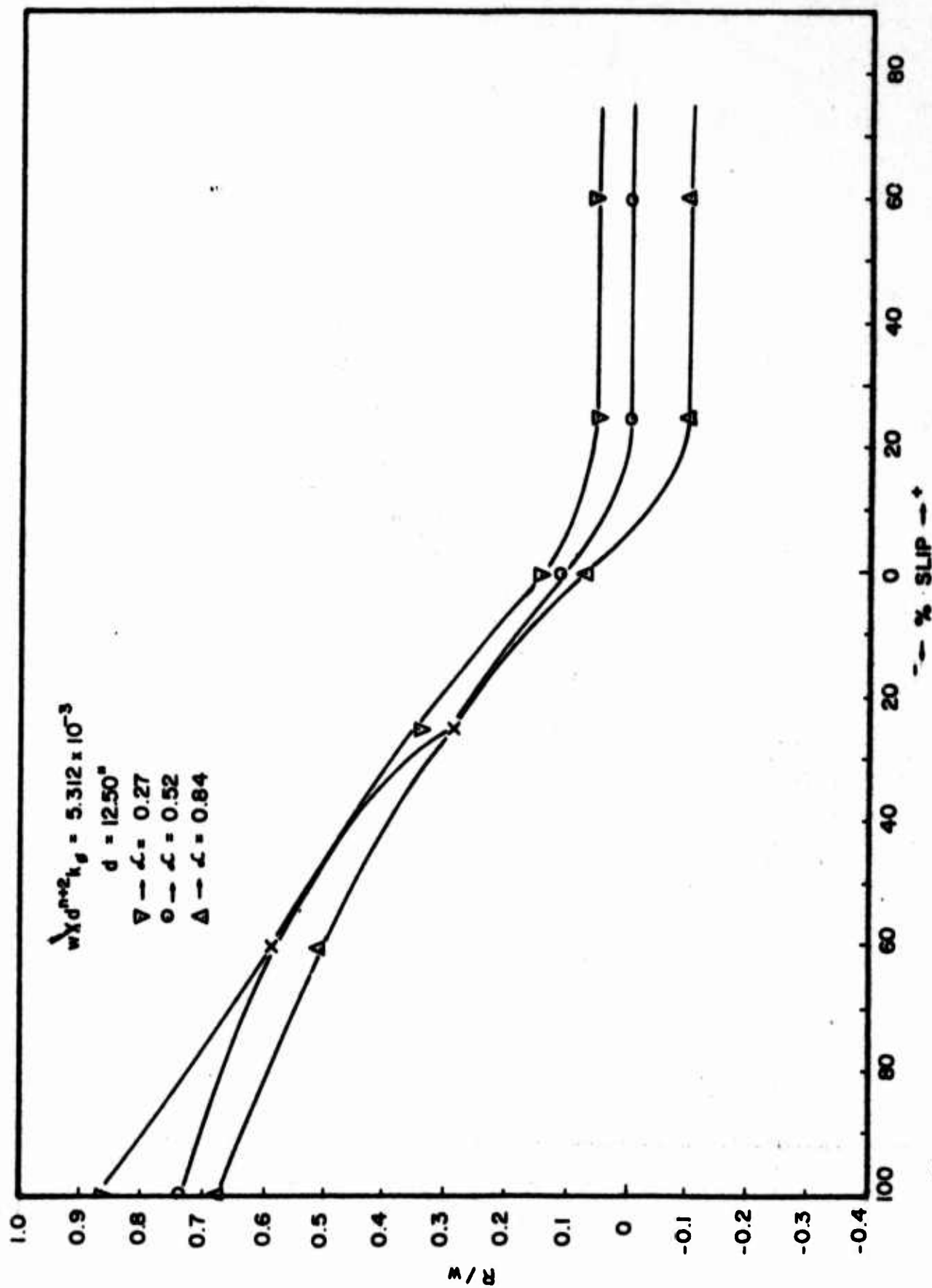


Fig. 28 Plot of (R/w) vs. % slip for $(w/d^{n+2} k_0 = 5.312 \times 10^{-3})$ at various aspect ratios.

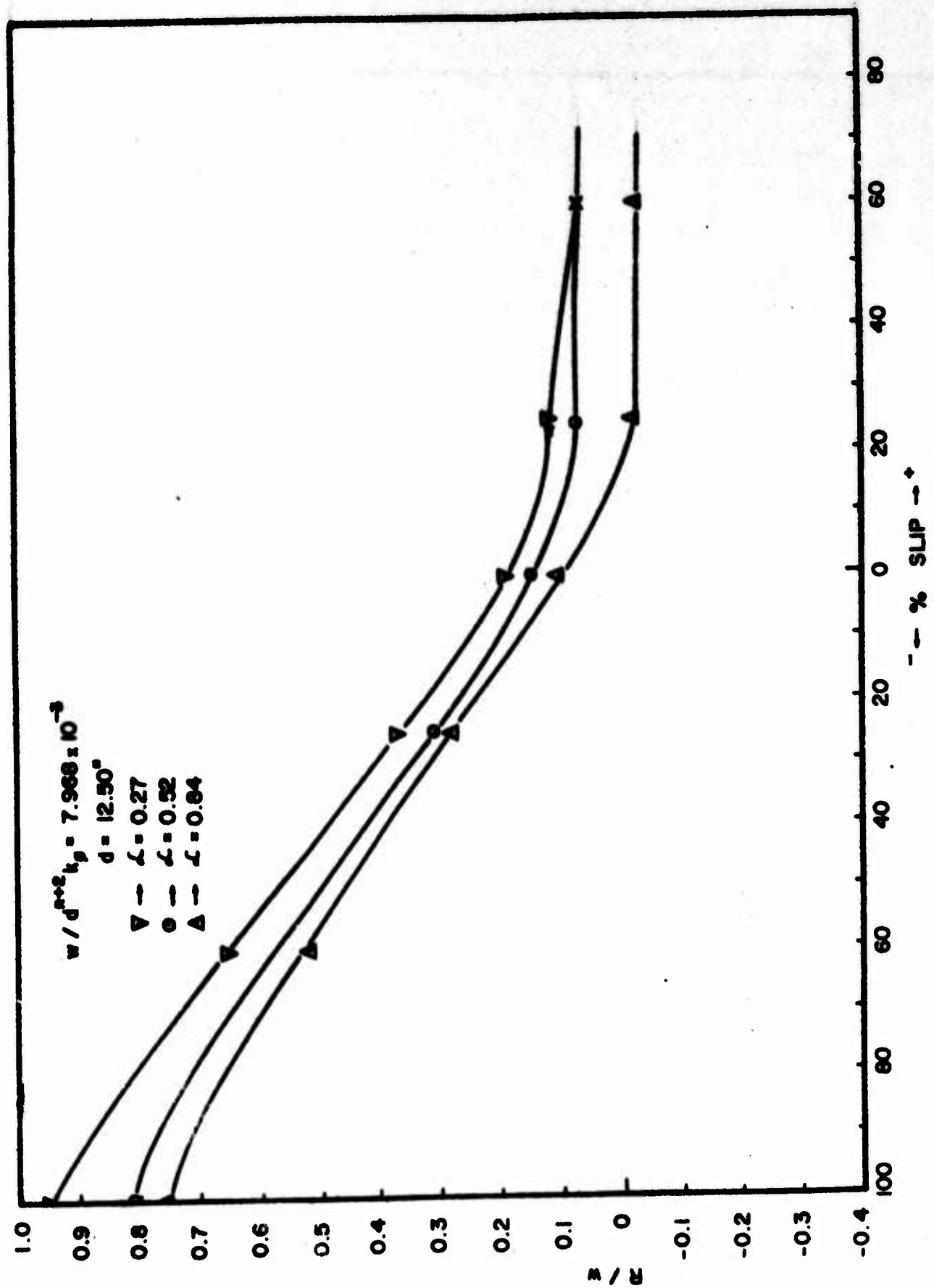


Fig. 29. Plot of (R/w) vs. $\%$ slip for $(w/d^{n+2}k_p = 7.968 \times 10^{-3})$ at various aspect ratios.

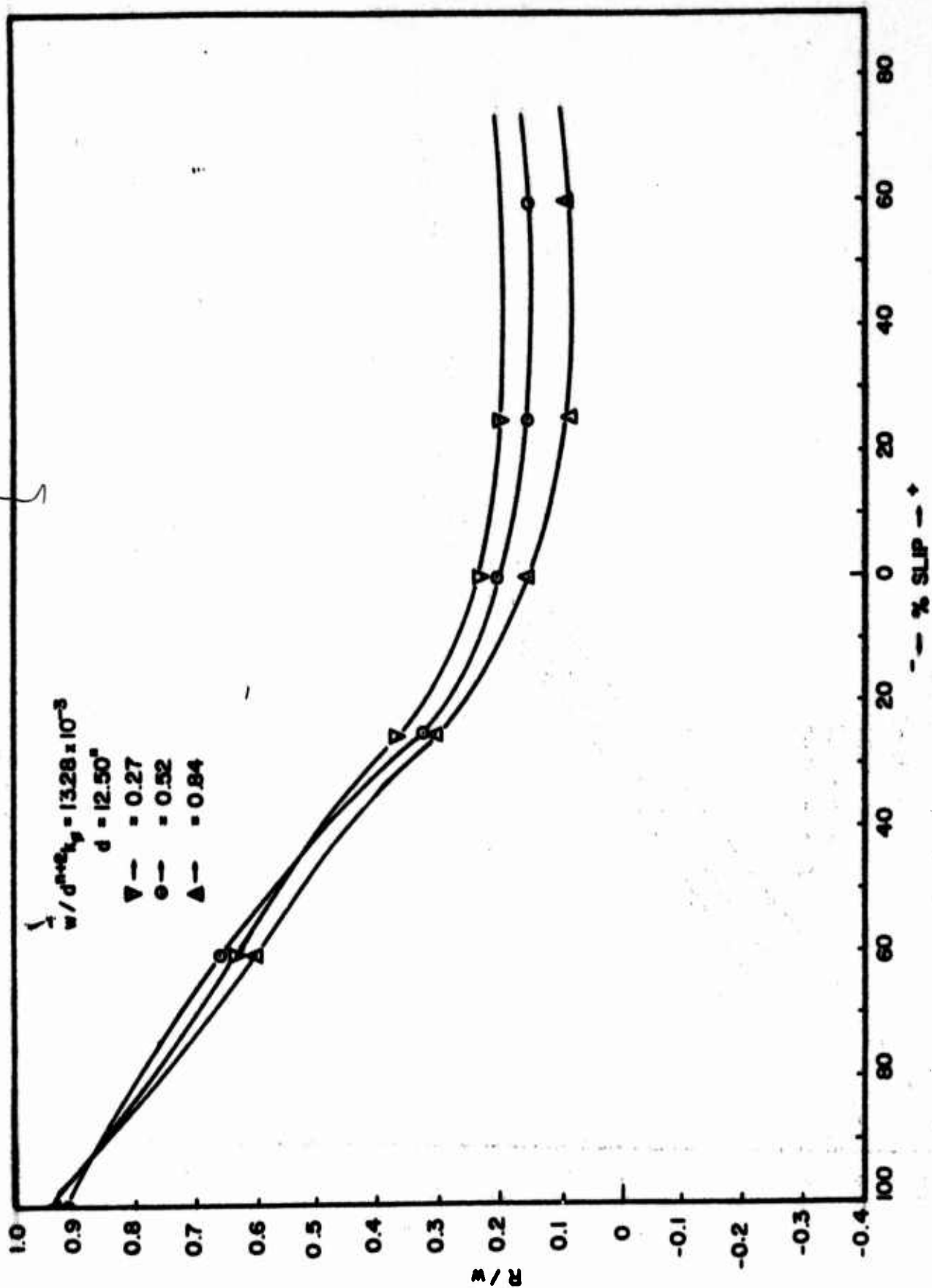


Fig. 30. Plot of (R/w) vs. $\% \text{ slip}$ for $(w/d^{n+2}k_p = 13.28 \times 10^{-3})$ at various aspect ratios.

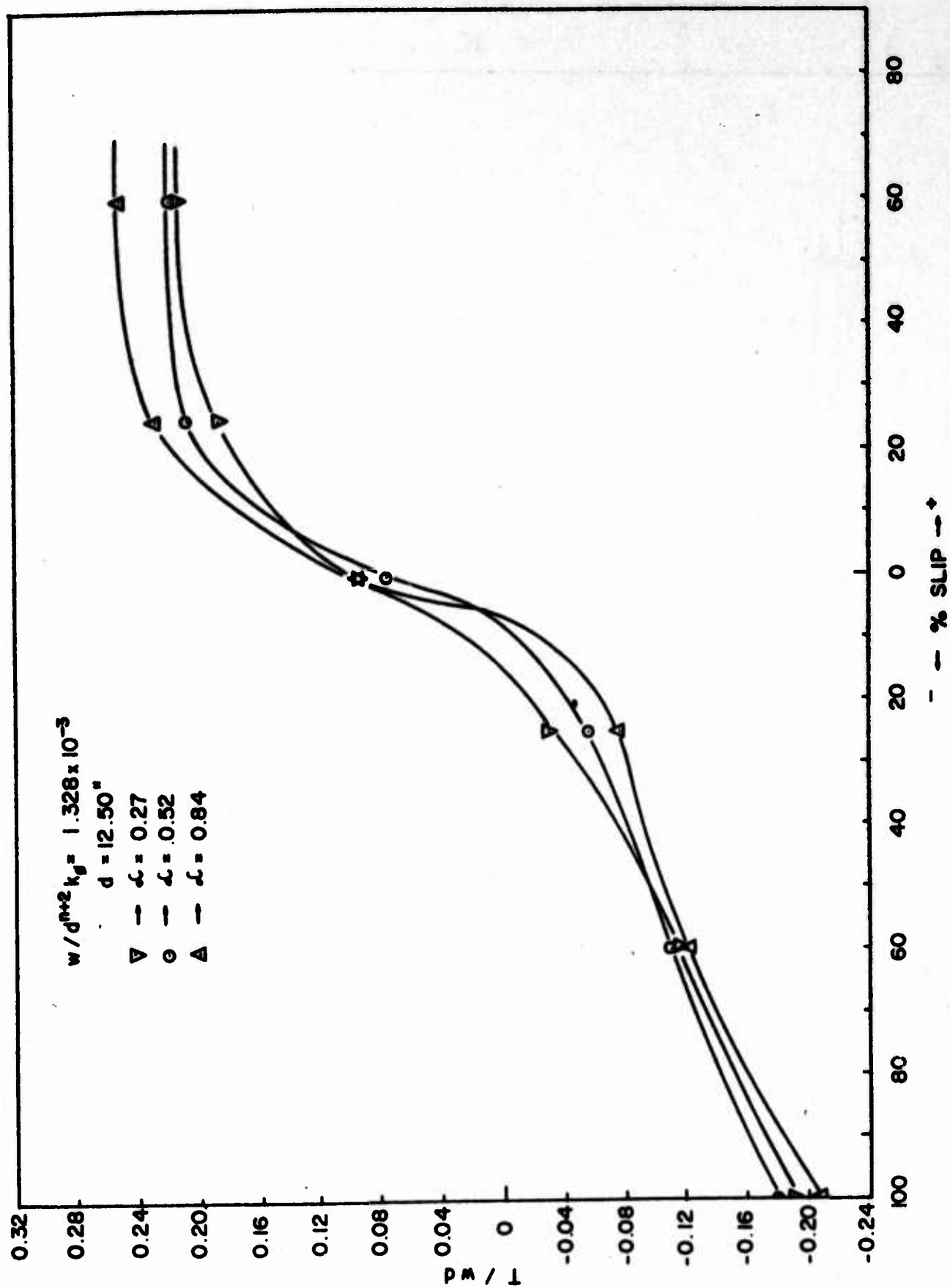


Fig. 31. Plot of (T/wd) vs. % slip for $(w/d^{n+2}k_g = 1.328 \times 10^{-3})$ at various aspect ratios.

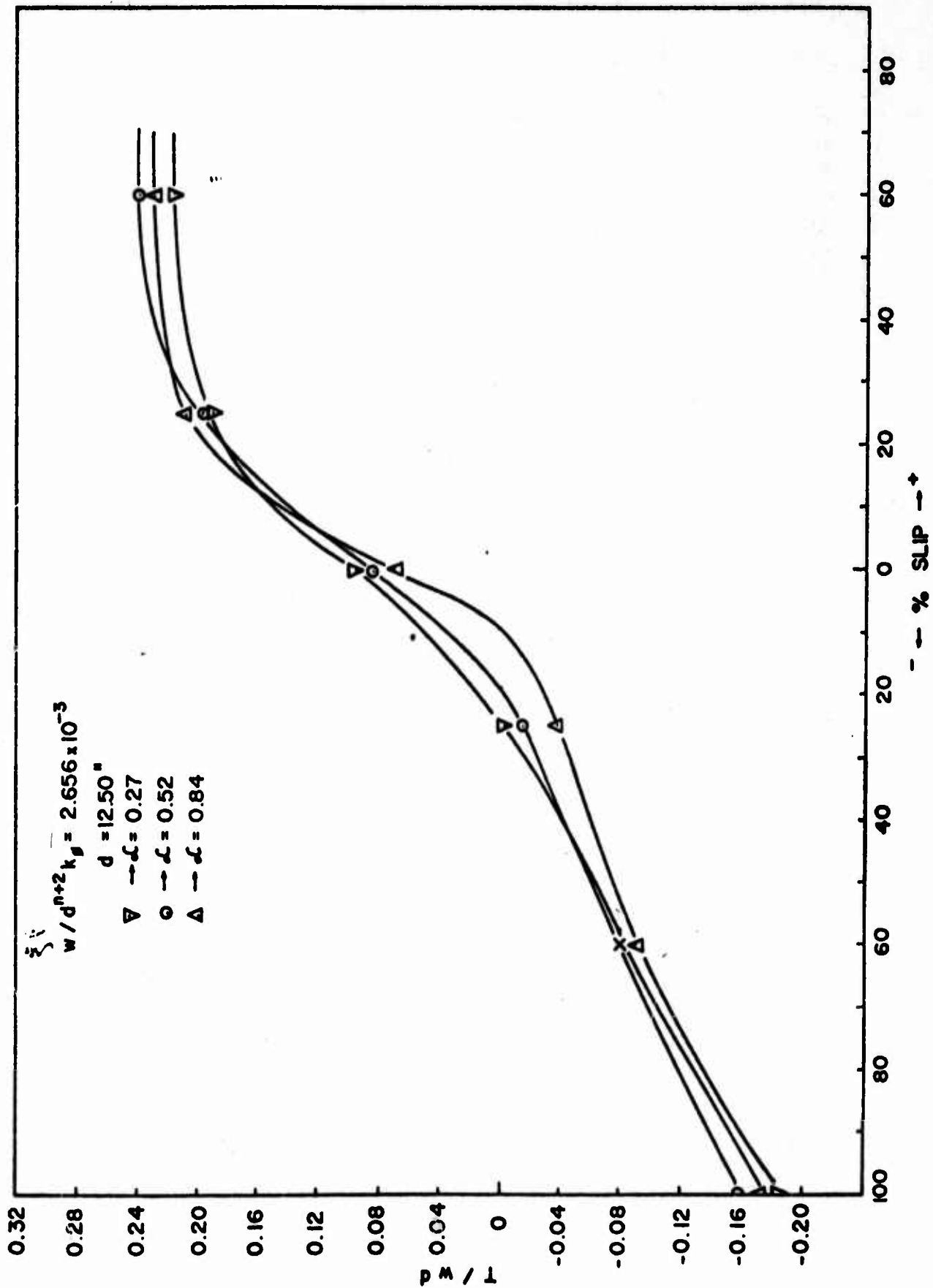


Fig. 32. Plot of (T/wd) vs. $\%$ slip for $(w/d^{n+2}k_g = 2.656 \times 10^{-3})$ at various aspect ratios.

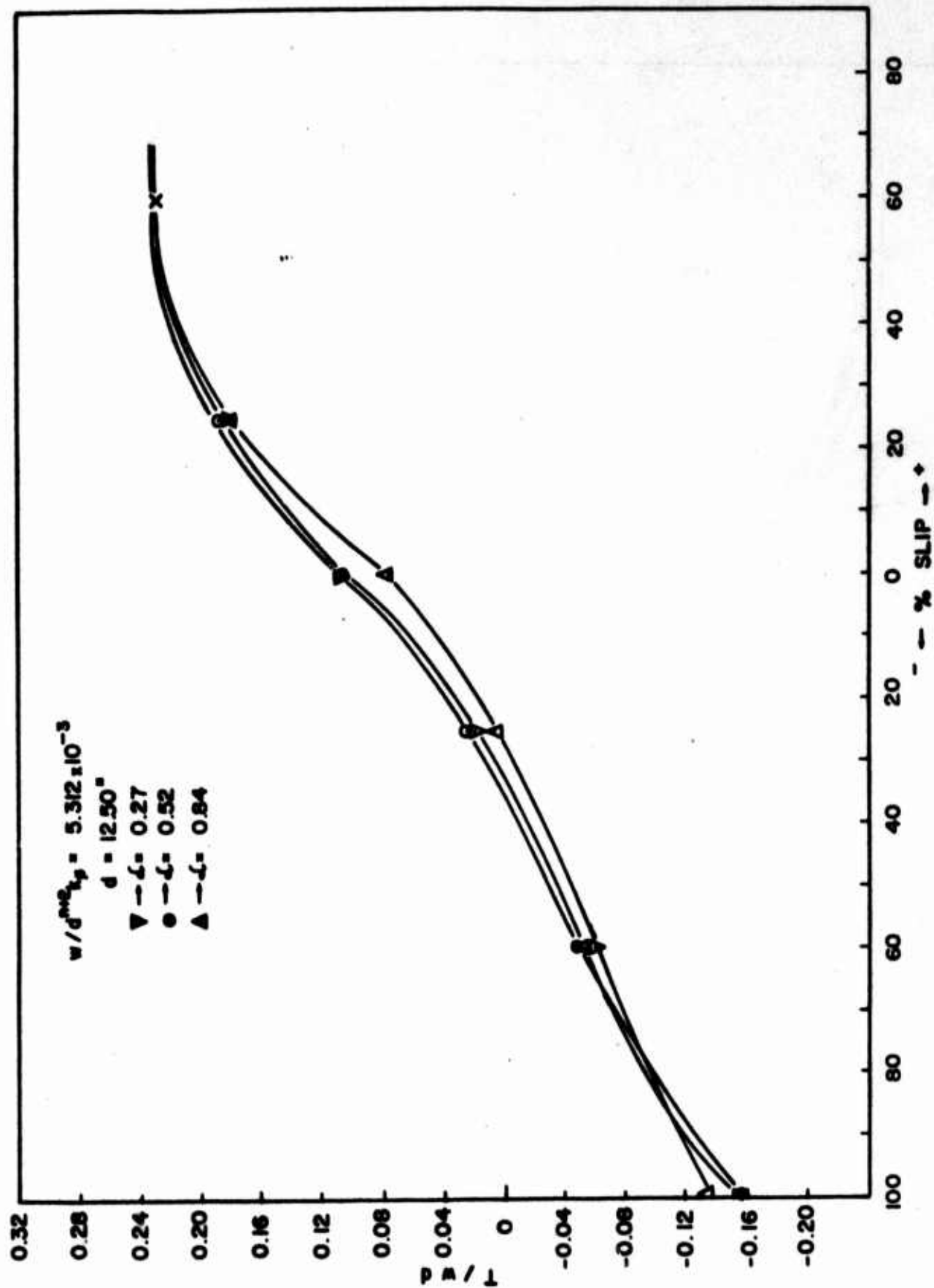


Fig. 33. Plot of (T/wd) vs. % slip for $(w/d^{n+2}k_0 = 5.312 \times 10^{-3})$ at various aspect ratios.

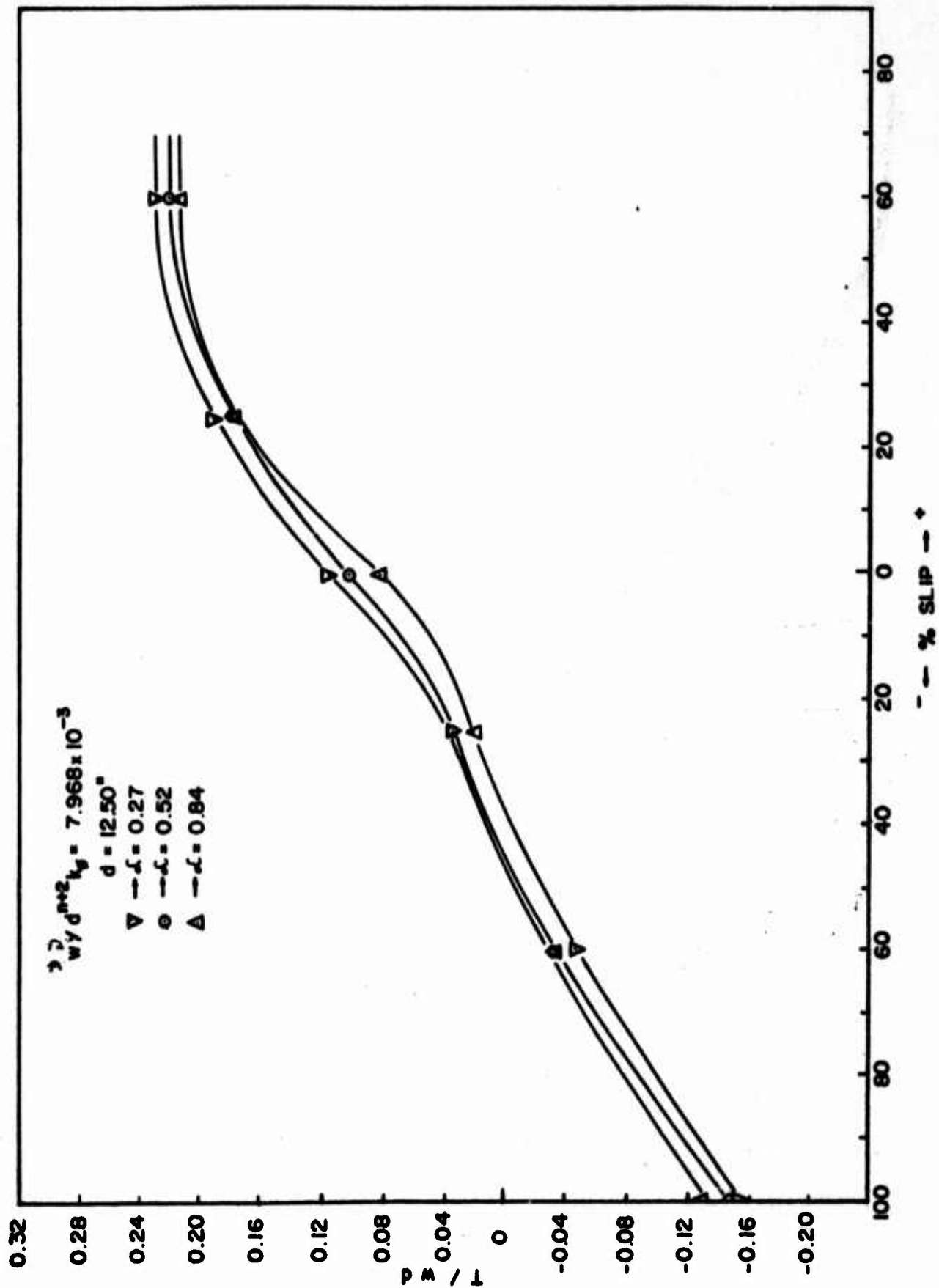


Fig. 34. Plot of (T/wd) vs. % slip for $(w/d^{n+2} k_p = 7.968 \times 10^{-3})$ at various aspect ratios.

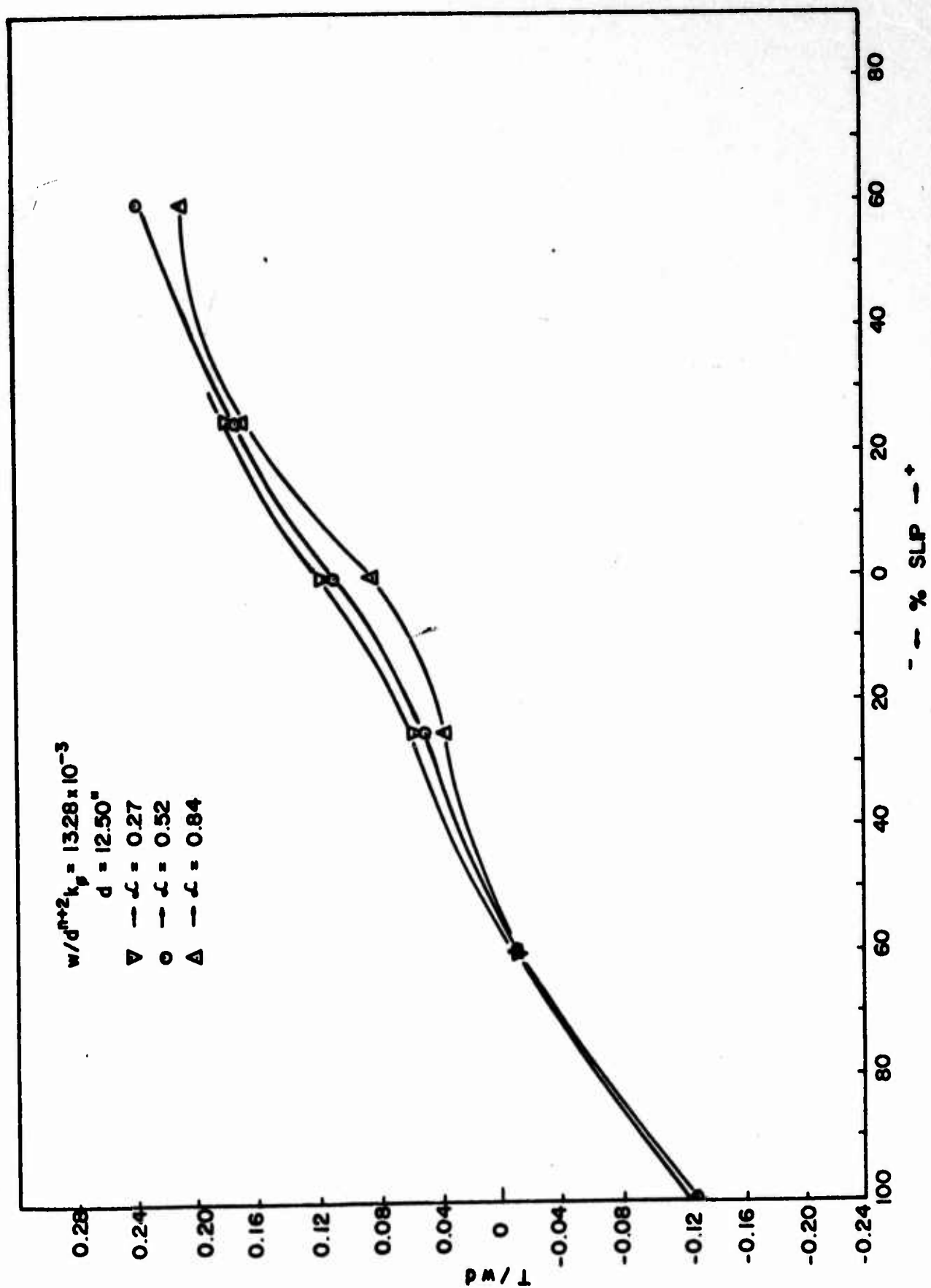


Fig. 35 Plot of (T/wd) vs. % slip for $(w/d^{n+2}k_\phi = 13.28 \times 10^{-3})$ at various aspect ratios.

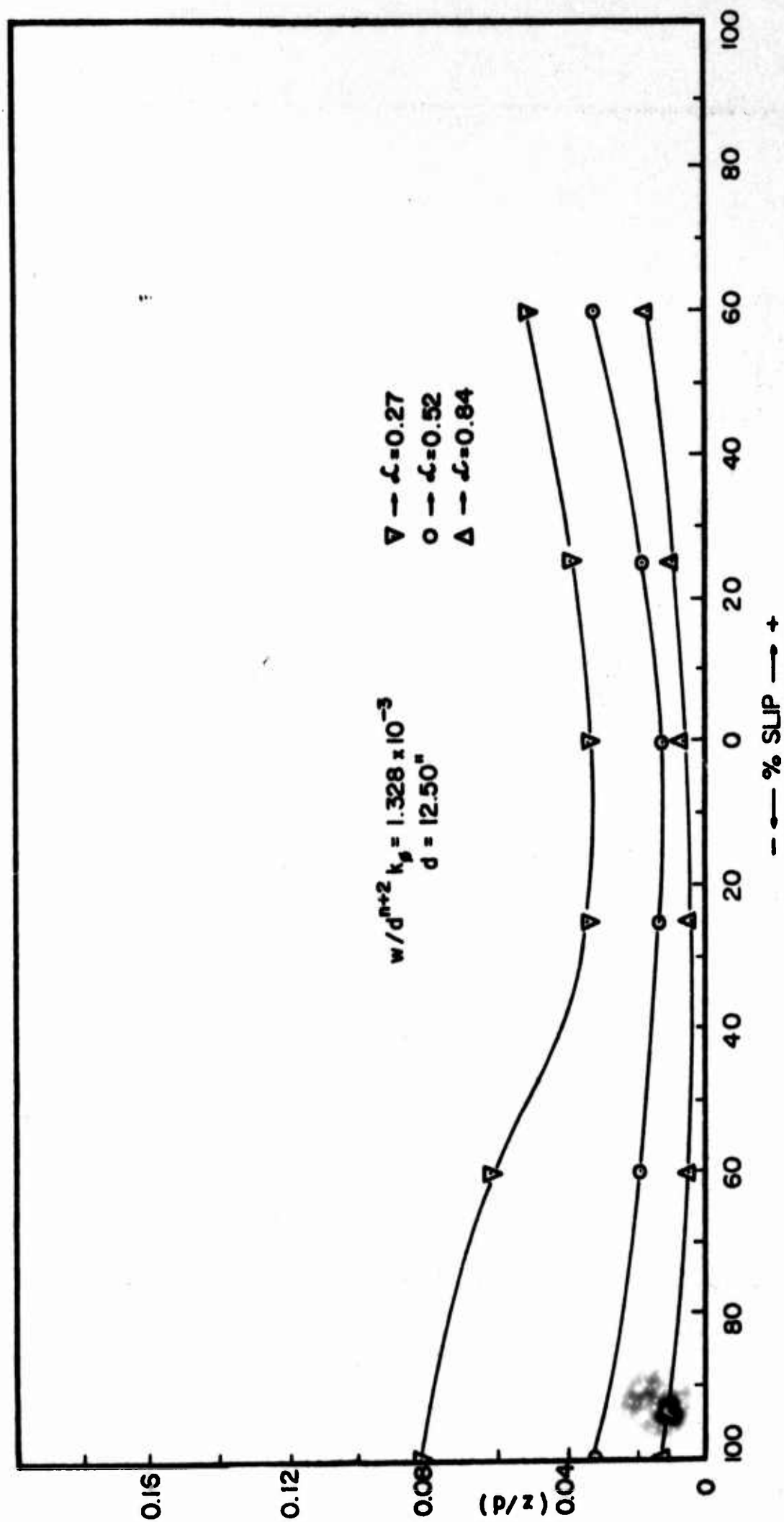


Fig. 36. Plot of (z/d) vs. % slip for $(w/d^{n+2}k_g = 1.328 \times 10^{-3})$ at various aspect ratios.

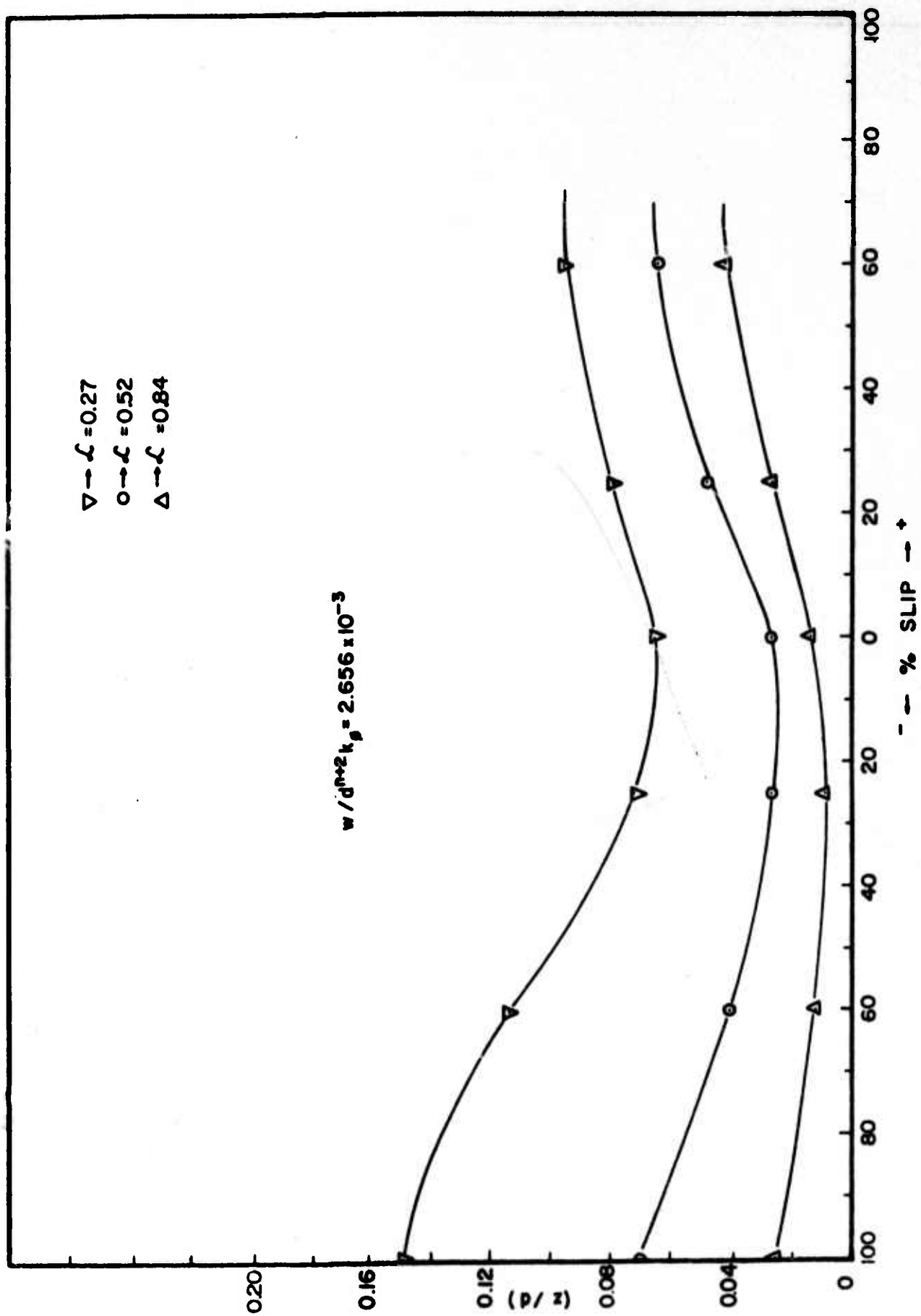


Fig. 37. Plot of (z/d) vs. $\%$ slip for $(w/d^{n+2}k_p = 2.656 \times 10^{-3})$ at various aspect ratios.

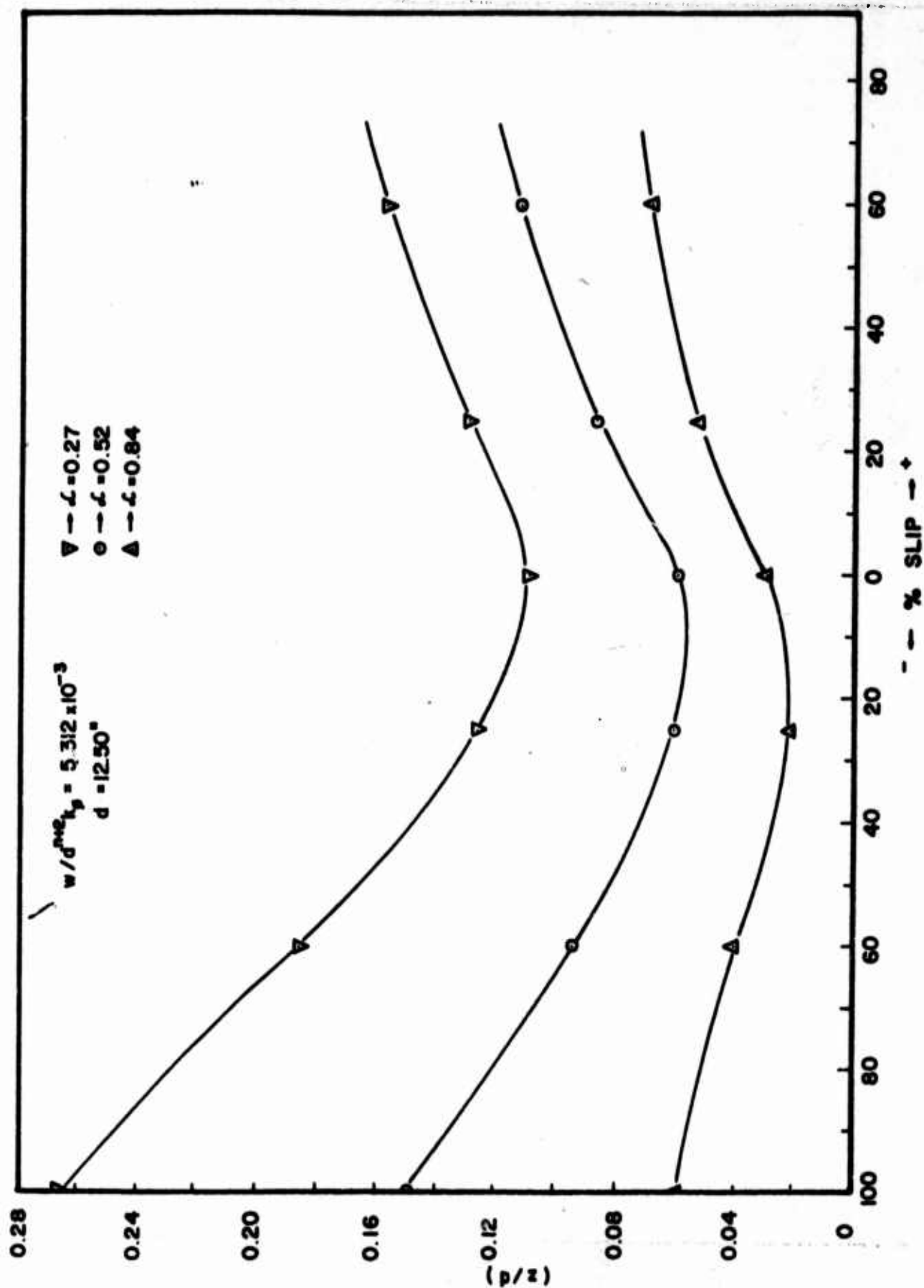


Fig. 38. Plot of (z/d) vs. $\%$ slip for $(w/d^{n+2}k_p = 5.312 \times 10^{-3})$ at various aspect ratios.

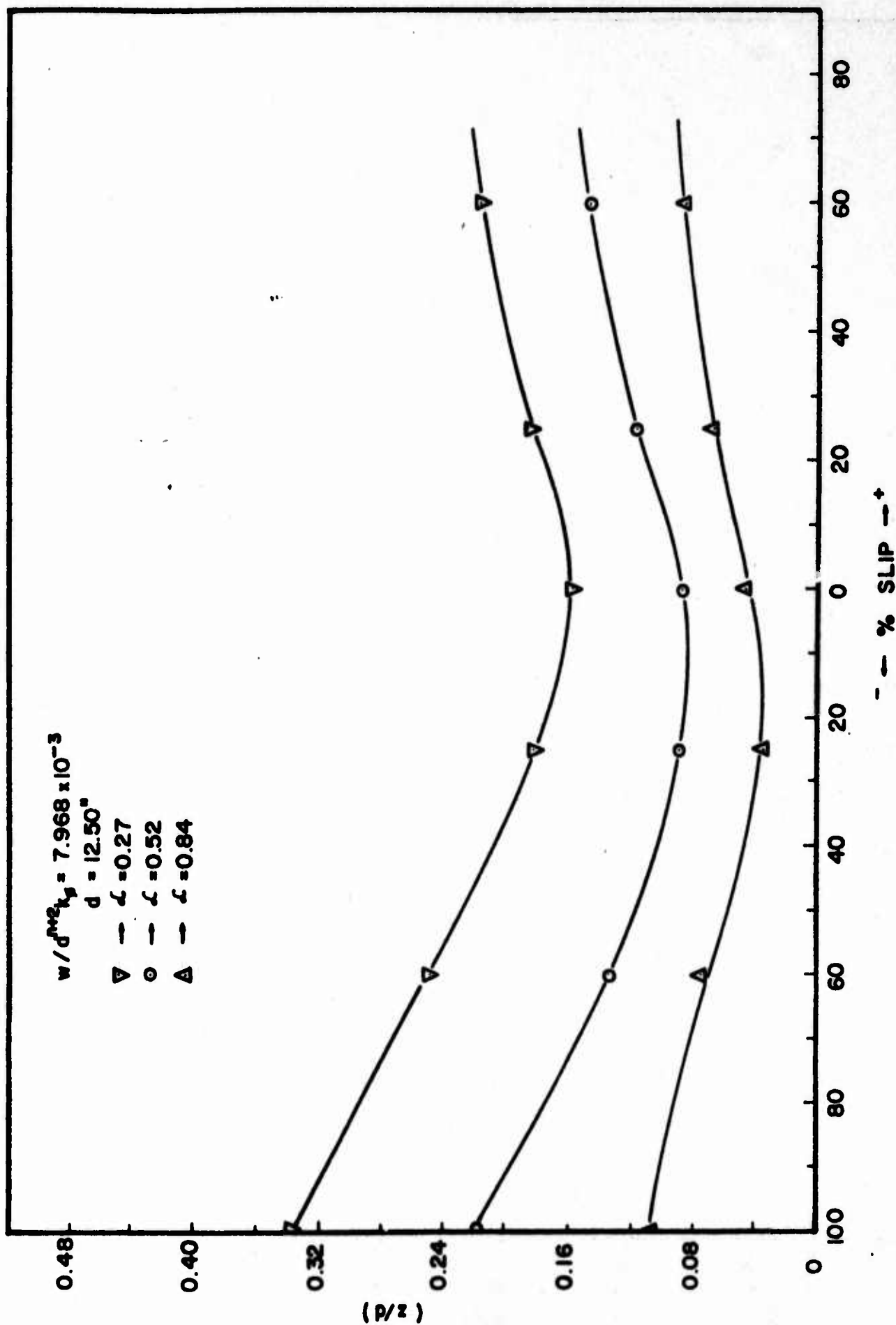


Fig. 39. Plot of (z/d) vs. % slip for $(w/d^{n+2}k_p - 7.968 \times 10^{-3})$ at various aspect ratios.

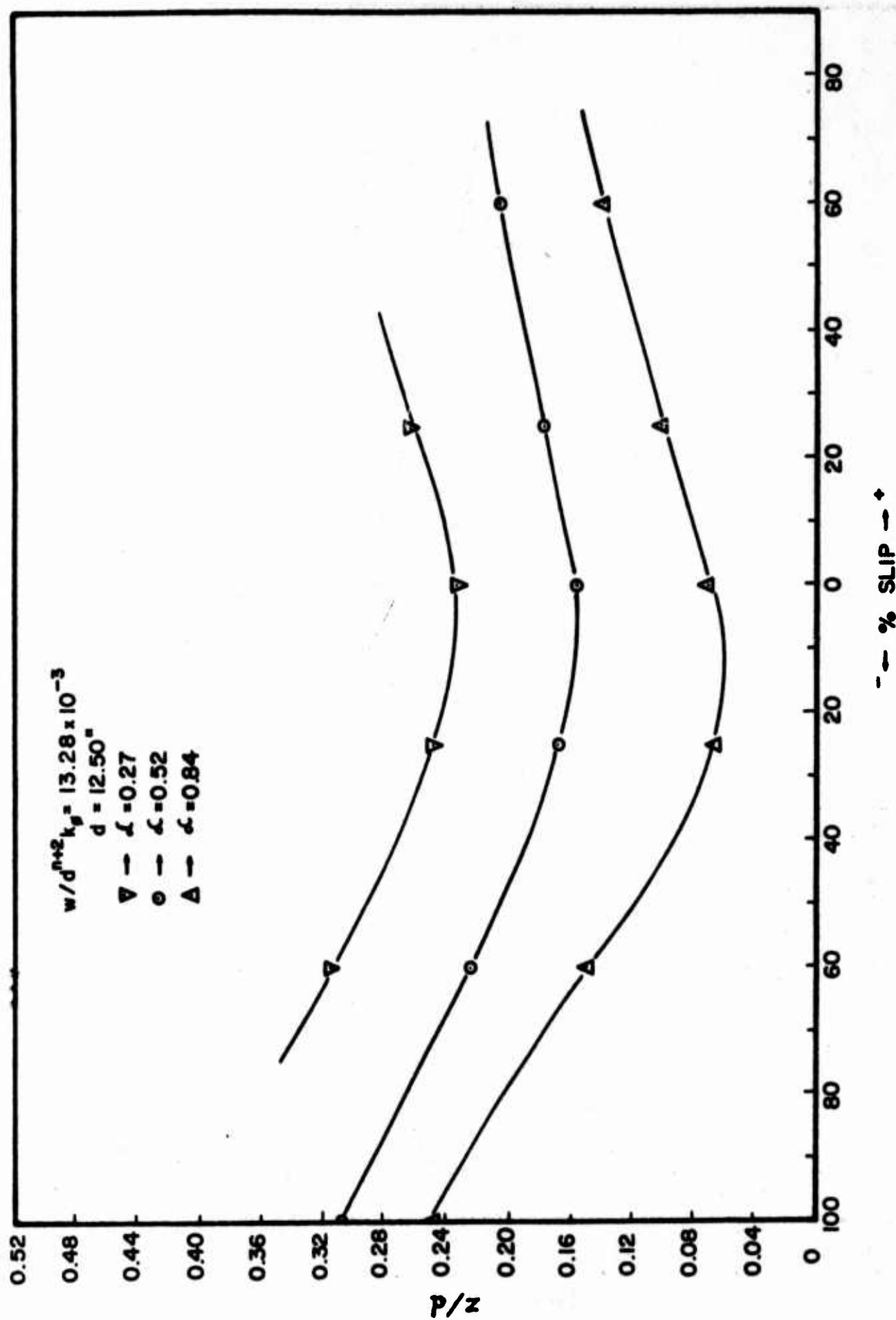


Fig. 40 Plot of (z/d) vs. % slip for $(w/d^{n+2} k_0 = 13.28 \times 10^{-3})$ at various aspect ratios.

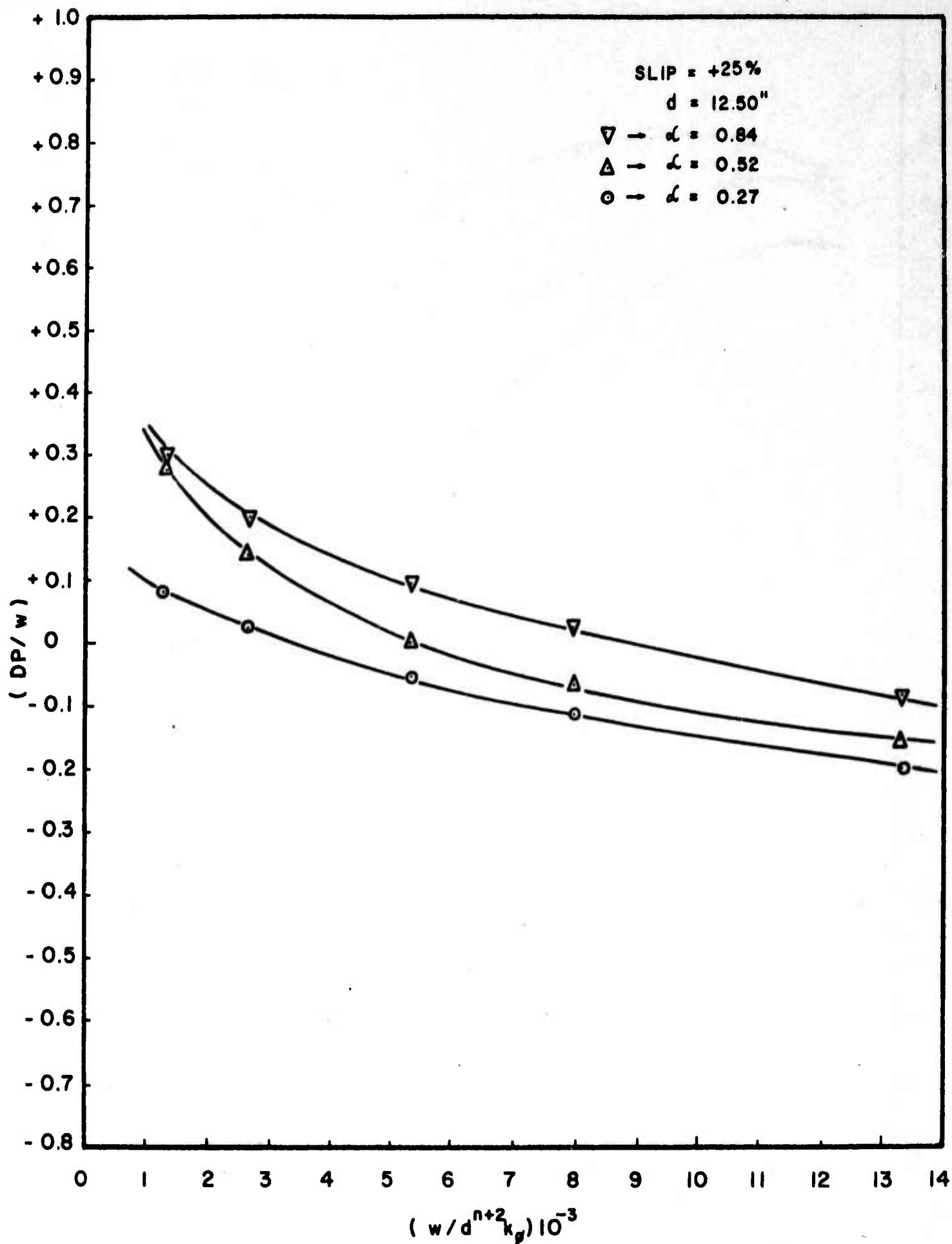


Fig. 41. Plot of (DP/w) vs. $(w/d^{n+2} k_{\phi}) 10^{-3}$ at +25% slip and various aspect ratios.

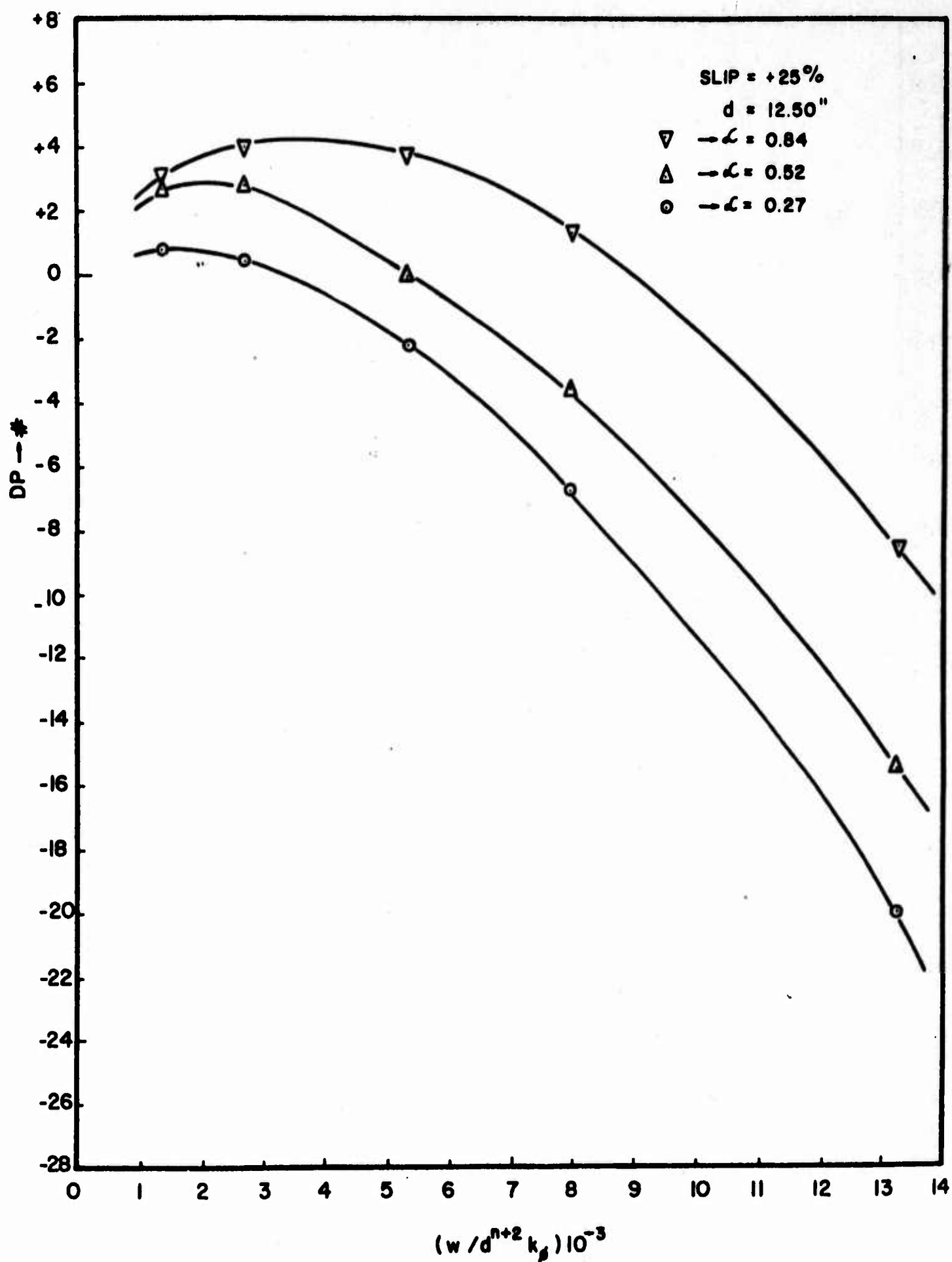


Fig. 42. Plot of DP vs. $(w/d^{n+2} k_{\phi}) 10^{-3}$ at +25% slip and various aspect ratios.

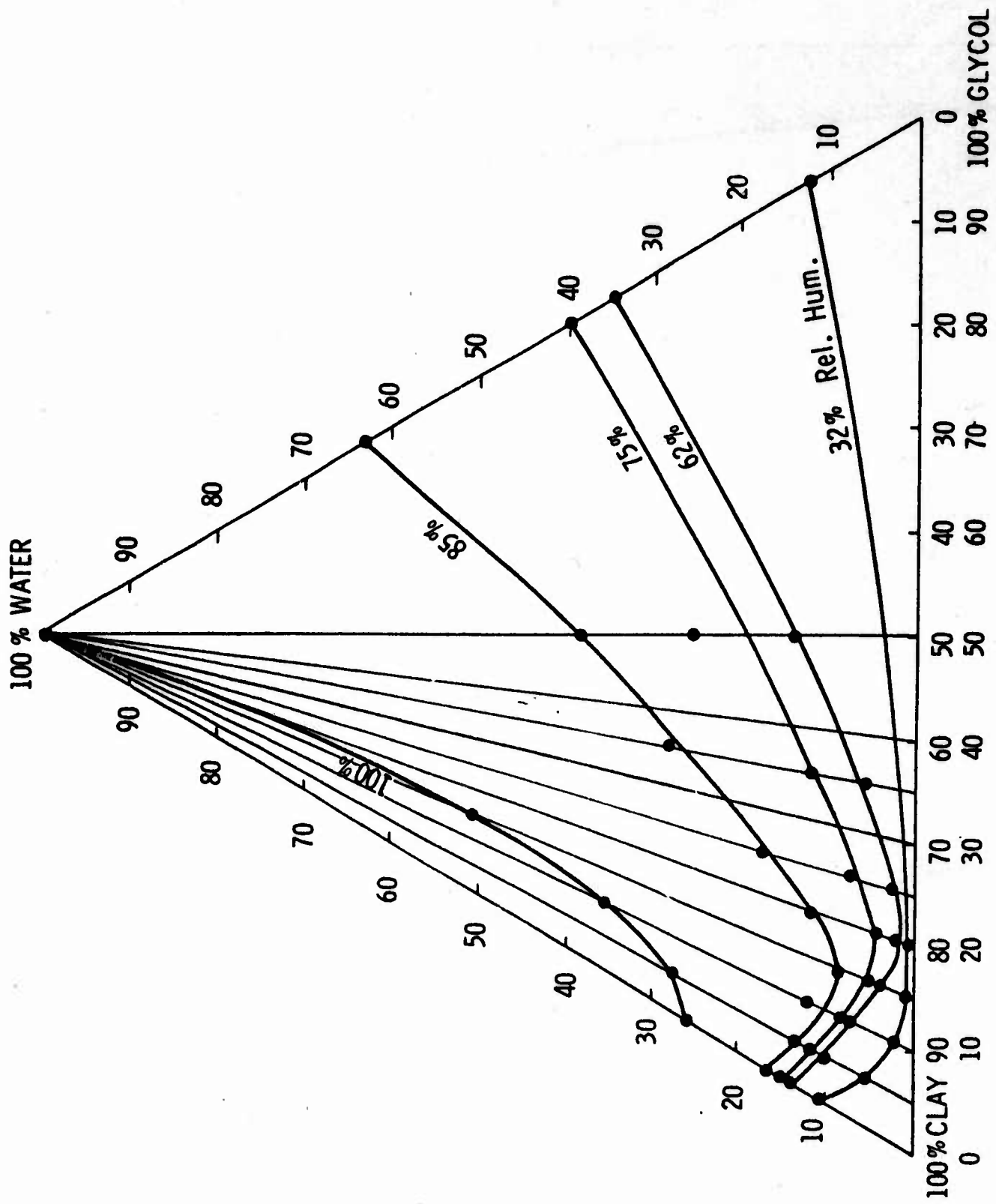


Fig. 43. Composition of the 3-component substance (water, clay, glycol) in equilibrium with humid air at 75°F, 1 atmos. pressure.

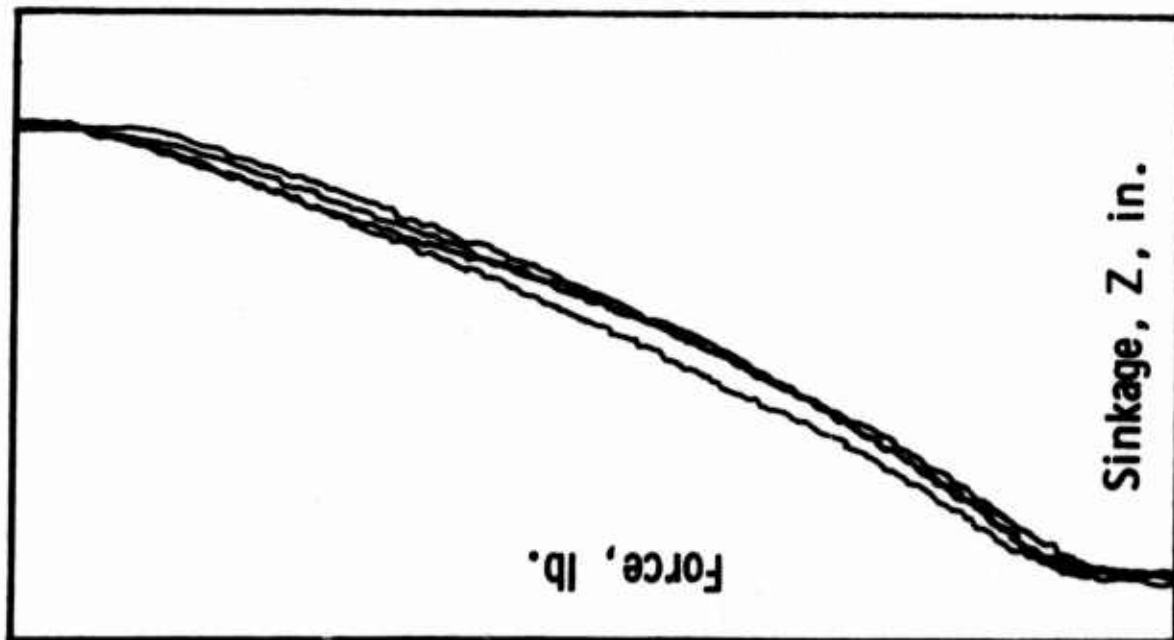


Fig. 44. Pressure and sinkage relationship of sand with stirring.

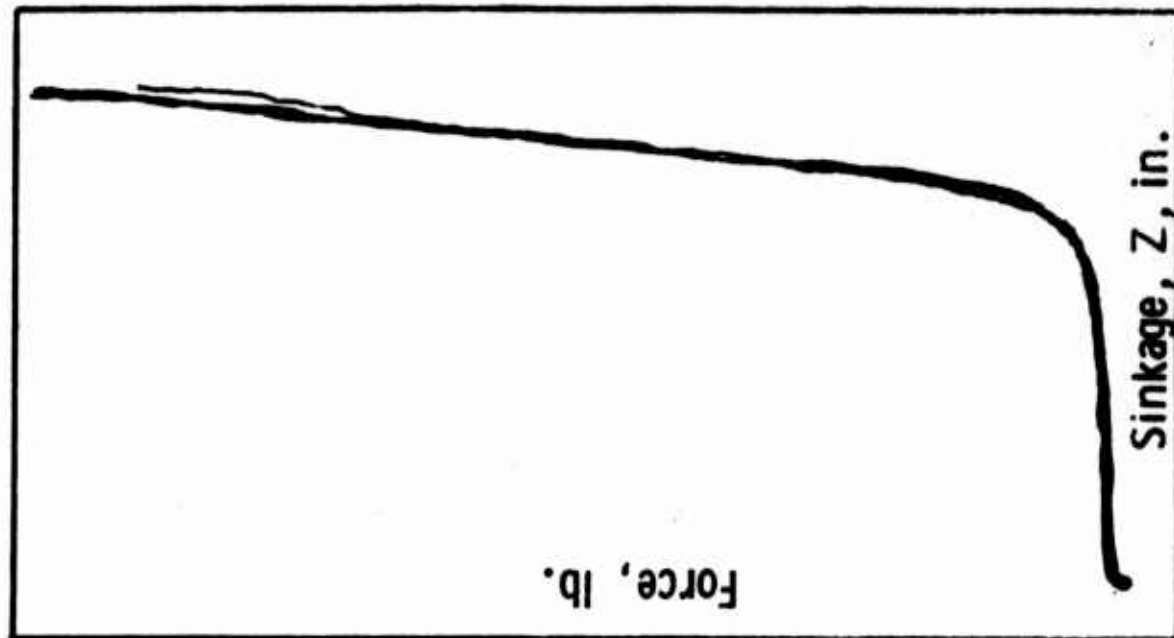


Fig. 45. Pressure and sinkage relationship of nonmagnetic barium ferrite with stirring.

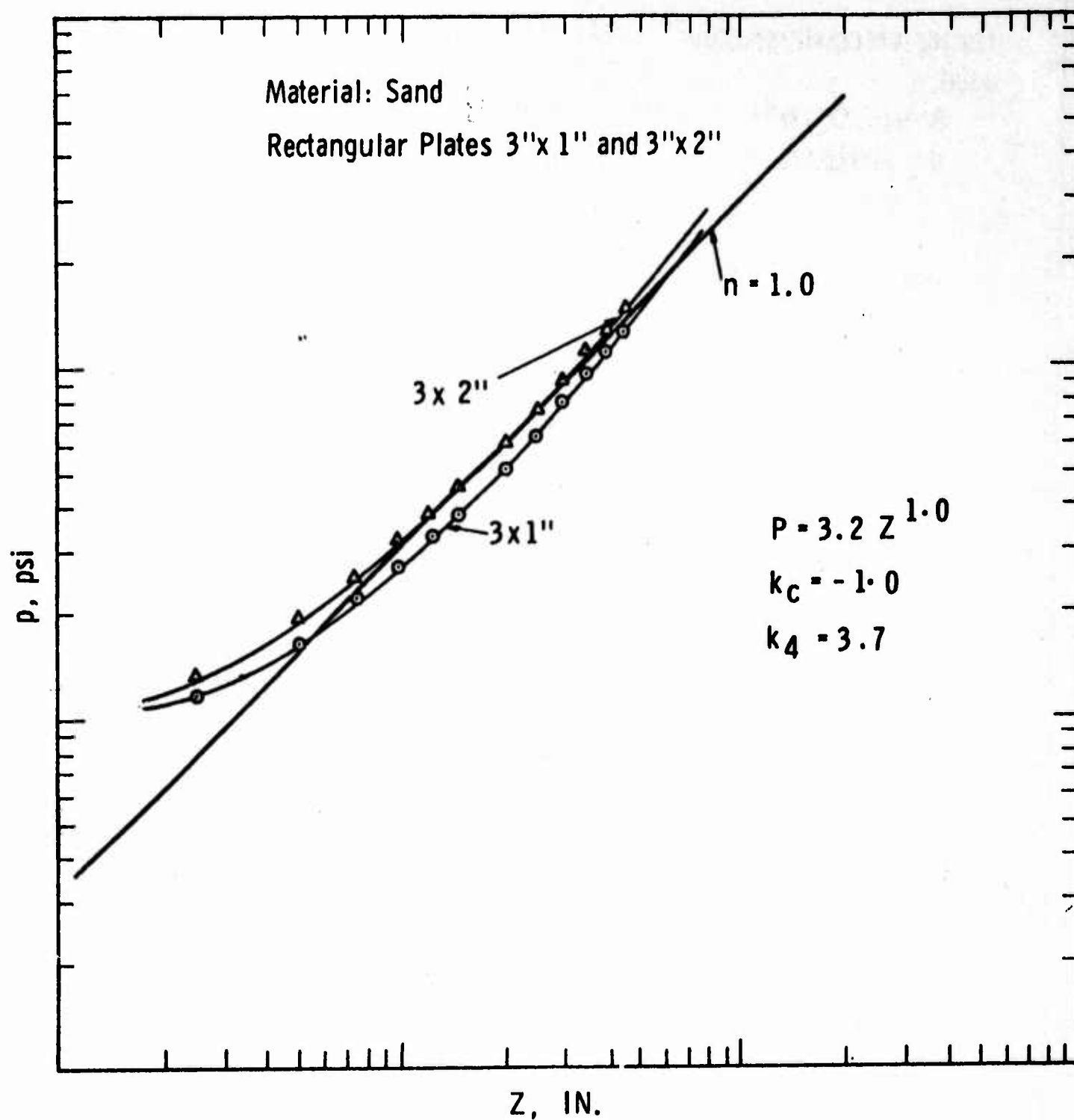


Fig. 46. Pressure vs. sinkage of a flat plate in sand.

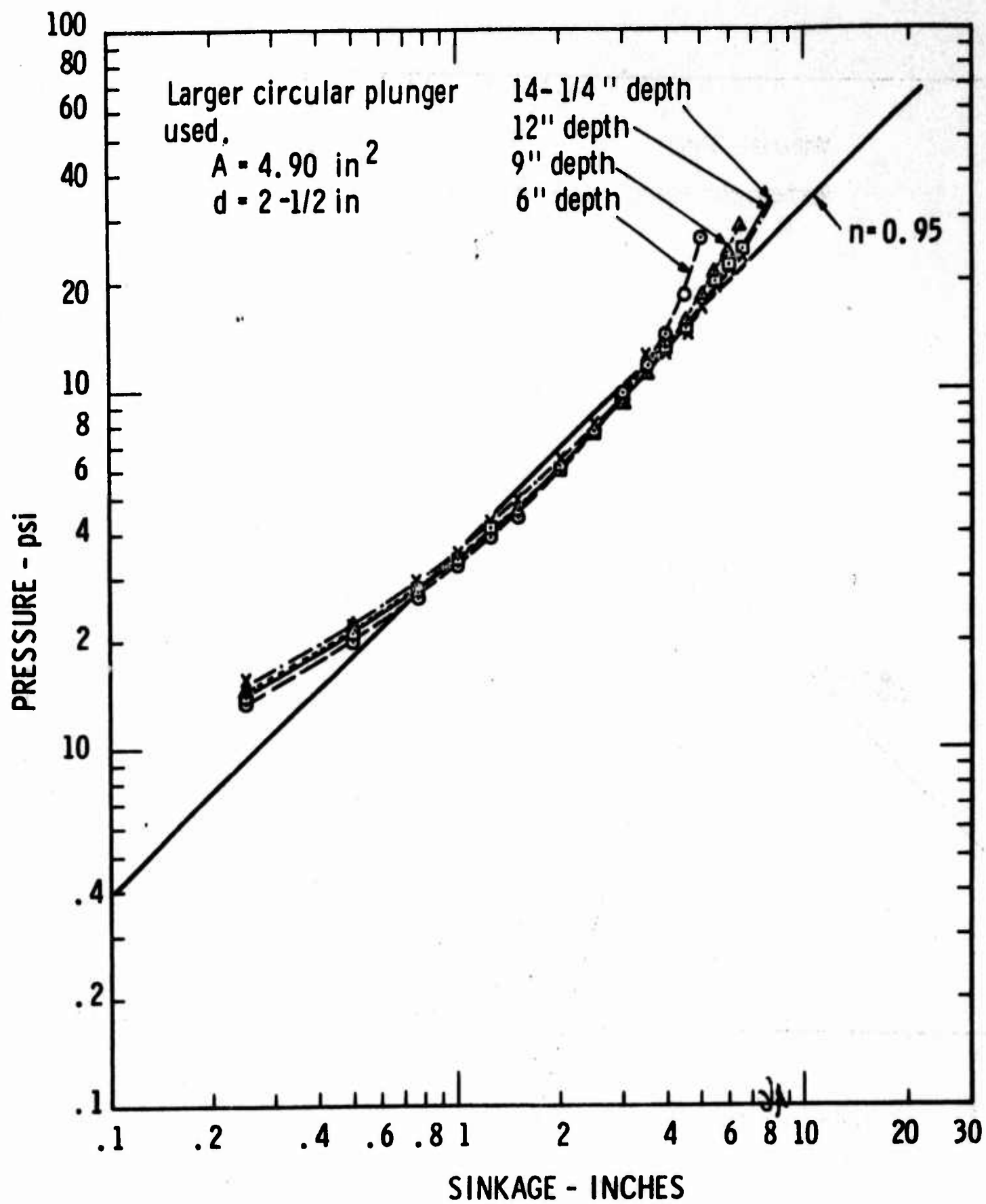


Fig. 47. 100% sand.

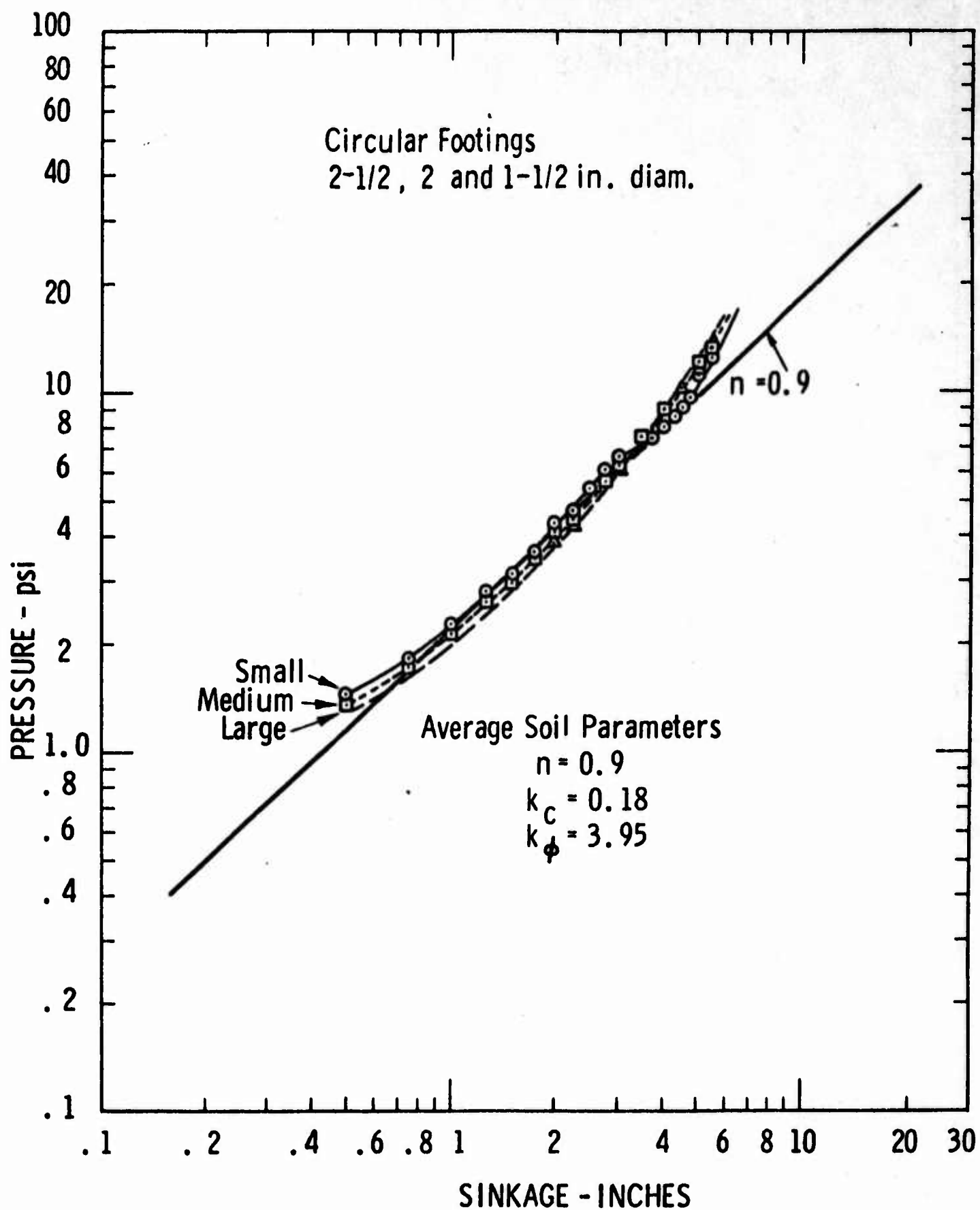


Fig. 48. 100% glass beads, 0.010 to 0.015 in. diam.

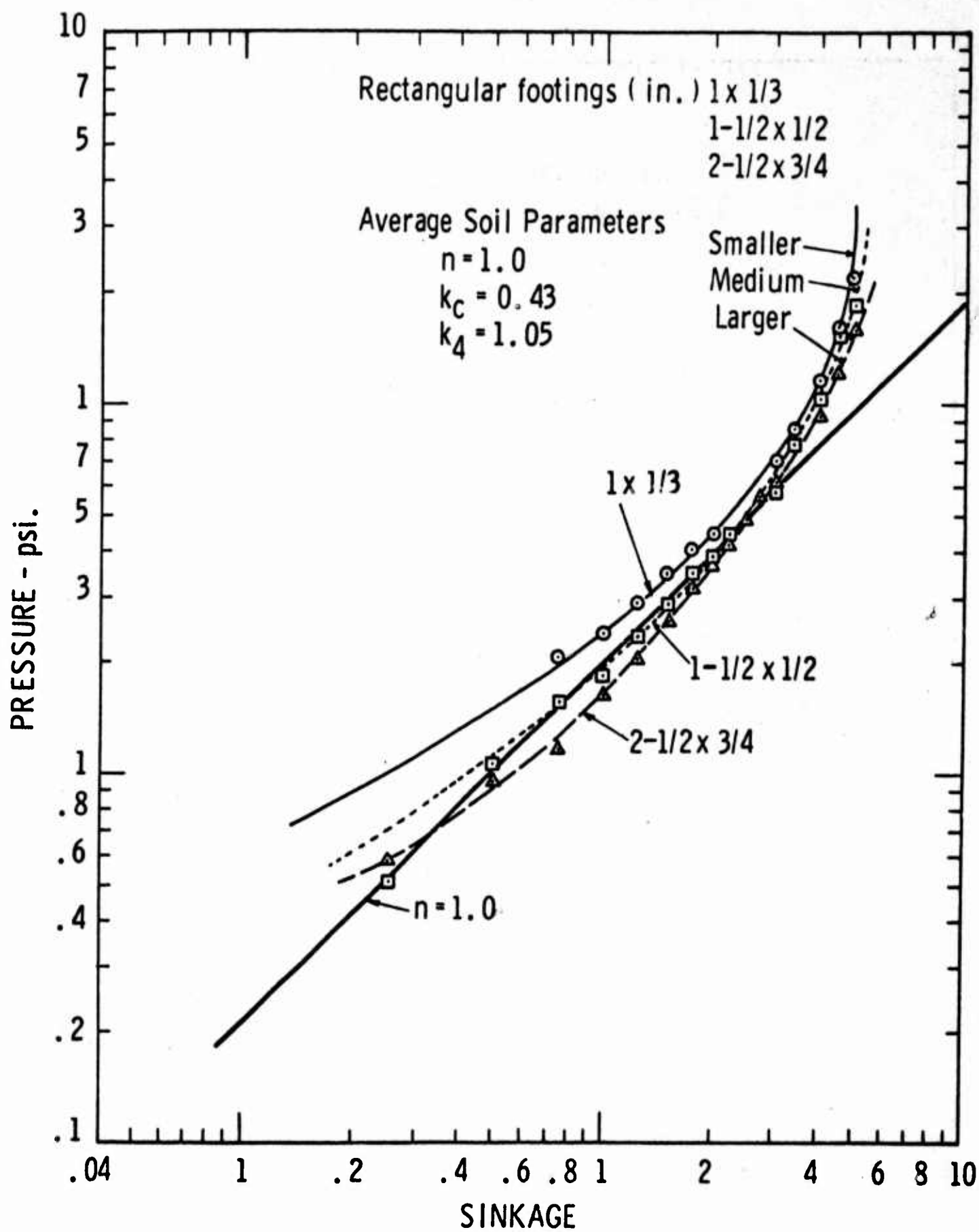


Fig. 49. Poured magnetic barium ferrite.

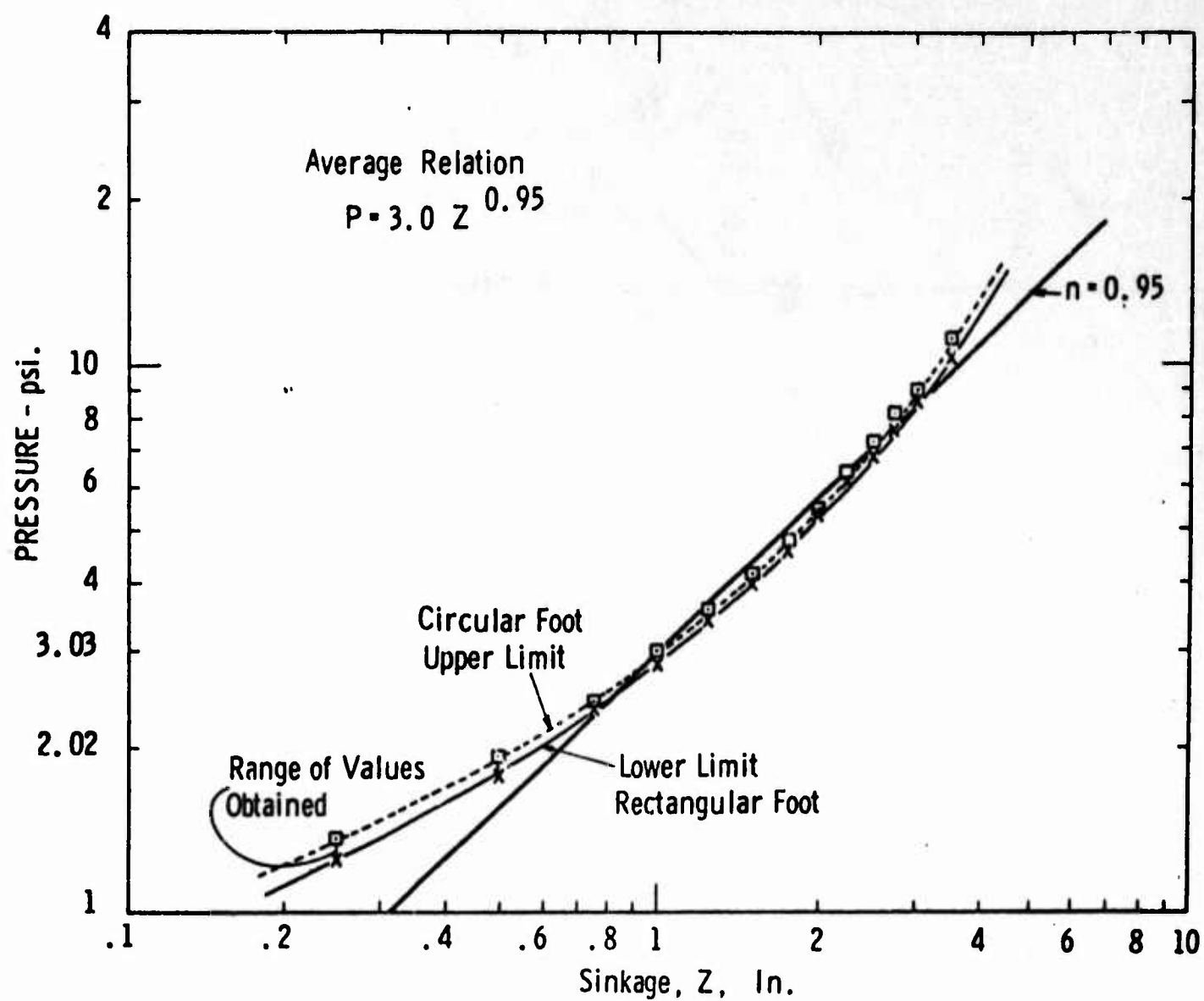


Fig. 50. Effect of speed of penetration in sand.

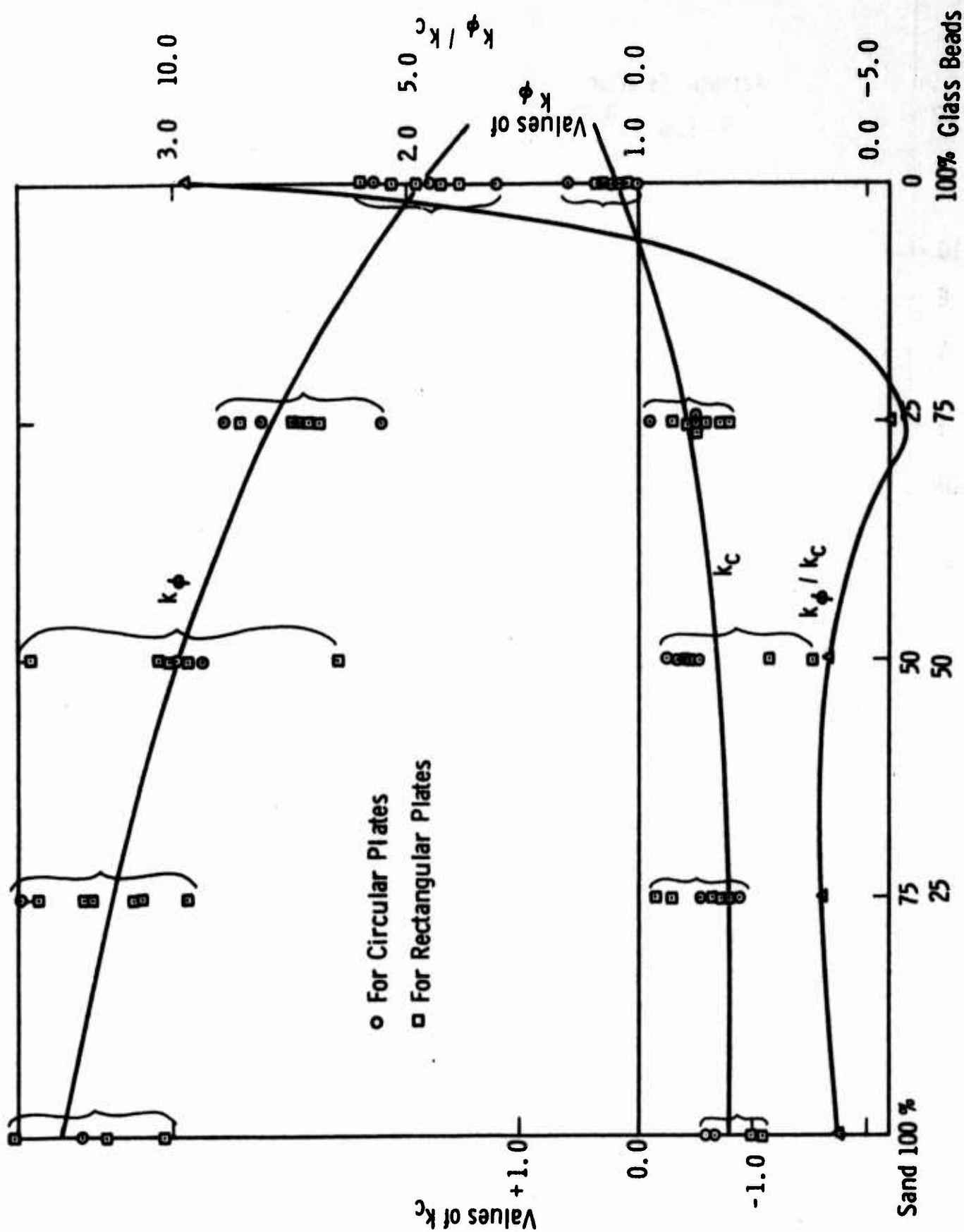


Fig. 51. Averaged values of actual test points.

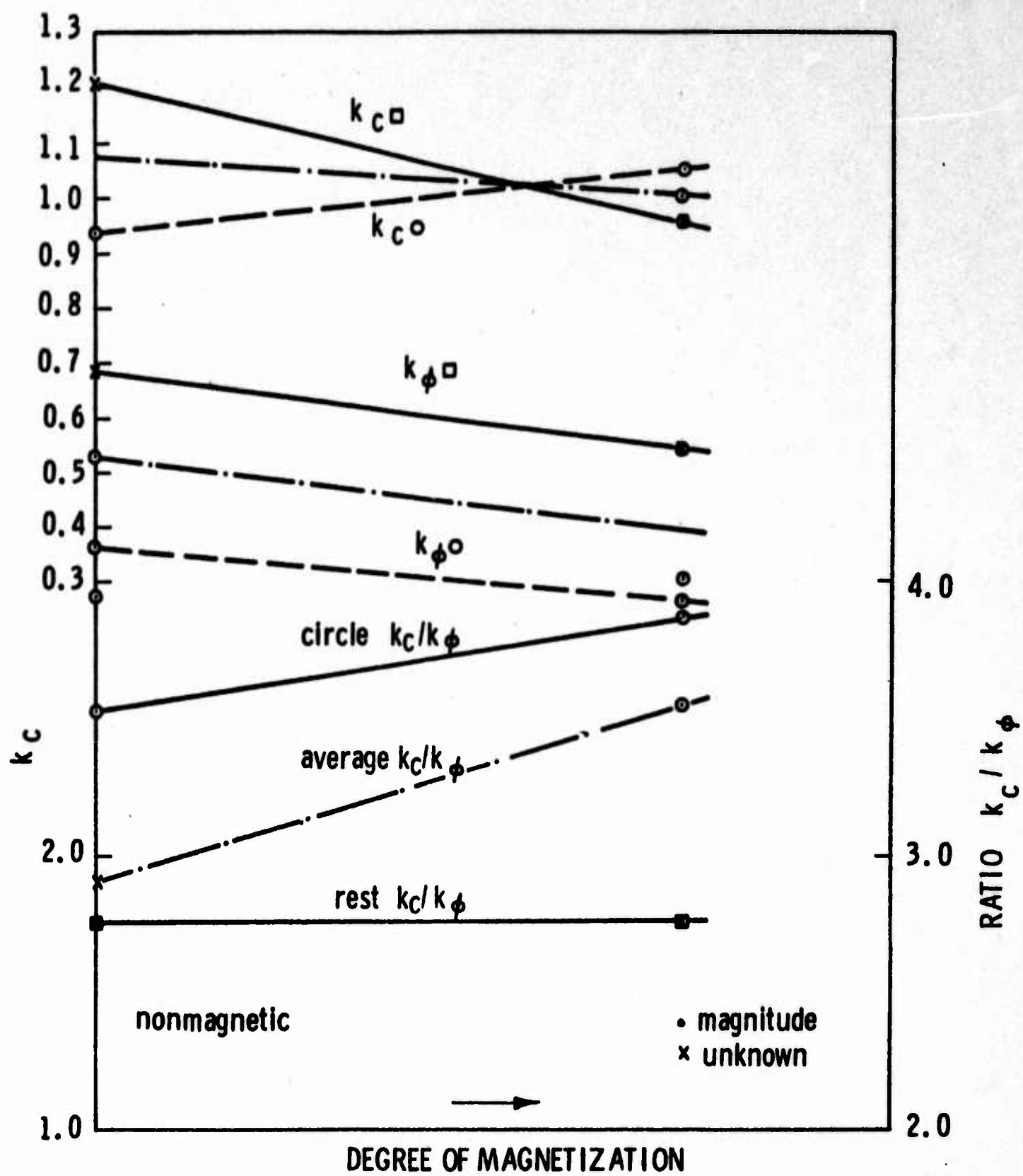


Fig. 52. Magnetic barium ferrite.

UNCLASSIFIED
Rigid Wheel
Studies by Means
of Dimensional
Analysis

1 Apr. 63

AD Accession No.
Components Research and Development Laboratories,
Detroit Arsenal, Center Line, Michigan
RIGID WHEEL STUDIES BY MEANS OF DIMENSIONAL ANALYSIS
Report No. 7841
Unclassified Report
103 PP-Tables-Illus.

In the work presented here, a successful similitude correlation of wheel performance in sand was obtained using the Bekker sinkage parameters. Tests were made in the laboratory under simulated field conditions and included an investigation of wheel sinkage, drag, and traction, as related to wheel shape, diameter, load and soil depth.

A series of experiments are reported using a precision Bevameter on sand and mixtures of sand with other materials. The object of the tests was to ascertain the range over which the cohesive and frictional moduli of sinkage of a soil could be controlled which would exert a controlling influence upon the dimensionless parameters developed.

The results indicate that such control is possible to a moderate degree when using the types of materials studied.

UNCLASSIFIED
Rigid Wheel
Studies by Means
of Dimensional
Analysis

1 Apr. 63

AD Accession No.
Components Research and Development Laboratories,
Detroit Arsenal, Center Line, Michigan
RIGID WHEEL STUDIES BY MEANS OF DIMENSIONAL ANALYSIS
Report No. 7841
Unclassified Report
103 PP-Tables-Illus.

In the work presented here, a successful similitude correlation of wheel performance in sand was obtained using the Bekker sinkage parameters. Tests were made in the laboratory under simulated field conditions and included an investigation of wheel sinkage, drag, and traction, as related to wheel shape, diameter, load and soil depth.

A series of experiments are reported using a precision Bevameter on sand and mixtures of sand with other materials. The object of the tests was to ascertain the range over which the cohesive and frictional moduli of sinkage of a soil could be controlled which would exert a controlling influence upon the dimensionless parameters developed.

The results indicate that such control is possible to a moderate degree when using the types of materials studied.

UNCLASSIFIED
Rigid Wheel
Studies by Means
of Dimensional
Analysis

1 Apr. 63

AD Accession No.
Components Research and Development Laboratories,
Detroit Arsenal, Center Line, Michigan
RIGID WHEEL STUDIES BY MEANS OF DIMENSIONAL ANALYSIS
Report No. 7841
Unclassified Report
103 PP-Tables-Illus.

In the work presented here, a successful similitude correlation of wheel performance in sand was obtained using the Bekker sinkage parameters. Tests were made in the laboratory under simulated field conditions and included an investigation of wheel sinkage, drag, and traction, as related to wheel shape, diameter, load and soil depth.

A series of experiments are reported using a precision Bevameter on sand and mixtures of sand with other materials. The object of the tests was to ascertain the range over which the cohesive and frictional moduli of sinkage of a soil could be controlled which would exert a controlling influence upon the dimensionless parameters developed.

The results indicate that such control is possible to a moderate degree when using the types of materials studied.

UNCLASSIFIED
Rigid Wheel
Studies by Means
of Dimensional
Analysis

1 Apr. 63

AD Accession No.
Components Research and Development Laboratories,
Detroit Arsenal, Center Line, Michigan
RIGID WHEEL STUDIES BY MEANS OF DIMENSIONAL ANALYSIS
Report No. 7841
Unclassified Report
103 PP-Tables-Illus.

In the work presented here, a successful similitude correlation of wheel performance in sand was obtained using the Bekker sinkage parameters. Tests were made in the laboratory under simulated field conditions and included an investigation of wheel sinkage, drag, and traction, as related to wheel shape, diameter, load and soil depth.

A series of experiments are reported using a precision Bevameter on sand and mixtures of sand with other materials. The object of the tests was to ascertain the range over which the cohesive and frictional moduli of sinkage of a soil could be controlled which would exert a controlling influence upon the dimensionless parameters developed.

The results indicate that such control is possible to a moderate degree when using the types of materials studied.

UNCLASSIFIED
Rigid Wheel
Studies by Means
of Dimensional
Analysis

1 Apr. 63

AD
Components Research and Development Laboratories,
Detroit Arsenal, Center Line, Michigan
RIGID WHEEL STUDIES BY MEANS OF DIMENSIONAL ANALYSIS
Report No. 7841
Unclassified Report

In the work presented here, a successful similitude correlation of wheel performance in sand was obtained using the Bekker sinkage parameters. Tests were made in the laboratory under simulated field conditions and included an investigation of wheel sinkage, drag, and traction, as related to wheel shape, diameter, load and soil depth.

A series of experiments are reported using a precision Bevameter on sand and mixtures of sand with other materials. The object of the tests was to ascertain the range over which the cohesive and frictional moduli of sinkage of a soil could be controlled which would exert a controlling influence upon the dimensionless parameters developed.

The results indicate that such control is possible to a moderate degree when using the types of materials studied.

AD
Components Research and Development Laboratories,
Detroit Arsenal, Center Line, Michigan
RIGID WHEEL STUDIES BY MEANS OF DIMENSIONAL ANALYSIS
Report No. 7841
Unclassified Report

UNCLASSIFIED
Rigid Wheel
Studies by Means
of Dimensional
Analysis

1 Apr. 63

In the work presented here, a successful similitude correlation of wheel performance in sand was obtained using the Bekker sinkage parameters. Tests were made in the laboratory under simulated field conditions and included an investigation of wheel sinkage, drag, and traction, as related to wheel shape, diameter, load and soil depth.

A series of experiments are reported using a precision Bevameter on sand and mixtures of sand with other materials. The object of the tests was to ascertain the range over which the cohesive and frictional moduli of sinkage of a soil could be controlled which would exert a controlling influence upon the dimensionless parameters developed.

The results indicate that such control is possible to a moderate degree when using the types of materials studied.

UNCLASSIFIED
Rigid Wheel
Studies by Means
of Dimensional
Analysis

1 Apr. 63

AD
Components Research and Development Laboratories,
Detroit Arsenal, Center Line, Michigan
RIGID WHEEL STUDIES BY MEANS OF DIMENSIONAL ANALYSIS
Report No. 7841
Unclassified Report

In the work presented here, a successful similitude correlation of wheel performance in sand was obtained using the Bekker sinkage parameters. Tests were made in the laboratory under simulated field conditions and included an investigation of wheel sinkage, drag, and traction, as related to wheel shape, diameter, load and soil depth.

A series of experiments are reported using a precision Bevameter on sand and mixtures of sand with other materials. The object of the tests was to ascertain the range over which the cohesive and frictional moduli of sinkage of a soil could be controlled which would exert a controlling influence upon the dimensionless parameters developed.

The results indicate that such control is possible to a moderate degree when using the types of materials studied.

AD
Components Research and Development Laboratories,
Detroit Arsenal, Center Line, Michigan
RIGID WHEEL STUDIES BY MEANS OF DIMENSIONAL ANALYSIS
Report No. 7841
Unclassified Report

UNCLASSIFIED
Rigid Wheel
Studies by Means
of Dimensional
Analysis

1 Apr. 63

In the work presented here, a successful similitude correlation of wheel performance in sand was obtained using the Bekker sinkage parameters. Tests were made in the laboratory under simulated field conditions and included an investigation of wheel sinkage, drag, and traction, as related to wheel shape, diameter, load and soil depth.

A series of experiments are reported using a precision Bevameter on sand and mixtures of sand with other materials. The object of the tests was to ascertain the range over which the cohesive and frictional moduli of sinkage of a soil could be controlled which would exert a controlling influence upon the dimensionless parameters developed.

The results indicate that such control is possible to a moderate degree when using the types of materials studied.